Resource Allocation and Performance Evaluation in Heterogeneous and Relay-based Wireless Networks

by

Hamidreza Boostanimehr

M.A.Sc., The University of British Columbia, 2010
B.Sc., Sharif University of Technology, 2008

A THESIS SUBMITTED IN PARTIAL FULFILLMENT OF
THE REQUIREMENTS FOR THE DEGREE OF

DOCTOR OF PHILOSOPHY

in

The Faculty of Graduate and Postdoctoral Studies

(Electrical and Computer Engineering)

THE UNIVERSITY OF BRITISH COLUMBIA

(Vancouver)

August 2014

Abstract

In the last decade, the mobile data demand has been exponentially growing. Telecommunication industry finds it increasingly difficult to cope with this exponential growth through conventional cellular networks with carefully planned high power macro base stations (BSs). Therefore, the densification of BSs through the introduction of low power BSs has been considered for implementation. The combination of macro BSs and low power BSs such as pico and femto BSs as well as relay nodes is referred to as heterogeneous networks (HetNets).

HetNets impose major technical challenges in implementation such as severe interference cases and imbalance of load among macro BSs and low power BSs. One of the problems that needs to be re-addressed in the context of HetNets is the cell association problem. Although centralized cell association schemes are important in realizing the potentials of HetNets, mobile operators are interested in distributed schemes in which network elements decide based on their local information. In this thesis, we consider distributed cell association algorithms with quality of service provisioning. First, we propose a unified cell association algorithm that is particularly designed for downlink. Next, we also consider uplink to have a downlink and uplink aware cell association scheme. The performances of the proposed schemes are examined through numerical simulations.

Cooperative relay-based communication combined with orthogonal frequency division multiplexing (OFDM) and its multi access variant, orthogonal frequency division multiple access (OFDMA) has gained an immense interest in the last decade. Among all the research topics in OFDM relay-based communication, analyzing the outage behavior has been an invariable concern to researchers. To analyze the outage behavior, most of the researchers ignore the correlation between OFDM subchannels, and also assume equal bit allocation on all the subchannels. In this thesis, we analyze the outage behavior of a three-node OFDM relay-based network when these two assumptions are relaxed. Next, we characterize the global outage probability of a multi-user single-relay OFDMA network. Finally, a network consisting of a cluster of source-destination pairs and a cluster of relays is considered where we propose a low complexity relay allocation scheme. The outage analyses and the relay allocation scheme are examined through numerical simulations.

Preface

Publications that have been resulted during the conduction of research in this thesis are as follows:

- H. Boostanimehr, V. K. Bhargava. Unified and Distributed QoS-Driven Cell Association Algorithms in Heterogeneous Networks. First round of revisions submitted to a peer reviewed journal, pages 1–13, Jul. 2014. (Linked to Chapter 2)

- H. Boostanimehr, V. K. Bhargava. Distributed and QoS-Driven Cell Association in HetNets to Minimize Global Outage Probability. Accepted to be presented in 2014 IEEE GLOBECOM, pages 1–7, Apr. 2014. (Linked to Chapter 2)

- H. Boostanimehr, V. K. Bhargava. Joint Downlink and Uplink Aware Cell Association in HetNets with QoS Provisioning. Submitted to a peer reviewed journal, pages 1–13, May 2014. (Linked to Chapter 3)

- H. Boostanimehr, V. K. Bhargava. Outage Capacity Analysis for OFDM Decode-and-Forward Systems in Frequency Selective Rayleigh Fading Channels. *IEEE Communications Letters*, 16(6):937–940, Jun. 2012. (Linked to Chapter 4)

- H. Boostanimehr, V. K. Bhargava. Outage Probability Analysis for Multi-User Single-Relay OFDMA DF Networks in Frequency Selective Rayleigh Fading Channels. *IEEE Communications Letters*, 18(2):245–248, Feb. 2014. (Linked to Chapter 5)

- H. Boostanimehr, V. K. Bhargava. Outage Analysis and Relay Allocation for Multi-stream OFDMA Decode-and-Forward Rayleigh Fading Networks. In *Proceedings of 2012 IEEE ICCC*, pages 630–635. (Linked to Chapter 6)

I am the primary researcher and author for all the research contributions made in this thesis. I conducted the literature review and identified the research problems. Moreover, I independently formulated the research problems and carried out the mathematical analysis and simulations. I also wrote the associated manuscripts for publication. My supervisor, Prof. Vijay K. Bhargava, is a co-author for contributions made in all the papers. I consulted

him during the identification and formulation of the research problems. He also provided technical and editorial feedback during the preparation of associated manuscripts.

Table of Contents

List of Tables

List of Figures

List of Abbreviations

2G	:	Second Generation of cellular networks
3GPP	:	3rd Generation Partnership Project
4G	:	Fourth Generation of cellular networks
ABS	:	Almost Blank Subframe
AF	:	Amplify-and-Forward
AMC	:	Adaptive Modulation Coding
AP	:	Access Point
CDF	:	Cumulative Distribution Function
CDMA	:	Code Division Multiple Access
CoMP	:	COordinated Multi-Point reception and transmission
CSR	:	Cell Specific Reference signal
DF	:	Decode-and-Forward
EBA	:	Equal Bit Allocation
eICIC	:	Enhanced Inter-Cell Interference Coordination
eNB	:	Evolved Node B
FCC	:	Federal Communications Commission
FDMA	:	Frequency Division Multiple Access
HARQ	:	Hybrid Automatic Repeat reQuest
HeNB	:	Home Evolved Node B
HetNet	:	HETerogenous NETworks
HSPA	:	High Speed Packet Access
ICIC	:	Inter-Cell Interference Coordination
i.i.d.	:	Independent and Identically Distributed
IP	:	Internet Protocol
KKT	:	Karush-Kuhn-Tucker
LOS	:	Line Of Sight
LTE	:	Long Term Evolution
LTE-Advanced	:	Long Term Evolution-Advanced
MIMO	:	Multiple Input Multiple Output

MRC	:	Maximum Ratio Combining
N-DFT	:	N point Discrete Fourier Transform
OFDM	:	Orthogonal Frequency Division Multiplexing
OFDMA	:	Orthogonal Frequency Division Multiple Access
PDF	:	Probability Distribution Function
QoS	:	Quality Of Service
RB	:	Resource Block
RN	:	Relay Node
RNC	:	Radio Network Controller
RV	:	Random Variable
SC-FDM	:	Single Carrier-Frequency Division Multiplexing
SC-FDMA	:	Single Carrier-Frequency Division Multiple Access
SINR	:	Signal to Interference plus Noise Ratio
SNR	:	Signal to Noise Ratio
TDMA	:	Time Division Multiple Access
UE	:	User Equipment

Acknowledgements

First and foremost, I would like to thank my supervisor, Prof. Vijay K. Bhargava, for the guidance and support that he has provided. This thesis would not have been possible without his suggestions, advice and constant encouragement.

Furthermore, I would like to extend my utmost gratitude to my lab mates for creating a friendly environment, in which I could carry out my research project.

Finally, heartfelt and deep thanks go to my family, who have always encouraged me and given their unconditional support throughout my studies at the University of British Columbia. Without their support, I could not have completed this thesis.

Dedication

To my parents...

Chapter 1

Introduction

In recent years, the proliferation of intelligent mobile devices that are connected to the Internet has changed the communication paradigms. Nowadays, users can communicate with each other at any time and through different mediums such as video, voice, instant message, and email. Users also are interested in sharing their everyday experiences with their circles through social media. The powerful mobile devices make generating data and consuming data from other users possible. Moreover, the number of machines that are connected to and controlled through the Internet is increasing everyday, extending the reach of Internet from users to machines [1]. It seems that the world is changing rapidly towards the Internet of everything. In fact, it is predicted that by the year 2020 more than 50 billion devices will be connected to the Internet [2]. The tendency of users to communicate through all sorts of media, the introduction of social networks and Internet of things, among other factors, have created an exponential growth in mobile data demand [3].

In order to cope with this exponential growth, the most immediate option seems to be increasing the spectral efficiency of the point to point communication. However, through the relentless efforts of industrial and academic researchers in recent decades, we are reaching the Shannon capacity in link level communication in wireless systems. Migrating from second generation of cellular wireless networks (2G) to today's fourth generation (4G), the spectral efficiency has been approaching the fundamental limit through the introduction of all sorts of technologies including powerful channel coding schemes, new multiple access schemes such as code division multiple access (CDMA) [4], orthogonal frequency division multiple access (OFDMA) [5], and multiple input multiple output (MIMO) antennas [6] (Fig. 1.1) [7]. Although the air interface in point to point communication keeps on improving, the anticipated improvement is not adequate to support the exponential growth of data demand. Therefore, other venues to improve the network capacity need to be investigated.

Data rate is directly proportional to communication bandwidth. Therefore, acquiring more spectrum seems to be another venue to enhance the capacity of wireless networks. However, the spectrum is highly regulated by Federal Communications Commission (FCC) and is already densely populated by various industries and applications. In fact, the scarcity of spectrum has given rise to technologies such as dynamic spectrum sharing and cognitive

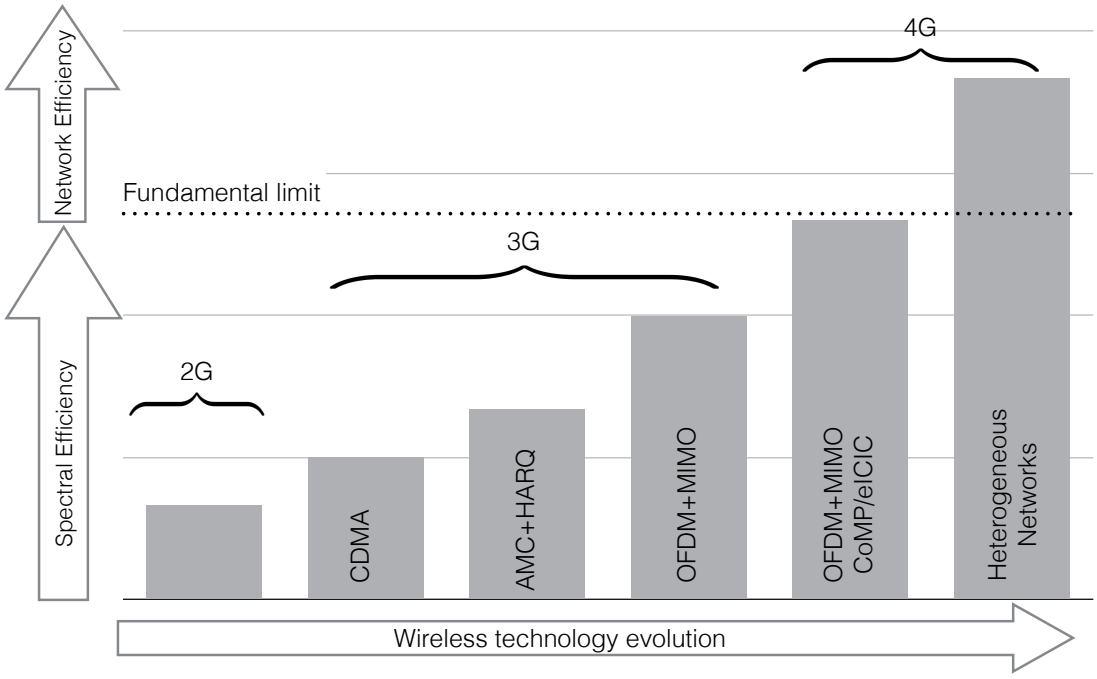

Figure 1.1: Wireless technology evolution

radio techniques [8] in the last decade as it is indicated by FCC that the spectrum has not been efficiently regulated and it is highly under-utilized in many cases [9]. The scarcity of the spectrum also contributes to making spectrum acquisition for wireless industries unreasonably costly. As a result, in an attempt to improve the network capacity by orders of magnitude, the tendency is to reuse the already available spectrum more efficiently by adding more base stations (BSs) to the network. In other words, the focus is to increase the network efficiency rather than the spectrum efficiency to meet this unprecedented mobile data demand.

Conventional cellular networks are composed of several cells. Each cell is served by one BS that is referred to as macro BS. The BSs in conventional cellular networks have high transmitting powers and cover large geographical areas. In a cellular network with sparse deployment of macro BSs, adding new macro BSs does not add significant inter-cell interference, and the frequency spectrum can be reused with considerable gains. However, few factors set back the use of extra macro BSs. One of the factors is the cost of deploying new macro BSs. In already dense deployment of macro BSs, it is expensive to acquire sites to install new macro BSs. In addition, the BS itself is an expensive device, and macro BSs require air conditioning on their power amplifier since they have high transmitting powers in the range of 2 to 40 W. Another factor is that the existence of coverage holes in

these large cells is expected since the urban environment conditions render the behavior of wireless channels random. The existence of coverage holes reduces the overall capacity of the network by increasing the likelihood of outage. Furthermore, there are hot spots during certain times of the day where many mobile users desire to have connectivity with good quality of service (QoS). Since BSs, including macro BSs, have finite resources to distribute among their users, all the users in hotspots may not be supported with acceptable QoS and further communication outage is resulted. The mentioned challenges of installing new macro BSs, among others, give rise to the idea of deploying low power BSs and relays to cover hot spots and coverage holes with considerably lower cost. Overlaying macro BSs with lower power BSs such as pico, femto, and relay stations constitutes what we call a *heterogeneous cellular network* [10].

In the next section, we provide a brief overview of heterogeneous networks (HetNets). Since some parts of the research presented in this thesis address relay-based cooperative communication, we will briefly go through the fundamentals of cooperative communication in Section 1.2. Finally, as the Long Term Evolution (LTE) standard is the most dominant standard defining 4G and highly correlated to the context of today's wireless communication research, some key features of this standard are overviewed in Section 1.3.

1.1 Overview of heterogeneous networks

HetNets can be defined as cellular networks composed of macro BSs overlaid with lower power BSs (lower tier BSs or smaller cells), in which the low power BSs are deployed with higher density. The lower tier BSs can be pico BSs, femto BSs, or relay stations. Macro BSs with their high transmitting power cover large geographical areas, while coverage holes and hot spots are covered by lower tier BSs. The lower tier BSs may be installed outdoor or cover indoor environments. Pico BSs usually are meant to be installed outdoor and have transmitting power in the range of 250 mW up to 2 W. Since the transmitting power is considerably low compared to macro BSs, air conditioning the power amplifier at the pico BSs is generally not required. In addition, as pico BSs are smaller in size and require smaller antennas, they are economically efficient to employ. Femto BSs are considered for serving indoor environments such as residential homes or a certain floor in an enterprise building [11]. As an example, a WiFi access point (AP) can be considered a femto BS [12]. However, in the case of WiFi AP, a different air interface is used compared to the air interface of outdoor BSs, and only authorized users may be served by the AP. Such femto BSs with restricted access are referred to as closed femto BSs [12]. As femto BSs are already installed in homes

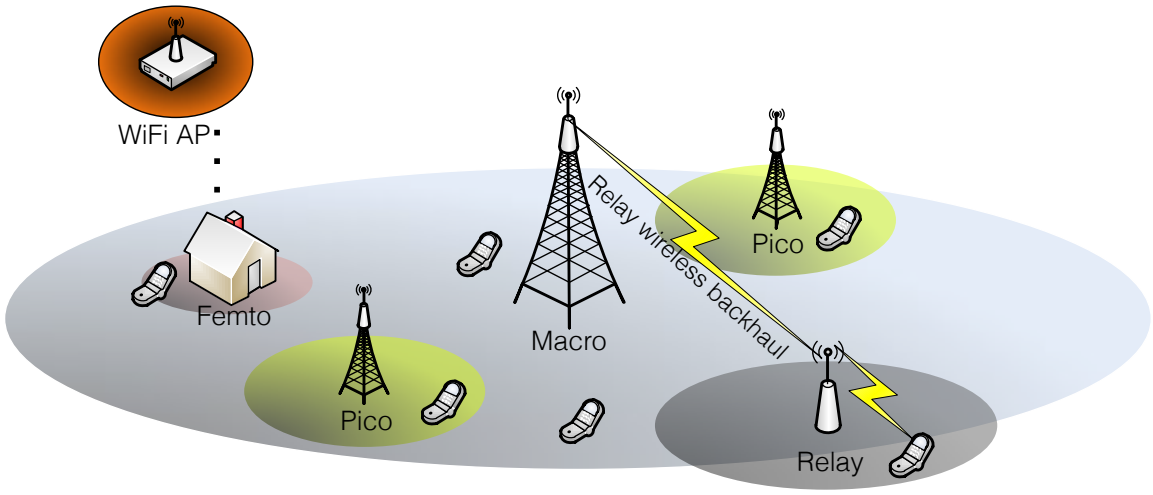

Figure 1.2: A HetNet composed of macro, pico, and femto BSs and relay nodes

or enterprises, utilizing them leads to significant reduction in cost. In fact, economics of pico and femto BSs have been the main driver of considering their deployment in cellular networks [13]. Macro, pico, and femto BSs are usually connected to the core network through wire or high speed optical fibre.

There are situations in which installing wired connection to the core network is not feasible. In these cases, a relay node can be used to extend the coverage of macro BS. Users under the coverage of a relay node communicate to the macro BS through the relay node. Relay node may use the same spectrum as the one users utilize or may be allocated dedicated spectrum to communicate to the macro BS. Re-using the spectrum for the BS to relay communication is more common. In this case, the relay node is equivalent to a BS from the user's perspective, and the macro BS perceives the relay node as another user [14]. The relay-based communication is a special case of a broader topic known as *cooperative communication* [1]. In summary, to define HetNets more precisely, the collection of macro, pico, femto, and relay BSs that can be connected to the core network through wired or wireless backhaul is referred to as HetNet [15]. A simplified HetNet is illustrated in Fig. 1.2.

As a legacy from conventional cellular networks, the most popular cell association scheme in wireless cellular networks is the maximum signal to interference plus noise ratio (SINR) scheme. A cell association scheme is a set of rules that determines which BS serves a particular user. In cellular wireless networks, BSs are constantly transmitting known reference or pilot signals to enable the users to measure some attributes of the downlink, including the received SINR. In maximum SINR scheme, each user associates itself to the BS that provides

[1] A brief overview of the fundamentals of cooperative communication is provided in the next section.

the best SINR. Following this scheme creates an imbalance in HetNets between macro BSs and lower tier BSs. Macro BSs with their high power have large coverage areas and lower tier BSs have boundaries that are relatively close to them. Moreover, BSs usually operate in the same frequency bands to achieve frequency re-use gains (referred to as co-channel deployment). Small coverage area of low tier BSs leads to underutilization of femto, pico, and relay stations that results in not achieving the expected gains from HetNets. In fact, the performance of co-channel deployment of multi-tier HetNets has been evaluated in early research [16, 17]. It is concluded in [16, 17] that higher gains would be achievable in HetNets, and the main reason that high gains are not reached is that the boundaries defined by low tier BSs is very close to those BSs. In addition, macro BSs cause significant downlink interference on the lower tier BSs that are located in the vicinity of macro BSs.

The small coverage area of low tier BSs causes an imbalance in the uplink interference at macro and lower tier BSs, as well. Let us explain the uplink interference situation through an example. Assume that a user is standing at a point where the downlink signal to noise ratio (SNR) received from a macro BS with nominal power of 40 dBm is equal to the SNR received from a femto BS with nominal power of 20 dBm. Assuming that only path loss is considered in the channel model, we can conclude that upon transmission of the user, the received power at the femto BS is 20 dB higher than the received power at the macro BS. Further assume that this boundary user is served by the macro BS, and 5 dB of power above the thermal noise is required by the macro BS to decode the user data correctly. This results in an interference that is 25 dB above the thermal noise power at the femto BS. This high level of interference corrupts the uplink connection of the users associated with the femto BS severely. Interference management techniques in the scope of 3G cellular networks is presented in [18] to handle the downlink and uplink interference scenarios in macro and femto deployment of HetNets. In [18], carrier selection and power control by the femto BS is proposed to handle the downlink interference scenarios, and adaptive attenuation of unwanted signals from macro user at the femto BS is proposed to cope with the uplink interference scenarios.

As the conventional maximum SINR cell association scheme creates the aforementioned drawbacks in HetNets, cell association needs to be done in a more wisely fashion in which the imbalance of load among BSs from different tiers and severe interference situations in downlink and uplink are reduced. One simple and yet effective technique to achieve load balancing in HetNets that has been envisioned by Third Generation Partnership Project (3GPP) in the context of LTE-Advanced [2] is called cell range expansion [15]. In cell range

[2]LTE-Advanced is the most dominant standard defining 4G wireless systems. The key features of LTE and LTE-Advanced are overviewed in Section 1.3.

expansion, the signal power of lightly loaded BSs are biased so that their coverage area increases and more users associate themselves with lightly loaded BSs. Intuitively, low tier BSs are usually under-utilized and cell range expansion is towards offloading the users from macro BSs to lower tier BSs. However, a negative bias value at low tier BSs can happen which indicates that offloading the users to macro or other low tier BSs should occur.

In cases which the location of the low tier BS is in the vicinity of the macro BS, high interference caused by the offloaded macro BS on the downlink of the low tier BS can cause link failure. Therefore, inter-cell interference coordination (ICIC) is needed along with cell range expansion to realize the offloading gains. In 4G standards, specifically LTE systems, a new structure for resources is used that is suitable for designing flexible resource allocation and ICIC schemes. The air interface of LTE standard is developed based on OFDMA. OFDMA technology makes possible a structure in which the time-frequency spectrum is divided into orthogonal resource blocks (RBs). The RB-based structure in LTE allows for more flexible resource allocation schemes which result in higher spectral efficiency [19]. One way of reducing interference among cells is to use resource partitioning in time, frequency, or space domain [20, 21]. Resource partitioning involves using orthogonal resources in cells that potentially interfere with each other. Through RB-based resources, BSs can coordinate so that the interfering BS gives up using parts of resources on certain frequency bands and during certain times so that the other BS can accomplish its communication with the user. In the context of LTE, this ICIC technique is accomplished through almost blank subframes (ABSs). Cell range expansion along with resource partitioning ICIC through ABS has shown to achieve considerable load balancing and interference avoidance gains [22, 23].

1.2 Overview of cooperative communication

During the last decade, the focus of wireless communication has been diverging from only voice applications towards applications such as wireless broadband Internet, online gaming, video streaming and many other applications. The data rate hungry nature of new applications has been driving the researchers to work on improving the spectral efficiency of the wireless communication links. MIMO systems are among the most successful technologies allowing for increasing the data rate by increasing the number of antennas at the transmitter and receiver sides. However, installing multiple antennas is not feasible at all the devices. In order to achieve MIMO gains, antennas must be separated enough so that spatial diversity through the reception or transmission of independent copies of the signal is realized. In addition, antennas can be prohibitively bulky devices themselves. Therefore, installing

multiple antennas on small devices such as cell phones and in applications such as sensor networks can prove infeasible. In order to resolve the prohibitive size of MIMO systems, cooperative communication came to the picture to harvest MIMO gains without installing multiple antennas. In cooperative communication, users cooperate with each other as relays to virtually create a MIMO system by transmitting a copy of each other's signals to the destination. The geographical separation of cooperative nodes creates enough spatial diversity so that the received copies of the signal go through independent fadings. Removing the extra antennas significantly reduces the cost of the system in cooperative communication.

The three-terminal cooperation model was first introduced by Van Der Meulen in [24]. The three-terminal cooperation model is composed of a source, a relay, and a destination, and is the building block of cooperative and relay-based communication. Then, the information theoretic aspects of the three-terminal model, including the calculation of Shannon capacity, have been investigated in [25]. Most of the ideas that came along later on cooperative communication can be traced back to the work in [25]. The technical complexity of the cooperative model at the time made it unattractive to the researches and it has been abandoned for a while. Then, the evolution of wireless technology made possible the practical implementation of the model and it regained popularity. Cooperative communication techniques are being used to improve coverage, enhance capacity and combat shadowing in wireless communication networks such as cellular or mesh networks [26]. As it has been mentioned before, cooperative communication also introduces spatial diversity by creating copies of the signal that have gone through independent channel fadings [27, 28]. Cooperative communication through multi-hop transmission can also contribute to energy efficient communication by breaking the long point to point distance into several short distance hops [29, 30]. In addition, low power relay nodes are being considered by 3GPP to be implemented in LTE-Advanced for planning HetNets efficiently. Relay nodes extend the coverage and capacity of HetNets at the cell boundaries without incurring high site acquisition and backhaul costs [31].

Fig. 1.3 illustrates the procedure in the fundamental three-node cooperation model. In order to avoid interference, the relay-based communication usually happens in two orthogonal phases. The orthogonality can be in time domain through time division multiple access (TDMA) or in frequency domain through frequency division multiple access (FDMA), while TDMA is more popular. In the first phase, the source broadcasts its information signal and both the relay and destination listen. In the second phase, the relay forwards the whole or parts of the source message to the destination through one of the fundamental relaying protocols or variants of them. The destination combines both copies of the received signal to have a more reliable detection. In many cases, there is no line of sight (LOS) between the

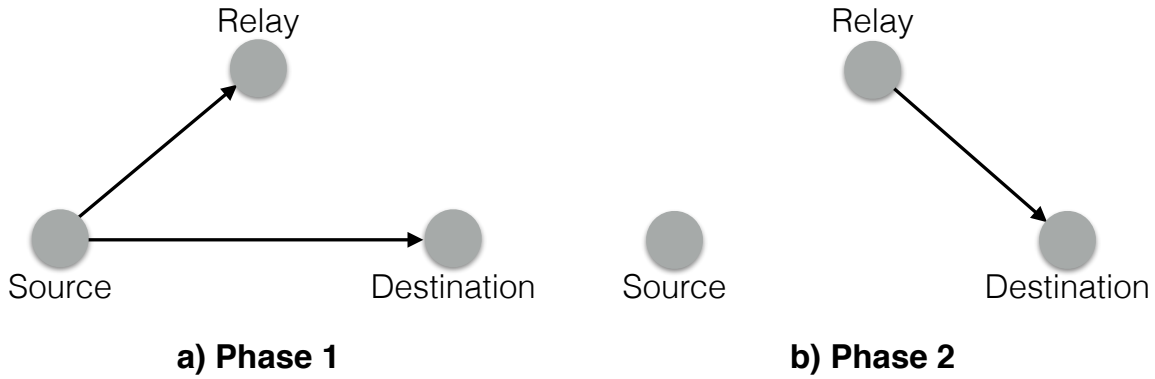

Figure 1.3: Simplified three-node cooperative model

source and destination. Therefore, the destination only relies on the message it has received from the relay. In this case, the relay is merely used for coverage extension.

Two fundamental relaying methods have been defined in [27]: Amplify-and-forward (AF), and decode-and-forward (DF). In AF protocol, the relay simply amplifies and forwards the analog signal it has received from the source. The destination combines the two copies of the signal, for instance using maximum ratio combining (MRC), to have a reliable detection. Naturally, the noise introduced at the relay also gets amplified and sent to the destination leading to higher noise level.

In DF protocol, the relay decodes the message it has received from the source, re-encodes a new one, and then forwards it to the destination. The relay may perform the decode-and-re-encode process in different fashions. For instance, the relay may decode the message fully and re-encodes a new one, it may add incremental redundancy for better channel coding, or it may decode it symbol by symbol knowing that the full decoding occurs at the destination. This degree of freedom in decode-and-re-encode process at the relay allows for a trade-off between performance and complexity [27]. In this thesis, only DF protocol is addressed.

1.3 Overview of 3GPP LTE standard

The first release of LTE, referred to as LTE Release-8, has been published in 2009 by 3GPP for 4G cellular networks [32, 33]. LTE is fully designed on packet-based radio access structure; thus, LTE only supports radio access technologies that provide Internet protocol (IP)-based functionalities. Compared to 3G standards such as 3GPP's High Speed Packet Access (HSPA), LTE allows for higher peak data rates by scaling the spectrum up to 20 MHz and utilizing higher number of MIMO antennas. LTE Release-8 supports up to 300 Mb/s and 75

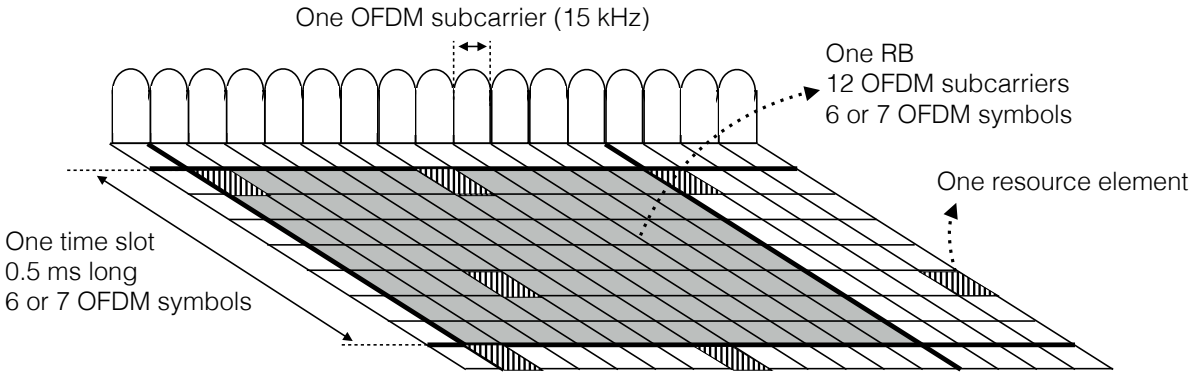

Figure 1.4: RB-based structure of resources in LTE

Mb/s of data rate in downlink and uplink, respectively. In LTE Release-8, up to 4 transmit and receive antennas are anticipated. The downlink of LTE is based on OFDM [5] technology, and the uplink is based on single carrier-frequency division multiplexing (SC-FDM) [34]. OFDM is one of the most attractive techniques to combat frequency selectivity in wide band channels. In OFDM, the wide band channel is divided into several narrow band flat faded subchannels. OFDMA [35] is the multiple access variant of OFDM in which simultaneous streams are possible by allocating each user a disjoint subset of available OFDM subchannels [3]. The multiple access variant of SC-FDM is referred to as single carrier-frequency division multiple access (SC-FDMA) [34]. SC-FDMA has a similar structure and complexity to those of OFDMA. However, SC-FDMA results in low peak to average power ratio which is suitable for mobile devices on which installing complex and high performance power amplifier is not feasible. Performance comparison of OFDMA and SC-FDMA can be found in [36] and [37].

The macro BSs in LTE are referred to as evolved node B (eNB), while pico and femto BSs are referred to as home eNB (HeNB). Relay stations are denoted by relay node (RN), and the BS that serves the RN is denoted as the donor eNB (DeNB). Finally, the mobile user is denoted by user equipment (UE). Furthermore, eNBs can directly talk and coordinate with each other through an interface denoted by X2 interface [38, 39]. In previous standards developed by 3GPP, a dedicated unit referred to as radio network controller (RNC) used to perform the functionalities regarding coordination among BSs. In LTE, the RNC is removed and its functionalities are transferred to eNBs which use X2 interface to exchange information regarding load balancing and ICIC.

As mentioned before, in LTE, OFDMA technology is used in downlink, and a variation of OFDMA called SC-FDMA is used in uplink. The channel bandwidth is divided into 15

[3]In this thesis, OFDM subchannel and OFDM subcarrier are used interchangeably.

kHz OFDM subcarriers in both downlink and uplink. The number of subcarriers available at each BS depends on the channel bandwidth that the BS has access to. In LTE, the channel bandwidth is intended to be scalable, and can be for example 1.4, 3, 5, 10, 15, or 20 MHz. The more the channel bandwidth, the higher number of OFDM subcarriers are available at the BS. The smallest resource structure over which a modulation occurs is called a resource element. A resource element spans over one OFDM subcarrier on the frequency axis, and one OFDM symbol duration on the time axis. The aggregation of 12 adjacent OFDM subcarriers and 6 or 7 OFDM symbols is referred to as an RB. Each RB spans over 180 kHz on the frequency axis and 0.5 ms on the time axis. An RB is the smallest resource structure that is given to a user for possible transmission [40]. The number of RBs allocated to each user depends on the QoS that the user requires. For instance, if a user requires a high data rate, the number of RBs allocated to that user is higher than a user requiring less data rate. The RB-based structure of the resources in LTE is illustrated in Fig. 1.4.

In the downlink of LTE, each antenna port of each eNB constantly transmits a cell specific reference (CSR) signal [41]. CSR signal is used by UEs for various purposes including cell search and initial cell association, and downlink channel estimation for demodulation and detection. The CRS symbols are spread over resource elements in a way that robust estimation of time and frequency is possible at the UE.

Last but not least, 3GPP released LTE Release-10 in 2011. LTE Release-10 along with later releases of LTE are also known as LTE-Advanced [33]. The last finalized release of LTE-Advanced is LTE Release-11 which was closed in 2013. 3GPP is now working on LTE Release-12. The peak data rate requirements in LTE-Advanced are 1 Gb/s and 500 Mb/s in downlink and uplink, respectively. Among the key features that are different in LTE-Advanced compared to the original LTE are supporting higher order of MIMO antennas (up to 8 antennas for downlink and 4 antennas for uplink), introducing carrier aggregation [42], introducing coordinated multi-point reception and transmission (CoMP) [43], enhancing the ICIC for deployment of co-channel HetNets, and focusing on RN features [40]. Overall, these advancements in LTE-Advanced result in a better user experience.

1.4 Scope, motivations, and objectives

This section is divided into two subsections. In the following subsection, the scope, motivations, and objectives behind the research contributions of this thesis in the context of HetNets are provided. Subsection 1.4.2 is dedicated to the scope, motivations, and objectives behind the research contributions of this thesis in the context of relay-based communication.

1.4.1 Scope, motivations, and objectives in HetNets

HetNets are built upon conventional cellular networks; thus, the research problems in conventional cellular networks such as cell association, ICIC, and resource allocation [15] need to be re-addressed in the context of HetNets. Cell association problem, which is to be addressed in this thesis, is involved with defining a set of rules to determine which BS serves a particular user. Most of the cell association schemes are designed based on the downlink maximum SINR scheme [44]. In maximum SINR scheme, users estimate the downlink SINR from the BSs in their range by listening to the BSs' reference signals and associate themselves with the best SINR providing BS. This scheme is not suitable for HetNets mainly because of two reasons. The first reason is that macro BSs in HetNets have higher transmitting powers and attract more users which leads to imbalance of load among the BSs. The resource budget of overpopulated BSs is distributed among more users which translates into lower throughput for those users. Therefore, load balancing should be achieved in the cell association phase in the context of HetNets. The second reason that renders maximum SINR cell association scheme unsuited for HetNets rises from the fact that there is an intrinsic asymmetry among uplink and downlink SINR levels in HetNets [44]. The sources of interference in the downlink are BSs with considerably high powers, while the sources of interference in the uplink are the mobile nodes with low levels of power and different geographical distribution. Therefore, an association rule designed for downlink is not necessarily suitable for the uplink, and vice versa.

From another perspective, wireless operators are interested in distributed cell association schemes where nodes decide based on their local measurements of the network, as opposed to centralized schemes where one central node decides for all the other nodes. The required message passing load in centralized algorithms renders them unappealing for practical implementation. The technical simplicity of distributed algorithms motivates us to address distributed cell association schemes in this thesis.

In cellular networks such as LTE, the BSs are constantly transmitting reference signals that enable the mobile users to measure some attributes of the downlink channel [41]. However, mobile users cannot measure the attributes of the uplink channel without communicating to the BS. Therefore, designing distributed cell association schemes is easier in downlink, while it is a major challenge in uplink. It should also be mentioned that cell association problem in downlink, although well-studied for conventional cellular networks, has not been thoroughly addressed in the context of HetNets. These factors motivate us to address distributed cell association schemes that can be whether downlink oriented, uplink oriented, or jointly downlink and uplink aware.

In newly emerged standards such as LTE-Advanced, the resources available in the downlink and uplink are broken into smaller building blocks referred to as RBs. An RB occupies a certain frequency range during a certain time interval. In LTE for instance, one RB spans over 12 OFDM subcarriers and 6 or 7 OFDM symbols, i.e., 180 kHz of bandwidth and 0.5 ms of time duration [33]. The number of available RBs at each BS in the downlink and uplink is proportional to the available bandwidth and scheduling interval at that BS. The number of RBs allocated to each user on the other hand, depends on the QoS that the user requires. For instance, if the QoS is defined in terms of the data rate that a user requires, more RBs are assigned to a user with higher rate requirement. Distributing the resources in terms of RBs among users introduces additional degrees of freedom in designing resource allocation schemes that results in higher spectral efficiency [19]. This motivates us to incorporate an RB-based model for the resources in this thesis in the context of cell association in HetNets.

Cell association problem in HetNets has drawn plenty of attention recently. The cell association problem has mostly been addressed in downlink [45–57], while the uplink, and the joint downlink and uplink cell association [58] have been barely touched.

Formulating the cell association problem naturally falls into the scope of integer or mixed integer programming since each user is to be mapped to a BS. There are several approaches to cope with these integer programs to achieve load balancing in the cell association phase. Solving the integer program directly by exploiting the structure of the problem [45, 46], relaxing the association constraints and using Lagrange dual decomposition method [47–49], Markov decision process frameworks [50, 51], game theoretic frameworks [52, 53], and stochastic geometry frameworks [54–57] are examples of these approaches among others. In the next two paragraphs, we focus on the first two approaches as they are more relevant to the works presented in this thesis.

Authors of [45] focus on flow level downlink cell load balancing and association under spatially inhomogeneous traffic distributions. A unified distributed and iterative algorithm is proposed that adapts to traffic loads and converges to the optimal point. The objective function of the defined optimization problem in [45] can be selected from a family of objective functions; each of which directs the solution towards a rate, throughput, delay, or load balanced optimal point. In [46], an online algorithm is developed based on the idea of associating users with BSs that provide the best expected throughput instead of associating users with the best SINR providing BS. Considerable interference avoidance and load balancing gains are achieved through the online algorithm proposed in [46]. In these two works, the association constraints are not relaxed and the proposed algorithms produce binary decision variables.

In many cases, formulating the cell association problem leads to NP-hard assignment

problems. Relaxing the association constraints and applying Lagrange dual decomposition method is a popular method to cope with these cases. This is because relaxing the association constraints usually converts the optimization problem into a convex or linear program for which efficient algorithms exist. Additionally, dual decomposition methods usually lead to distributed algorithms in which the nodes in the network decide based on their local information, as opposed to centralized solutions which require global information access at one central node or all the nodes. Examples of distributed cell association algorithms for downlink can be found in [47, 48]. In these works, the resources at each BS is distributed evenly among the users associated with that BS. In [47], it is proven that distributing the resources equally among the users connected to a given BS is optimal for a logarithmic objective function. Based on this observation, a distributed algorithm is proposed that converges to a near optimal point to improve the long term rate. The framework provided in [47] is suitable for environments that undergo slow fading (low mobility environments). Cell range expansion technique by biasing the SINR of lightly loaded BSs to make them more attractive to the users is also incorporated in the distributed algorithm in [47]. Extending over [47], in [48], the joint optimization of load balancing and enhanced intercell interference coordination (referred to as eICIC by 3GPP) via ABS is considered. Lastly, [49] is another work in which a dynamic cell association and cell range expansion algorithm for load balancing through relaxation of association constraints is proposed. The algorithm presented in [49] is in a centralized fashion.

Authors of [51] adopt an approach based on Markov decision process to tackle the cell association problem, and game theoretic approaches are considered in [52, 53]. Recently, stochastic geometry has been introduced as a mean to analyze the downlink SINR distribution and devise cell association algorithms. It is assumed in such works that the low tier BSs are distributed according to a point Poisson process, then the probability distribution of downlink SINR is calculated over space. Examples of this approach can be found in [54–57]. Finally, a centralized algorithm has been proposed in [58] to jointly maximize the downlink system capacity while minimizing the users' uplink transmitting powers.

At least one of the following shortcomings has been identified in the research works mentioned in this subsection:

- In most of the related works, providing QoS is not considered, and further it is assumed in the system models that the BSs are distributing all the resources among the users. In the case of having QoS constraints, once the users receive enough resources to satisfy their QoS constraints, the need for expending more resources is eliminated. In addition, allowing the users to use more resources than their QoS requirements translates into

spending unnecessary power whether by the BS in downlink or user in the uplink. Spending power for extra resources reduces the energy efficiency. Energy efficiency is in particular important at the mobile user side, considering their limited battery life.

- All the cell association works mentioned above, including the maximum SINR scheme, are downlink oriented. The only work in which one parameter of uplink is also considered is [58]. The considered parameter is uplink transmit power. The uplink load or interference on the BS is not considered in [58]. As it has been mentioned earlier, a cell association algorithm specifically designed for downlink does not show an acceptable performance in the uplink.

- The distributed cell association schemes are not investigated completely in the literature. This is in particular the case for the uplink since users cannot measure the attributes of uplink by listening to the BS reference signals.

- The RB-based structure of the resources is not explicitly considered in the system models.

- In most of the related works, only low mobility environments suffering from slow fading are considered in the system models for designing distributed algorithms. This is the case since most researchers choose to work with data rate, for which only the long term variation is measurable at the users by listening to the reference signals of BSs. Link outage probability which is a venue to deal with fast fading environments has not been incorporated in the context of cell association in HetNets.

The above shortcomings in the literature motivated us to pursue the following objectives in the context of cell association in HetNets:

1. Designing distributed cell association schemes with QoS provisioning in the downlink of a HetNet considering that BSs have finite number of RBs as their resource budget.

2. Designing distributed cell association schemes in the downlink of a HetNet, that are suitable for fast fading environments as well as slow fading environments.

3. Designing distributed cell association schemes with QoS provisioning in a HetNet where BSs have finite number of RBs as their resource budget in downlink and uplink, that are jointly aware of downlink and uplink and yet are not complex and require low amount of message passing.

The contributions in Chapter 2 revolve around the first and second objectives, and the third objective is addressed in Chapter 3. The contributions made regarding these objectives are clarified in the beginning of each chapter.

1.4.2 Scope, motivations, and objectives in relay-based communication

Introducing relays to wireless networks opens many interesting research problems. Among these problems, analyzing the outage behavior of relay-based systems seems to be one of the invariable concerns. Allocating relays to source-destination streams is also among these topics, which can be tackled to satisfy different kinds of objectives such as minimizing the global outage probability of the system. Authors of [27] first characterized the outage behavior of fundamental relaying protocols, namely DF and AF protocols, in high SNR regimes. Closed form solutions to the outage probability have been obtained in [59–61], for AF and DF multi-hop communication systems assuming no direct link between source and destination. In all the aforementioned works, it is assumed that the channel is suffering from Rayleigh flat fading.

Data rate hungry applications have driven the wireless industry into using wider frequency channels which undergo frequency selective fading. OFDM technology is among the best candidates combating frequency selectivity by dividing the wide band channel into narrower flat faded subchannels. In OFDM, the user is free to transmit on all the available subcarriers. Therefore, only one source-destination link can be realized in a specific frequency band and time slot. The multiple access variant of OFDM on the other hand, OFDMA, allows for multiple simultaneous source-destination links to be realized by limiting the users to occupy non-overlapping subsets of available subcarriers. Analyzing the outage event in OFDM and OFDMA relay systems imposes another challenge upon researchers.

In the context of single stream OFDM cooperative communications with single or multiple relays, most researchers assume that the event of outage occurs if one or more OFDM subcarriers are in outage [62–64]. This assumption is the result of considering the case of equal bit allocation (EBA) to all the OFDM subcarriers. However, this case may not capture the general scenario where the nodes are free to allocate arbitrary number of bits to different subcarriers in the modern wireless technologies. For instance, if a subset of subcarriers is enjoying good channel gains, more bits with the same level of power can be assigned to them so that they compensate for other subcarriers which are in deep fade. This motivates us to consider the general case of arbitrary number of bit allocation to OFDM subcarriers in the link outage analysis.

Moreover, most of the analyses evaluating the outage performance rely on the assumption that the subcarrier gains are independent and identically distributed (i.i.d) random variables (RVs) [62–65]. It is well known that OFDM subcarrier gains in frequency domain are correlated. This motivates us to consider the correlation between the OFDM subcarrier gains in the link outage analysis.

The problem of analyzing the outage behavior of OFDM cooperative networks becomes more challenging when simultaneous streams are allowed to coexist. Two scenarios are possible in the case of multi-stream networks. The first case is when multiple users are communicating through a single relay to the destination using OFDMA, and the second case is when multiple relays exist in the network as well as multiple sources. In both of these multi-stream cases, the link outage behavior does not capture the global outage behavior of the network. Therefore, the global outage probability needs to be defined in some sense and evaluated.

Regarding the OFDMA multi-user single-relay case, the simultaneous links are also statistically correlated. This is because all the streams are sharing the channel between the relay and destination. Although these simultaneous streams are realized on disjoint subsets of OFDM subcarriers, the OFDM subcarriers on the common relay-destination channel are correlated with each other. Therefore, on the common relay-destination channel, there is a statistical correlation not only between the subcarriers in each subset, but also among subcarriers in different subsets. This causes the simultaneous links realized on these OFDM subcarriers to be correlated. This also makes the global outage analysis more complex. To the best of our knowledge, this correlation has not been detected and addressed in the literature; thus, there is motivation to consider this correlation in the outage analysis of OFDMA relay-based networks with single relay and multiple users.

In the case of multiple users and multiple relays, assigning relays to individual source-destination pairs becomes crucial, as well. Regarding the multi-stream scenarios, an immense amount of research exists on uplink and downlink of cellular systems in which multiple nodes are communicating with a single BS. For instance, in [66], cellular multi-user cooperative networks under OFDM modulation are addressed, where a circular cell is divided into equal area sectors, and one relay serves all the nodes in a each sector. The outage probability of this system is also analyzed and used as the performance metric. Compared to cellular systems, non-cellular systems, e.g., ad hoc and mesh topologies, in which simultaneous streams can co-exist among multiple sources and destinations are less explored.

The above shortcomings in the literature motivates us to pursue the following objectives in the context of outage analysis and relay allocation in DF OFDM and OFDMA relay-based communication with Rayleigh frequency selective channels:

1. Analyzing the outage behavior of a three-node DF OFDM cooperative model allowing for arbitrary number of bits on OFDM subcarriers and correlated OFDM subcarriers.

2. Defining the global outage probability in the case of multi-stream DF OFDMA relay-based communication.

3. Taking into account the correlation between simultaneous streams in the global outage analysis in the case of multi-stream single-relay DF OFDMA cooperative model.

4. Evaluating the global outage probability and using it as an objective to be optimized through relay allocation to source-destination streams in the case of multi-user multi-relay DF OFDMA cooperative model.

The first objective is tackled in Chapter 4. The second and third objectives are addressed in Chapter 5, and the last objective is the topic of Chapter 6. The contributions made regarding these objectives are clarified in the beginning of each chapter.

1.5 Thesis outline

The rest of this thesis is organized as follows:

- Chapter 2 addresses the cell association problem in the downlink of a multi-tier HetNet in which BSs have finite number of RBs available to distribute among their associated users. Two problems are defined and treated in Chapter 2: Sum utility of long term rate maximization with long term rate QoS constraints, and global outage probability minimization with outage QoS constraints. The first problem is well-suited for low mobility environments, while the second problem provides a framework to deal with environments with fast fading. The defined optimization problems in Chapter 2 are solved in two phases: Cell association phase followed by the optional RB distribution phase. We show that the cell association phase of both problems have the same structure. Based on this similarity, we propose a unified distributed algorithm with low levels of message passing for the cell association phase. This distributed algorithm is derived by relaxing the association constraints and using Lagrange dual decomposition method. In the RB distribution phase, the remaining RBs after the cell association phase are distributed among the users. Simulation results show the superiority of our distributed cell association scheme compared to schemes that are based on maximum SINR.

- Chapter 3 addresses the joint downlink and uplink aware cell association problem in a multi-tier HetNet in which BSs have finite number of RBs to distribute among the users. An optimization problem is defined to maximize the sum of weighted utility of long term data rate in downlink and uplink through cell association and RB distribution, while maintaining QoS. Separate outage QoS constraints are considered for downlink and uplink of a user. Using outage QoS constraints renders the problem suitable for fast fading environments. We propose a distributed scheme for the cell association problem. As users cannot measure the uplink attributes by listening to the reference signals of BSs, a limited amount of feedback is added to the reference signals of BSs to inform the users of the uplink interference and make the distributed algorithm design possible. Moreover, by assigning different weights to the downlink and uplink data rates, the proposed scheme can be only downlink oriented, only uplink oriented, or both downlink and uplink aware. Comparing the proposed scheme with the downlink oriented SINR scheme, significant uplink rate gains are observed. This is while the gains in downlink rates are also considerable. In the end, the remaining RBs after the cell association phase are distributed among users separately in downlink and uplink to further improve the rate.

  It also should be mentioned that Chapter 3 is an extension to Chapter 2, in which uplink is considered as well as downlink. Therefore, the downlink cell association problems defined in Chapter 2 can be developed by shutting down the uplink in Chapter 3 and applying necessary modifications in the objective functions and the QoS constraints. However, since Chapter 2 is dedicated to cell association in downlink, more in depth remarks and simulations on the behavior of the downlink problems are provided. On the other hand, the remarks and simulation results in Chapter 3 are towards the relationship between downlink and uplink.

- In Chapter 4, we investigate a DF two-hop relaying system consisting of one source, one relay and one destination, in which OFDM is used. We present an outage probability analysis based on approximating the probability distribution function of the total capacity by a Gaussian distribution. Tight approximations on the outage probability assuming correlated OFDM subchannels and arbitrary number of bits on OFDM subcarriers are found. As a special case, i.i.d. OFDM subchannels are also addressed, where a closed form solution to the variance of the total capacity is obtained, leading us to even tighter approximations on the outage probability.

- In Chapter 5, we study a multi-user single-relay DF OFDMA system, where the channel

model is Rayleigh frequency selective. We provide analytical approximations for the global outage probability in the sense that the outage event occurs when at least one link goes into outage. The main contribution of Chapter 5 is the consideration of the statistical correlation between the link capacities which is created by the relay-destination channel that is common to all the links. The analysis is carried out by fitting the multi-variate normal distribution to the joint probability distribution function of the link capacities.

- In Chapter 6, we study a clustered two-hop DF network consisting of a set of source-destination pairs, and a cluster of relays. We consider the case in which channels are Rayleigh frequency selective, OFDMA is employed, and there is no line of sight (LOS) between source and destination clusters. Approximating the capacity of a single source-relay-destination link by a Gaussian RV, the global outage probability of this network is characterized allowing for correlated OFDM subcarrier gains and arbitrary number of bits on each subcarrier. The obtained global probability of outage is used as an objective function to formulate an optimization problem to allocate relays to source-destination pairs. The outage probability minimization problem through relay allocation then is converted to a standard assignment problem for which a low complexity algorithm based on Hungarian method is proposed. The numerical results show the precision and effectiveness of our analysis and proposed relay allocation technique.

- Conclusions and possible future research directions are discussed in Chapter 7.

Chapter 2

Unified and Distributed QoS-Driven Cell Association Algorithms in HetNets

The accomplished works and research contributions in this chapter are briefly described in the following.

This chapter addresses the cell association problem in the downlink of a multi-tier HetNet. It is assumed that BSs have finite number of RBs available to distribute among their associated users. We investigate distributed algorithms where users and BSs decide based on their local measurements of the wireless environment. We also focus on providing QoS in terms of minimum achievable long term rate or maximum outage probability.

Two problems are defined and treated in this chapter: Sum utility of long term rate maximization with long term rate QoS constraints, and global outage probability minimization with outage QoS constraints. The first problem is well-suited for low mobility environments, and the second problem provides a framework to deal with environments with fast fading. In defining the optimization problems in this chapter, we consider a general scenario where unity frequency reuse factor and no interference coordination schemes are assumed. Both problems are to be optimized through cell and RB association.

The defined optimization problems in this chapter are solved in two phases: Cell association phase followed by the optional RB distribution phase. We show that the cell association phase for both problems have the same structure. Based on this similar structure, we design and propose a unified distributed algorithm with low levels of message passing and complexity for the cell association phase. The distributed cell association algorithm is derived by relaxing the association constraints and using Lagrange dual decomposition method. Our distributed cell association algorithm is QoS-driven since users receive only enough number of RBs to satisfy their QoS constraints while maximizing the sum utility of rate or minimizing the global outage probability. Extensive simulation results that are brought in this chapter show that our distributed cell association scheme outperforms the maximum SINR scheme. For instance, rate gains of up to 2.4x have been observed in the simulations for the

cell edge users in our distributed cell association algorithm over maximum SINR scheme.

In the RB distribution phase, the remaining RBs after the cell association phase are distributed among the users for further improvement of the network performance. However, the RB distribution phase is kept optional since once the users can satisfy their QoS requirements, expending more resources seems unnecessary. In addition, giving users resources beyond their QoS requirements calls for spending more power which is not appealing from energy saving perspectives. We show that the RB distribution phase for the rate problem is a convex program. In fact, RB distribution to maximize the rate has a similar structure to that of the well-known water-filling problem. Therefore, the closed form solution of this problem is obtained by writing the Karush-Kuhn-Tucker (KKT) conditions. However, distributing the remaining RBs for the outage problem is a complex non-convex non-linear problem. Therefore, we propose a sub-optimal greedy algorithm to allocate the remaining RBs to minimize the global outage probability.

Before proceeding further into this chapter, it should be pointed out that in the next chapter, a more general case of downlink and uplink cell association in HetNets is considered. Therefore, defined problems in this chapter can be considered as special case of the general problem in Chapter 3 with different objective functions and QoS constraints. Nevertheless, as this chapter is dedicated to downlink, the remarks and simulation results go in depth regarding the behavior of HetNets in downlink, while in Chapter 3, the remarks and simulation results are more towards realizing the differences in downlink and uplink.

The rest of the chapter is organized as follows: In the next section, the chosen system model is described. The cell association problem with QoS constraints is formulated in Section 2.2. Our distributed solution to the cell association problem is presented in Section 2.3. Section 2.4 will address distributing the remaining RBs after the cell association phase. In Section 2.5, we examine the performance of our proposed algorithms through numerical simulations.

2.1 System model

The focus of this chapter is on a downlink HetNet consisting of multiple tiers of BSs, where different tiers represent different types of BSs. As an example, tier 1 BSs can be macro BSs with high transmit power and large coverage areas. Tier 2 BSs (pico BSs) are regarded as smaller BSs with lower powers compared to tier 1 BSs, but with higher deployment density. Finally, tier 3 BSs (femto BSs) model indoor APs with very small transmit powers.

The set of all BSs is denoted by $\mathcal{B} = \{1, \ldots, N_{\mathcal{B}}\}$, and the set of all users is denoted by

Table 2.1: List of key parameters in Chapter 2

$\mathcal{U}$	Set of users
$\mathcal{B}$	Set of BSs
i	User $i \in \mathcal{U}$
j	BS $j \in \mathcal{B}$
N_j	Resource budget of BS j
n_{ij}	# of RBs given to user i by BS j
P_j	Transmitting power of BS j
$H_{ij} = G_{ij}F_{ij}$	Channel power gain between user i and BS j
G_{ij}	Large scale component of H_{ij}
F_{ij}	Small scale component of H_{ij}
$\lambda_{ij} = \frac{1}{G_{ij}}$	Exponential parameter of H_{ij}
SINR_{ij}	Instantaneous SINR at user i from BS j
$\overline{\mathrm{SINR}}_{ij}$	Long term SINR at user i from BS j
c_{ij}	Instantaneous RB capacity at user i from BS j
$\bar{c}_{ij}$	Long term RB capacity at user i from BS j
r_{ij}	Instantaneous rate at user i from BS j
$\bar{r}_{ij}$	Long term rate at user i from BS j
P_{ij}^{out}	Probability of outage when user i is served by BS j
γ_i	Rate requirement of user i
T_i	Outage probability requirement of user i
$\bar{n}_{ij}^R$	Minimum # of required RBs of user i from BS j for rate QoS constraint
$\bar{n}_{ij}^O$	Minimum # of required RBs of user i from BS j for outage QoS constraint

$\mathcal{U} = \{1, \ldots, N_{\mathcal{U}}\}$. The cardinality of $\mathcal{B}$ is $N_{\mathcal{B}}$, and the cardinality of $\mathcal{U}$ is $N_{\mathcal{U}}$. Each BS $j \in \mathcal{B}$ has a fixed power of P_j W available. All the BSs are assumed to be connected by a high speed backhaul through which information exchange with negligible delay is possible. In order to follow RB-based structure of resources in recent standard such as LTE and LTE-Advanced, we asssume that each BS $j \in \mathcal{B}$ has access to N_j RBs to distribute among its associated users. The resource budget of BS j in terms of N_j depends on the available bandwidth and scheduling interval at BS j.

2.1.1 The channel model, instantaneous rate, long term rate and outage probability

We denote the positive channel power gain between user i and BSs j by H_{ij}, i.e., the received power at user i from BS j is $H_{ij}P_j$. Furthermore, H_{ij} embodies the effects of path loss, log normal shadowing and antenna gains as large scale fading component (denoted by G_{ij}), and multi-path Rayleigh fading as small scale fading component (denoted by F_{ij}). By adopting these notations we have

$$H_{ij} = G_{ij}F_{ij}, \quad \forall (i,j) \in \mathcal{U} \times \mathcal{B}, \tag{2.1}$$

where $(\cdot) \times (\cdot)$ denotes the Cartesian product. The large scale fading component G_{ij} is assumed to be constant during one association period, while the small scale fading component F_{ij} fluctuates fast enough so that a mobile user can average it out in its channel measurements. F_{ij}s are modelled by statistically independent exponentially distributed RVs with unit variance. They are exponentially distributed since in Rayleigh fading, the envelope of the signal is assumed to follow a Rayleigh distribution, and in turn the channel power is exponentially distributed [67]. F_{ij}s are statistically independent random variables since they model geographically separated wireless channels which show independent multi-path fading behaviours. Based on these assumptions, H_{ij}s are statistically independent exponentially distributed random variables with parameter λ_{ij}, where

$$\lambda_{ij} = \frac{1}{\mathrm{E}[H_{ij}]} = \frac{1}{G_{ij}}, \tag{2.2}$$

where $\mathrm{E}[\cdot]$ denotes the expected value. As it is mentioned before, user i can measure G_{ij} (and equivalently λ_{ij}) for all the BSs $j \in \mathcal{B}$.

In such a setting, the instantaneous SINR seen by user $i \in \mathcal{U}$ from BS $j \in \mathcal{B}$ is

$$\mathrm{SINR}_{ij} = \frac{P_j H_{ij}}{\sum_{k \in \mathcal{B} \setminus \{j\}} P_k H_{ik} + \Delta f N_0}, \tag{2.3}$$

and the long term SINR that is measured by user $i \in \mathcal{U}$ from BS $j \in \mathcal{B}$ [45, 47, 48] is

$$\overline{\mathrm{SINR}}_{ij} = \frac{P_j G_{ij}}{\sum_{k \in \mathcal{B} \setminus \{j\}} P_k G_{ik} + \Delta f N_0}. \tag{2.4}$$

In equations (2.3) and (2.4), the constant Δf denotes the bandwidth over which an RB is realized, N_0 denotes the thermal noise spectral power, and $\mathcal{B} \setminus \{j\}$ is the set of all BSs except BS j.

Accordingly, the instantaneous and long term spectral efficiency at user i, if it is served by BS j, denoted by c_{ij} and $\bar{c}_{ij}$, respectively, can be written as

$$c_{ij} = \log_2(1 + \mathrm{SINR}_{ij}), \tag{2.5}$$

$$\bar{c}_{ij} = \log_2(1 + \overline{\mathrm{SINR}}_{ij}). \tag{2.6}$$

Without loss of generality, c_{ij} and $\bar{c}_{ij}$ can be regarded as achievable rate and long term achievable rate on an RB. For example, if c_{ij} is multiplied by the RB bandwidth and time duration and divided by the scheduling interval, it will be the achievable rate on one RB.

Given that n_{ij} RBs are given to user i by BS j, the instantaneous and long term data rates seen by user i are

$$r_{ij} = n_{ij} c_{ij}, \tag{2.7}$$

$$\bar{r}_{ij} = n_{ij} \bar{c}_{ij}. \tag{2.8}$$

The above equations are valid if we assume flat fading on the bandwidth of BSs from users' point of view. The flat fading assumption is made to preserve simplicity in the system model. The study of the frequency selective scenario in which users see different channel gains on different RBs (and in turn, different SINR levels and capacities on different RBs) is left for future work.

We define the outage event of a single user i served by BS j to be the event where the instantaneous rate seen by user i drops below a certain threshold γ_i. We denote the

probability of this event by P_{ij}^{out} and formally define it as

$$P_{ij}^{\text{out}} = \Pr\{r_{ij} < \gamma_i\} = \Pr\left\{ n_{ij} \log_2 \left(1 + \frac{P_j H_{ij}}{\sum_{k \in \mathcal{B} \setminus \{j\}} P_k H_{ik} + \Delta f N_0}\right) \leq \gamma_i \right\}, \tag{2.9}$$

where $\Pr\{\cdot\}$ denotes the probability of the input argument. This probability of outage is derived in [68, 69] (an easy to read proof is available in [68]), which is

$$P_{ij}^{\text{out}} = 1 - \left(e^{\frac{-\lambda_{ij}\Delta f N_0}{P_j}\Gamma_{ij}}\right) \prod_{k \in \mathcal{B} \setminus \{j\}} \left(\frac{\frac{\lambda_{ik}}{P_k}}{\frac{\lambda_{ij}}{P_j}\Gamma_{ij} + \frac{\lambda_{ik}}{P_k}}\right), \tag{2.10}$$

where

$$\Gamma_{ij} = 2^{\frac{\gamma_i}{n_{ij}}} - 1. \tag{2.11}$$

Note that P_{ij}^{out} is measurable by user i since users can measure λ_{ij} for all the BSs $j \in \mathcal{B}$. Moreover, It can easily be verified that P_{ij}^{out} is a strictly decreasing function of n_{ij}, i.e., more RBs improves the outage behaviour.

2.1.2 Rate and outage QoS constraints

In this chapter, we define two QoS constraints, namely, long term rate QoS and outage QoS constraints. We refer to the long term QoS constraint simply as rate QoS constraint hereafter. In the case of rate QoS constraint, each user intends to keep its *long term rate* above its requested rate threshold. In the beginning phase of cell association, each user i requests a certain rate QoS class in terms of minimum required long term rate γ_i. Therefore, if user i is associated with BS j, it is the duty of the BS to satisfy the following rate QoS constraint

$$\bar{r}_{ij} \geq \gamma_i. \tag{2.12}$$

By substituting (2.8) in the above equation, we have

$$n_{ij} \geq \frac{\gamma_i}{\bar{c}_{ij}}. \tag{2.13}$$

We indicate the smallest integer greater than the right hand side of the above equation by $\bar{n}_{ij}^{R}$ as follows

$$\bar{n}_{ij}^{R} = \lceil \frac{\gamma_i}{\bar{c}_{ij}} \rceil, \tag{2.14}$$

where $\lceil \cdot \rceil$ represents the ceiling function. Inequalities (2.12) and (2.13) and equality (2.14) indicate that if user i requires rate QoS class of minimum rate γ_i, BS j will be obliged to allocate at least $\bar{n}_{ij}^{R}$ RBs to that user, i.e.,

$$n_{ij} \geq \bar{n}_{ij}^{R}. \tag{2.15}$$

In the case of outage QoS constraint, each user intends to keep its *instantaneous rate* above its requested rate threshold with a certain probability. In the beginning of cell association phase, each user requests a certain outage QoS class. An outage QoS class is defined in terms of user's rate threshold γ_i, and probability of user's rate dropping below that threshold T_i. Therefore, if user i is associated with BS j, it is the duty of BS j to satisfy the following constraint for that user

$$P_{ij}^{\text{out}} = \Pr\{r_{ij} \leq \gamma_i\} \leq T_i. \tag{2.16}$$

The probability of outage is given in (2.10) as a function of n_{ij}. Since this probability is a strictly decreasing function of n_{ij}, a lower bound on n_{ij} exists above which the outage QoS constraint is satisfied. Since n_{ij}s can take only positive integer values, this lower bound can easily be found numerically by setting $n_{ij} = 1$ in (2.10) and incrementing it until the constraint is satisfied. We indicate the smallest integer for which (2.16) is satisfied by $\bar{n}_{ij}^{O}$. Therefore, if user i requires outage QoS class of rate threshold γ_i and probability of outage T_i, BS j will be obliged to allocate at least $\bar{n}_{ij}^{O}$ RBs to that user, i.e.,

$$n_{ij} \geq \bar{n}_{ij}^{O}. \tag{2.17}$$

The key parameters that are used in this chapter are listed in Table 2.1.

2.2 Problem formulation

Two optimization problems are considered in this chapter: Sum utility of long term rate maximization with rate QoS constraints (referred to as **P1**), and global outage probability minimization with outage QoS constraints (referred to as **P2**), both through cell association

and RB allocation. We formulate these two problems in the rest of this section. Before proceeding further, we define binary association indices $x_{ij} \in \{0,1\},\ \forall (i,j) \in \mathcal{U} \times \mathcal{B}$, where $x_{ij} = 1$ indicates that user i is associated with BS j, and $x_{ij} = 0$ indicates the opposite.

2.2.1 Sum utility of long term rate maximization with rate QoS constraints

In this problem, the objective is to maximize a function of long term rate while satisfying the rate QoS constraints. Since we are working with the notion of long term rate, this framework is well-suited for environments with users with low mobility so that the channels remain unchanged in one resource allocation period. We select the sum utility of users' long term rate to be our objective function. Utility of rate can be regarded as a measure of user's satisfaction with the rate it gets. A utility function, in general, is a strictly increasing and concave function. For instance, logarithm function is a suitable candidate. However, in order to preserve generality, the notion of $U(\cdot)$ is used as a general strictly increasing and concave utility function. The sum utility of long term rate maximization problem with rate QoS provisioning (**P1**) is

$$\mathbf{P1}: \underset{\mathbf{x},\mathbf{n}}{\text{maximize}} \quad \sum_{i\in\mathcal{U}} \sum_{i\in\mathcal{B}} x_{ij} U(\bar{r}_{ij}) \tag{2.18}$$

$$\text{subject to} \quad (\text{RC}): \sum_{i\in\mathcal{U}} x_{ij} n_{ij} \leq N_j,\ \forall j \in \mathcal{B}$$

$$(\text{AC}): \sum_{j\in\mathcal{B}} x_{ij} \leq 1,\ \forall i \in \mathcal{U}$$

$$\sum_{j\in\mathcal{B}} x_{ij} \bar{r}_{ij} \geq \gamma_i,\ \forall i \in \mathcal{U} \tag{2.19}$$

$$x_{ij} \in \{0,1\},\ \forall (i,j) \in \mathcal{U} \times \mathcal{B} \tag{2.20}$$

$$n_{ij} \in \{0,1,\ldots,N_j\},\ \forall (i,j) \in \mathcal{U} \times \mathcal{B}. \tag{2.21}$$

In the above optimization problem, $\mathbf{x}$ and $\mathbf{n}$ are matrices containing x_{ij} and n_{ij} elements. Furthermore, the first constraint is referred to as the resource constraint (RC). This constraint ensures that the number of RBs given to the associated users does not exceed the resource budget of that BS. The second constraint is referred to as association constraint (AC). This constraint guarantees that each user is connected to at most one BS. The third constraint (2.19) is the rate QoS constraint which is derived based on inequality (2.12). In the end, constraints (2.20) and (2.21) indicate that the association indices are binary variables, and n_{ij}s can take integer values between zero and the maximum number of RBs at

BS j.

2.2.2 Global outage probability minimization with outage QoS constraints

The motivation behind formulating this problem is to take into account the stochastic behaviour of wireless channels without adding signalling overhead to the system. Guaranteeing a constant instantaneous rate to users in wireless environments that suffer from fast fading is not achievable. However, it is possible to guarantee a certain rate with a certain probability, which suggests formulating the problem in the context of outage probability. In the context of outage probability, the eventual goal is to associate the users with BSs and RBs such that the global outage probability is minimized. In order to achieve this goal, the first step is to define the global outage probability in some sense and evaluate it as a function of system model parameters. We define the global outage event as the event where one or more users experience outage, i.e., if at least one user experiences an instantaneous data rate below its requested threshold, a global outage will be declared. The outage probability of a single link is given in (2.10). Considering that the outage events for different users are statistically independent, it can be argued that the probability of no users experiencing outage is $\prod_{i\in\mathcal{U}}\prod_{j\in\mathcal{B}}\left(1-P_{ij}^{\text{out}}\right)^{x_{ij}}$. Therefore, the global outage probability indicated by $\widehat{P_{\text{out}}}$ is

$$\widehat{P_{\text{out}}} = 1 - \prod_{i\in\mathcal{U}}\prod_{j\in\mathcal{B}}\left(1-P_{ij}^{\text{out}}\right)^{x_{ij}}. \tag{2.22}$$

Now, we define the global outage probability minimization problem with outage QoS provisioning (**P2**) as

$$\mathbf{P2}: \underset{\mathbf{x},\mathbf{n}}{\text{minimize}} \;\; 1 - \prod_{i\in\mathcal{U}}\prod_{j\in\mathcal{B}}\left(1-P_{ij}^{\text{out}}\right)^{x_{ij}} \tag{2.23}$$

$$\text{subject to} \;\; \text{(RC), (AC), (2.20), (2.21)},$$

$$\prod_{j\in\mathcal{B}}\Pr\{n_{ij}c_{ij}\leq\gamma_i\}^{x_{ij}} \leq T_i, \;\forall i\in\mathcal{U}. \tag{2.24}$$

Comparing the constraints in **P2** and **P1**, the only different constraint is the QoS constraint; in **P2** the outage QoS constraint has replaced the rate QoS constraint in **P1** for each user. Constraint (2.24) is derived based on inequality (2.16).

2.3 Cell association phase

Optimization problems **P1** and **P2** are combinatorial problems in $\mathbf{x}$ and $\mathbf{n}$ which are involved to solve. In order to make the problem tractable, we solve them in two steps. First, we fix n_{ij}s and find association indices x_{ij}s. This step is equivalent to solving the association problem. In the next step, given the association indices, we solve the optimization problem with respect to n_{ij}s. In this section, we address the association problem, while optimizing with respect to n_{ij}s is addressed in the next section. It should be noted that n_{ij}s can not be fixed at arbitrary values since the QoS constraints need to be satisfied in the cell association phase. Therefore, we replace the rate QoS constraints in **P1** by $n_{ij} = \bar{n}_{ij}^R$, and outage QoS constraints in **P2** by $n_{ij} = \bar{n}_{ij}^O$, for all $(i,j) \in \mathcal{U} \times \mathcal{B}$. According to inequalities (2.15) and (2.17), $\bar{n}_{ij}^R$ and $\bar{n}_{ij}^O$ are the minimum number of RBs required by user i from BS j to satisfy the rate QoS and outage QoS constraints, respectively.

From another perspective, if we replace n_{ij}s by constant 1 in (RC), it can be shown that both problems become a two dimensional assignment problem with respect to x_{ij}s, and algorithms such as Hungarian method solves them efficiently [70] in a centralized fashion. However, optimizing over x_{ij}s is an NP-hard problem because of the (RC) constraint [71]. In order to change the combinatorial nature of the problem into a continuous one, and hopefully a convex program, we relax the constraints (2.20) in both optimization problems, i.e., we replace constraints (2.20) by $0 \leq x_{ij} \leq 1$ for all $(i,j) \in \mathcal{U} \times \mathcal{B}$.

Next, we show that by fixing n_{ij}s, problems **P1** and **P2** become equivalent optimization problems. After the aforementioned modifications, problem **P1** transforms into problem $\mathbf{P1_x}$ as follows

$$\begin{aligned}
\mathbf{P1_x}: \ \underset{\mathbf{x}}{\text{maximize}} \quad & \sum_{i\in\mathcal{U}}\sum_{j\in\mathcal{B}} x_{ij} a_{ij}^R && (2.25)\\
\text{subject to} \quad & \text{(RC), (AC)},\\
& n_{ij} = \bar{n}_{ij}^R, \ \forall (i,j) \in \mathcal{U} \times \mathcal{B}, && (2.26)\\
& 0 \leq x_{ij} \leq 1, \ \forall (i,j) \in \mathcal{U} \times \mathcal{B}, && (2.27)
\end{aligned}$$

where

$$a_{ij}^R = U(\bar{r}_{ij}) = U(\bar{n}_{ij}^R \bar{c}_{ij}).$$

a_{ij}^R is treated as a constant since $\bar{n}_{ij}^R$ is a constant.

It seems that the objective function in **P2** has a different structure compared to the objective function in **P1**. However, applying the following changes unifies these two objective functions. Inspecting the objective function (2.23), it can be seen that the first term is a con-

stant and can be removed. Moreover, removing the negative sign changes the minimization to a maximization problem. Finally, taking the natural logarithm of the objective function does not change the optimum argument and transforms multiplication to addition. After these modifications, problem **P2** transforms into problem $\mathbf{P2_x}$ as follows

$$\mathbf{P2_x}: \underset{\mathbf{x}}{\text{maximize}} \quad \sum_{i\in\mathcal{U}}\sum_{j\in\mathcal{B}} x_{ij}a_{ij}^{O} \tag{2.28}$$

$$\text{subject to} \quad \text{(RC), (AC)},$$

$$n_{ij} = \bar{n}_{ij}^{O},\ \forall (i,j) \in \mathcal{U}\times\mathcal{B}, \tag{2.29}$$

$$0 \le x_{ij} \le 1,\ \forall (i,j) \in \mathcal{U}\times\mathcal{B}, \tag{2.30}$$

where

$$a_{ij}^{O} = \log\left(1 - P_{ij}^{\text{out}}\right).$$

a_{ij}^{O} is also treated as a constant since P_{ij}^{out} is a function of n_{ij} which is set to $\bar{n}_{ij}^{O}$.

By comparing $\mathbf{P1_x}$ and $\mathbf{P2_x}$, it is trivial that these two optimization problems have the same structure. Therefore, we remove the superscripts R and O from a_{ij}^{R}, a_{ij}^{O}, $\bar{n}_{ij}^{R}$, and $\bar{n}_{ij}^{O}$ and replace them by a_{ij} and $\bar{n}_{ij}$ to have the unified optimization problem $\mathbf{P_x}$ as follows

$$\mathbf{P_x}: \underset{\mathbf{x}}{\text{maximize}} \quad \sum_{i\in\mathcal{U}}\sum_{j\in\mathcal{B}} x_{ij}a_{ij} \tag{2.31}$$

$$\text{subject to} \quad \sum_{i\in\mathcal{U}} x_{ij}\bar{n}_{ij} \le N_j,\ \forall j \in \mathcal{B}, \tag{2.32}$$

$$\sum_{j\in\mathcal{B}} x_{ij} \le 1,\ \forall i \in \mathcal{U}, \tag{2.33}$$

$$0 \le x_{ij} \le 1,\ \forall (i,j) \in \mathcal{U}\times\mathcal{B}. \tag{2.34}$$

The objective function of $\mathbf{P_x}$ is a linear function in x_{ij}s, and all the constraints are linear and affine in x_{ij}s. Therefore, $\mathbf{P_x}$ is a convex optimization problem with respect to x_{ij}s [72].

2.3.1 Cell association solution

In order to devise a distributed solution to $\mathbf{P_x}$, we use a similar approach to the one suggested in [47], that is employing the Lagrange dual decomposition method [73]. Note that the strong duality property holds for $\mathbf{P_x}$, that is the optimum value of $\mathbf{P_x}$ is equal to the optimum value of its Lagrange dual function. According to Slater's theorem, strong duality holds for a convex optimization problem if Slater's condition holds for the constraints of that problem. Moreover, if the problem is convex and all the equality and inequality constraints are linear

and affine, Slater's condition reduces to feasibility condition [72]. As discussed in the previous subsection, $\mathbf{P_x}$ is a convex optimization problem with linear and affine constraints. Therefore, if a set of x_{ij}s exists for which $\mathbf{P_x}$ is feasible, then the strong duality holds. For instance, $x_{ij} = 0$, for all $(i, j) \in \mathcal{U} \times \mathcal{B}$ is always a feasible point in $\mathbf{P_x}$, thus, strong duality always holds for $\mathbf{P_x}$.

We define the Lagrangian of $\mathbf{P_x}$ by taking the resource constraint (2.32) inside the objective function and indicate it by $\mathcal{L}(\mathbf{x}, \mu)$. The Lagrangian of $\mathbf{P_x}$ is

$$\mathcal{L}(\mathbf{x}, \mu) = \sum_{i\in\mathcal{U}} \sum_{j\in\mathcal{B}} x_{ij} a_{ij} - \sum_{j\in\mathcal{B}} \mu_j \big(\sum_{i\in\mathcal{U}} x_{ij} \bar{n}_{ij} - N_j \big), \tag{2.35}$$

where μ_js are Lagrange multipliers associated with resource constraints at BSs. Then, the Lagrange dual function represented by $g(\mu)$ is

$$g(\mu) = \sup_{\mathbf{x}} \quad \sum_{i\in\mathcal{U}} \sum_{j\in\mathcal{B}} x_{ij}(a_{ij} - \mu_j \bar{n}_{ij}) + \sum_{j\in\mathcal{B}} \mu_j N_j \tag{2.36}$$

$$\text{subject to} \;\; 0 \le x_{ij} \le 1, \; \forall (i, j) \in \mathcal{U} \times \mathcal{B}, \tag{2.37}$$

$$\sum_{j\in\mathcal{B}} x_{ij} \le 1, \; \forall i \in \mathcal{U}. \tag{2.38}$$

The strong duality holds, therefore, we can first maximize over $\mathbf{x}$ and then minimize over μ. In order to find $g(\mu)$ for fixed μ_js, we rewrite the Lagrange dual function as

$$g(\mu) = \sum_{i\in\mathcal{U}} g_i(\mu) + \sum_{j\in\mathcal{B}} \mu_j N_j, \tag{2.39}$$

where $g_i(\mu)$ is defined for all $i \in \mathcal{U}$ as

$$g_i(\mu) = \sup_{x_{ij}, j\in\mathcal{B}} \quad \sum_{j\in\mathcal{B}} x_{ij}(a_{ij} - \mu_j \bar{n}_{ij}) \tag{2.40}$$

$$\text{subject to} \;\; 0 \le x_{ij} \le 1, \; j \in \mathcal{B}$$

$$\sum_{j\in\mathcal{B}} x_{ij} \le 1.$$

It can be seen that for fixed μ_js, $g(\mu)$ is separable with respect to users i as in (2.40). Therefore, each user i needs to solve the optimization problem (2.40). For a given user i, the objective function in (2.40) is a weighted average of $(a_{ij} - \mu_j \bar{n}_{ij})$, where the weights are between 0 and 1 and they sum up to unity. Therefore, (2.40)'s unique solution is yielded by keeping the maximum argument of $(a_{ij} - \mu_j \bar{n}_{ij})$ over js and diminishing the contribution of

other elements. We call the term $(a_{ij} - \mu_j \bar{n}_{ij})$ the qualification index of BS j from user's i point of view and indicate it by QI_{ij} as follows

$$\mathrm{QI}_{ij} = a_{ij} - \mu_j \bar{n}_{ij}. \tag{2.41}$$

Accordingly, (2.40)'s unique solution for each user i is

$$x_{ij} = \begin{cases} 1 & \text{if } j = j^* \\ 0 & \text{if } j \neq j^* \end{cases}, \ \forall i \in \mathcal{U}, \tag{2.42}$$

where

$$j^* = \underset{j \in \mathcal{B}}{\operatorname{argmax}}(\mathrm{QI}_{ij}), \ \forall i \in \mathcal{U}. \tag{2.43}$$

After finding x_{ij}s for fixed μ_js, we update the vector μ by using gradient descent method [72]. The partial derivative of the Lagrange dual function with respect to μ_j is

$$\frac{\partial \mathcal{L}(\mathbf{x}, \mu)}{\partial \mu_j} = N_j - \sum_{i \in \mathcal{U}} x_{ij} \bar{n}_{ij}, \ \forall j \in \mathcal{B}. \tag{2.44}$$

Therefore, the updating rule for μ is

$$\mu_j(t+1) = \Big[\mu_j(t) - \beta(t) \big(N_j - \sum_{i \in \mathcal{U}} x_{ij} \bar{n}_{ij} \big) \Big]^+, \forall j \in \mathcal{B}, \tag{2.45}$$

where the operator $[\cdot]^+$ indicates the maximum of the argument of the operator and 0. We applied the operator $[\cdot]^+$ on μ_js because the Lagrange multipliers are non-negative parameters [72]. Furthermore, $\beta(t)$ is some step size that satisfies the following two conditions

$$\lim_{t \to \infty} \beta(t) = 0 \quad , \text{ and } \quad \sum_{t=1}^{\infty} \beta(t) = \infty. \tag{2.46}$$

According to proposition 6.3.4 in [74], if the step size $\beta(t)$ satisfies the above conditions, the convergence of the gradient descent method will be guaranteed assuming that the association indices are continuous variables of the form $0 \leq x_{ij} \leq 1$. These conditions do not guarantee the convergence for the binary association indices. However, we have used $\beta(t) = 0.5/t$ in our simulations, and in all cases the distributed algorithm converged in less than 25 iterations; most of the times the convergence was reached in less than 10 iterations.

We iteratively update the association variables according to (2.42), and the Lagrange multipliers according to (2.45), until the convergence is reached. Note that updating rule for the association variables automatically generates binary values. Consequently, no further approximations is required.

2.3.2 Feasibility problem and admission control

In the cell association procedure described in the previous subsection, the users find their desired BS through (2.43). The users are not aware of how many other users are associating themselves with the desired BS and how much resources that BS has access to. As a result, many users may associate themselves with a BS and exhaust its resources, leading to violating the resource constraint (2.32). This condition not only affects the convergence of the algorithm, but also takes the solution out of the feasible set. As it is described in [72], the Lagrange dual function is an upper bound on the original maximization problem only if we are in the feasible set of the problem defined by the constraints. Beyond the feasible set, not only the Lagrange dual function may not be an upper bound on the original problem, but also iterating with gradient descent method may divert the solution from the desired optimal point. Therefore, once an iteration is out of the feasible set, it needs to be projected back to the feasible set, i.e., gradient projection method [75] should be used.

In the context of cell association in HetNets, we use a heuristic to project the iteration back to the feasible set once one or more BSs receive association requests from too many users. First, we require all the users $i \in \mathcal{U}$ to sort the BSs in their range in descending order based on their qualification index QI_{ij} given in (2.41), and send this sorted list to the BS they want to connect to (BS j^* in (2.43)). Let us say BS j receives too many association requests, i.e., upon acceptance of all those requests the resource constraint at BS j is violated. Then, BS j finds the users who are consuming the highest number of RBs (highest number of $\bar{n}_{ij}$), and removes them until its resource constraint is satisfied. BS j sends those removed users' requests to the second best BSs the users have requested. If the resource constraints are satisfied at all BSs now, the projection is accomplished. Otherwise, this procedure continues until the solution is back to the feasible set. As we have mentioned before, it is assumed that BSs are connected through a high speed back-haul, and the message passing required for projecting the solution back to the feasible set takes place in negligible time period. Moreover, the admission control described here achieves load balancing in the network since it avoids over populating the BSs.

2.3.3 Distributed cell association protocol design

The proposed distributed algorithm of cell association described in previous sections is summarized here:

Step 1: Initialization Each BSs $j \in \mathcal{B}$ initializes its associated Lagrange multiplier μ_j and broadcasts it in the network.

Step 2: User request In this step, all users $i \in \mathcal{U}$ listen to the pilot signals broadcasted by BSs and measure the SINR from each BS and channel gains between themselves and all the BSs. Based on these measurements and the desired QoS, user i calculates the number of RBs it needs from each BS. Then, user i calculates the QI_{ij} in equation (2.41) for all the BSs in its range and sorts the BSs in descending order. A request containing this sorted list along with the required number of RBs from the BSs in the list is sent to the BS with the best QI_{ij}.

Step3: User admission BSs process the requests they have received. If BS j can accommodate all the requests it has received, an admission message is sent to all those that find BS j to be the best candidate. Otherwise, BS j forwards the requests from users consuming the highest amount of resources to the next best BS the users have requested. This procedure continues until the solution is feasible.

Step 4: BS Lagrange multiplier update After all the users are accommodated, BSs update their Lagrange multipliers according to (2.45) and broadcast the new multipliers. The algorithm continues by going back to step 2.

This algorithm solves the cell association problem in a distributed fashion for either of the rate maximization with rate QoS constraints problem, or global outage probability minimization with outage QoS constraints problem ($\mathbf{P1_x}$ or $\mathbf{P2_x}$).

2.4 RB distribution phase

After the cell association phase is completed, some of the BSs may have extra RBs not allocated to any users. In this section, in order to allocate the remaining RBs, given the association indices x_{ij}s, we solve the optimization problems **P1** and **P2** for n_{ij}s. Before addressing either of **P1** and **P2**, we define $\mathcal{U}_j$ as the set of users associated with BS j

$$\mathcal{U}_j = \{i | x_{ij} = 1\}, \forall j \in \mathcal{B}. \tag{2.47}$$

2.4.1 Sum utility of rate maximization

Assuming fixed x_{ij}s, problem **P1** is reduced to the following optimization problem at each BS j

$$\mathbf{P1_{n},}_{j}: \underset{n_{ij}^{'}, i\in\mathcal{U}_j}{\text{maximize}} \quad \sum_{i\in\mathcal{U}_j} U(n_{ij}\bar{c}_{ij}) \tag{2.48}$$

$$\text{subject to} \quad \sum_{i\in\mathcal{U}_j} n_{ij} = N_j, \tag{2.49}$$

$$n_{ij} = \bar{n}_{ij}^{R} + n_{ij}^{'}, \quad \forall i \in \mathcal{U}_j, \tag{2.50}$$

where $\bar{n}_{ij}^{R}$ is the number of already allocated RBs to user i by BS j satisfying the rate QoS constraint of user i, and $n_{ij}^{'}$ is the share of user i from the remaining RBs available at BS j. Moreover, It is implicitly assumed that $n_{ij}^{'}$s are integer values that satisfy $\bar{n}_{ij} \leq n_{ij}^{'} \leq N_j$. If we assume that $n_{ij}^{'}$ are continuous variables, it can be shown that problem $\mathbf{P1_{n},}_{j}$ is a convex optimization problem with strong duality property. In fact, $\mathbf{P1_{n},}_{j}$ has a similar structure to that of the water-filling problem [72]. Therefore, we solve $\mathbf{P1_{n},}_{j}$ using KKT conditions [72]. Introducing the Lagrange multiplier ν for the resource constraint (2.49), the solution is

$$n_{ij}^{'} = \left[\frac{1}{\bar{c}_{ij}}(U^{'})^{-1}\big(\frac{\nu}{\bar{c}_{ij}}\big) - \bar{n}_{ij}^{R}\right]^{+}, \ \forall i \in \mathcal{U}_j, \tag{2.51}$$

where ν is the unique solution of the following equation

$$\sum_{i\in\mathcal{U}_j} \max\left\{\frac{1}{\bar{c}_{ij}}(U^{'})^{-1}\big(\frac{\nu}{\bar{c}_{ij}},\big), \bar{n}_{ij}^{R}\right\} = N_j. \tag{2.52}$$

In addition, $(U')^{-1}(\cdot)$ is the inverse of the derivative of $U(\cdot)$ with respect to n_{ij}. The solution of the above equation is unique since $U(\cdot)$ is a concave and strictly increasing function, hence, $(U^{'})^{-1}(\cdot)$ is a strictly increasing (monotonic) function of ν. This equation can be solved efficiently through a numerical search method. In the end, the optimal solution of the $\mathbf{P1_{n},}_{j}$ is rounded to the closest integer value since the procedure described here does not necessarily produce integer values for n_{ij}s.

2.4.2 Global outage probability minimization

Assuming fixed x_{ij}s, removing the constant 1 in the objective function of **P2**, flipping the negative sign to positive sign, and taking the logarithm of the remaining term, **P2** reduces

to the following optimization problem at each BS j

$$\mathbf{P2}_{\mathbf{n},j}: \underset{n'_{ij}, i\in\mathcal{U}_j}{\text{maximize}} \quad \sum_{i\in\mathcal{U}_j} \log\left(1-P_{ij}^{\text{out}}\right) \tag{2.53}$$

$$\text{subject to} \quad \sum_{i\in\mathcal{U}_j} n_{ij} = N_j, \tag{2.54}$$

$$n_{ij} = \bar{n}_{ij}^{O} + n'_{ij}, \quad \forall i \in \mathcal{U}_j, \tag{2.55}$$

where $\bar{n}_{ij}^{O}$ is the number of already allocated RBs to user i by BS j satisfying the outage QoS constraint of user i, and n'_{ij} is the share of user i from the remaining RBs available at BS j. The optimization problem $\mathbf{P2}_{\mathbf{n},j}$ is a non-convex problem, and finding the closed form solution to it is involved. However, it can be shown that the objective function in $\mathbf{P2}_{\mathbf{n},j}$ is strictly increasing in n_{ij}s. In other words, increasing each of n_{ij}s or a subset of n_{ij}s increases the objective function. As this problem is a monotonic combinatorial optimization problem, applying a greedy algorithm is a natural approach to solving it [76]. We propose a greedy algorithm where in each iteration one RB is given to the user that benefits the most in terms of the outage probability (the user that has the highest decrement in P_{ij}^{out} given in (2.10)) until the RBs at BS j are exhausted. At BS j, given that there are $K_j = (N_j - \sum_{i\in\mathcal{U}_j} \bar{n}_{ij}^{O})$ RBs left, the algorithm terminates in K_j iterations.

2.5 Numerical simulation results

In this section, we evaluate the performance of our distributed cell association algorithm and the effects of distributing the remaining RBs through numerical simulations. Three tiers of BSs are considered to exist in the HetNet. The transmitting powers of macro, pico and femto BSs are set to $46, 35$ and 20 dBm, respectively. The macro BSs' locations are assumed to be fixed and for each macro BS, 5 micro BSs, 10 femto BSs, and 200 users are randomly located in a square area of 1000 m$\times$1000 m, unless stated otherwise. The macro BSs are fixed at the center of each square cell. Regarding the channel model, large scale path loss and small scale Rayleigh multi-paths fading are considered. The path loss between the macro or pico BSs, and the users is modelled as $L(d) = 34 + 40\log_{10}(d)$, and the path loss between femto BSs and users is $L(d) = 37 + 30\log_{10}(d)$, where d is the distance between users and BSs in meters. The small scale fading is modelled by statistically independent exponentially distributed RVs with unit variance. The noise power at all the receivers is set to -111.45 dBm, which corresponds to thermal noise at room temperature and bandwidth of 180 kHz (Bandwidth of an RB in LTE standard). The mobile users in their SINR and

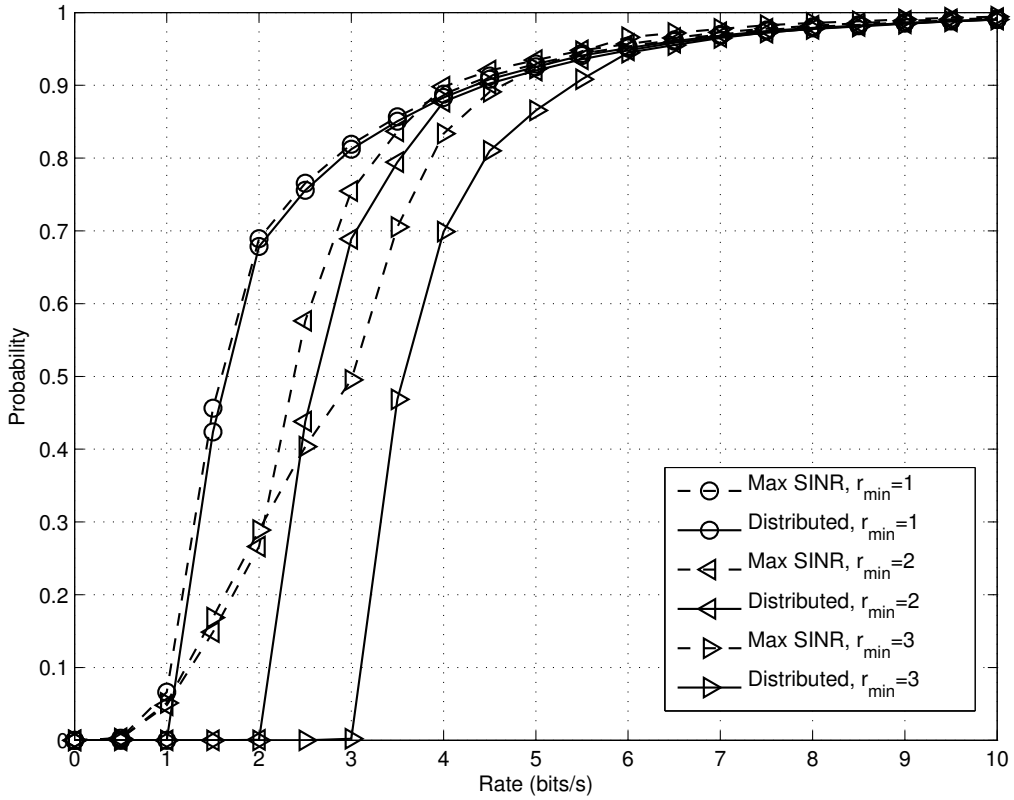

Figure 2.1: The CDFs of users' long term rate for the rate problem in a static setting

channel gain measurements average out the Rayleigh multi-paths fading and see the effects of large scale path loss, while their instantaneous rate depends on both the large scale and small scale fading. The number of RBs available at macro, pico and femto BSs are $N_{\text{macro}} = 200$, $N_{\text{pico}} = 100$, and $N_{\text{femto}} = 50$. Without loss of generality, the scheduling interval of 1 second is considered in the simulations.

2.5.1 Rate cumulative distribution functions

As mentioned in [44], when it comes to HetNets, the rate distribution is a more meaningful metric compared to SINR or spectral efficiency distribution to compare different schemes. This is because with rate distribution metric, the effect of BS load on the data rate the users perceive is observable, while this is not the case with SINR or spectral efficiency distribution metrics.

Fig. 2.1 shows the cumulative distribution function (CDF) of the long term rate for the maximum SINR scheme (Maximum SINR scheme is referred to as Max SINR in the rest of

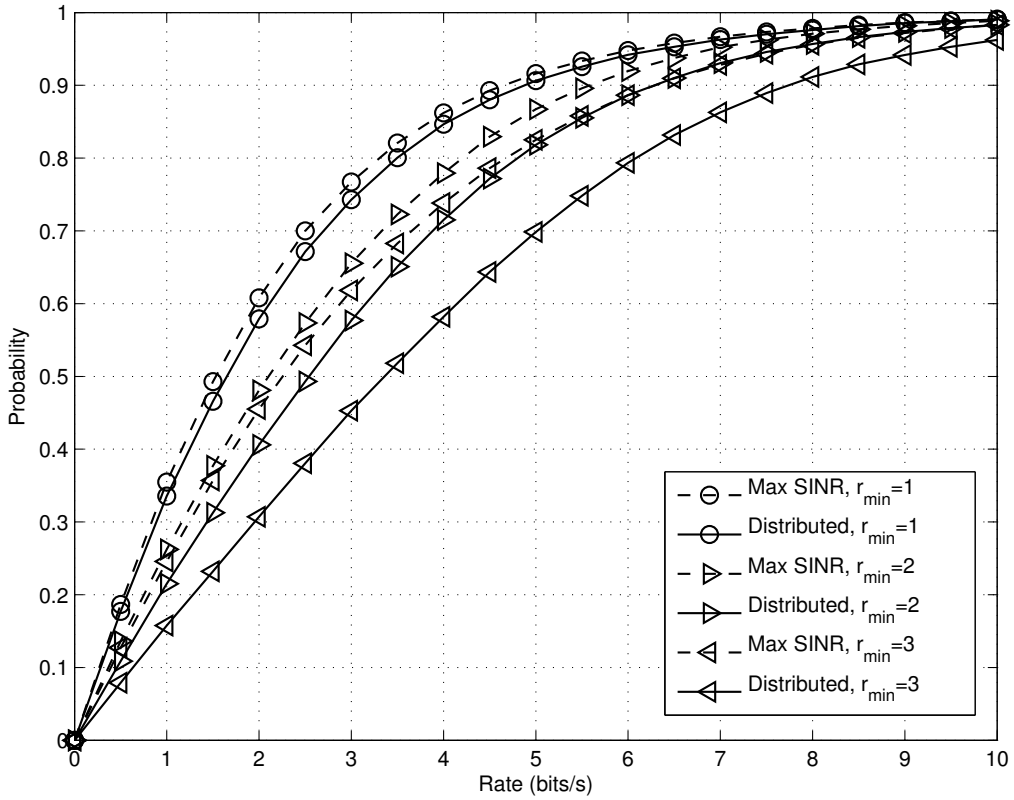

Figure 2.2: The CDFs of users' instantaneous rate for the rate problem in a stochastic setting

this chapter) and the distributed cell association algorithm for the rate problem in a static simulation environment. The simulation environment is static in the sense that Rayleigh multi-path fading is not considered, and only large scale path loss is taken into account. Fig. 2.2 shows the CDFs of instantaneous rate for the Max SINR and the distributed cell association algorithm for the rate problem in a stochastic setting where both large scale and small scale fading are taken into account. In both figures, the results for the rate threshold of $\gamma = 1, 2$, and 3 bits/s are shown. In the case of Max SINR scheme, some of the BSs may get overloaded when users associated with a BS require more RBs than the BS budget; thus, those users are needed to be scheduled in the next scheduling interval. The rate reduction caused by the over-loaded BSs is taken into account in the simulations. As it can be seen in Fig. 2.1, the long term rate of the users never drops below the rate threshold in the case of the distributed algorithm, while Max SINR algorithm is not able to satisfy the rate QoS constraints in a static setting. Furthermore, the rate CDFs of the distributed algorithm always lie below the corresponding CDFs resulted by employing the Max SINR algorithm,

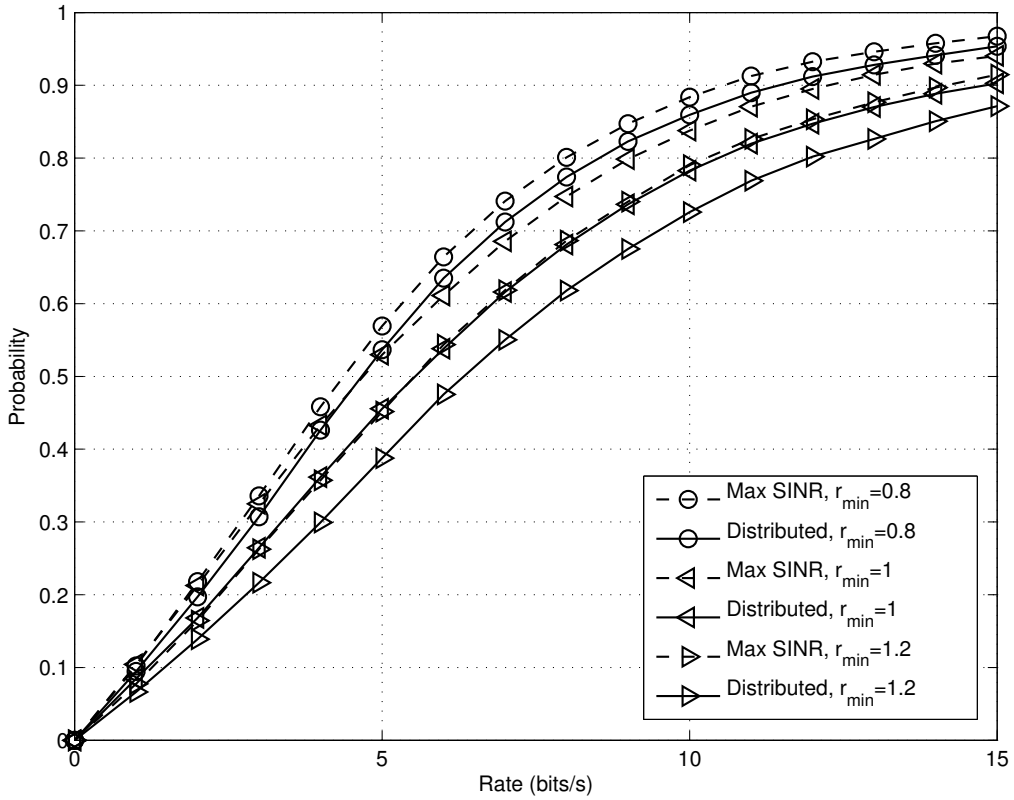

Figure 2.3: The CDFs of users' instantaneous rate for the outage problem and outage probability of $T = 10\%$ in a stochastic setting

especially for the cell edge users (worst 10% users). The rate gain for the cell edge users obtained by using the distributed algorithm over the Max SINR algorithm increases by increasing the rate threshold. To be more specific, rate gains of $\alpha = 2.4, 1.6$, and 1.1 are observed for minimum thresholds of $\gamma = 3, 2$, and 1 bits/s, respectively, in a static setting. Likewise, in a stochastic setting, as it can be seen in Fig. 2.2, the rate CDFs of the distributed algorithm always lie below the corresponding CDFs obtained by employing the Max SINR algorithm. In this case, the rate gains for the cell edge users of $\alpha = 1.75, 1.3$, and 1.08 are observed for minimum thresholds of $\gamma = 3, 2$, and 1 bits/s. However, the instantaneous rate seen by the users can go below the rate threshold since the users' measurements are based on the average channel gains, while the instantaneous rate is dictated by both the average channel gain and the small scale Rayleigh fading. Since lower rates than the rate threshold are also achievable, the average rates and the rate gain of the cell-edge users drop in the stochastic setting compared to the static setting.

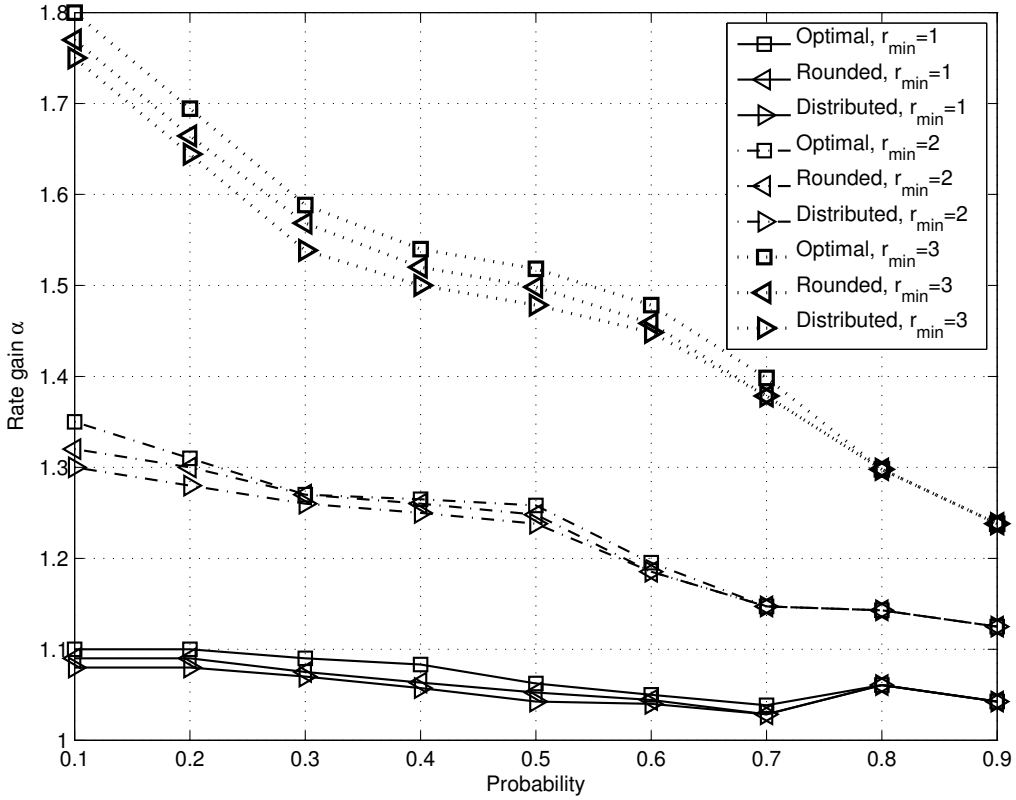

Figure 2.4: The rate gain of the optimal linear program algorithm, the rounding algorithm, and our distributed algorithm over maximum SINR algorithm for the rate problem in a stochastic setting

The CDFs of the instantaneous rate for the Max SINR and the distributed cell association algorithm for the outage problem is shown in Fig. 2.3. Only a stochastic setting is considered for the outage problem since outage probability cannot be defined in a static setting. The maximum outage probability is set to $T = 10\%$ for all the users. By zooming in this figure, it can be seen that the outage probability for the distributed algorithm and the cases of $\gamma = 0.8, 1$, and 1.2 bits/s is $T = 7.9\%, 8.4\%$, and 8.1%, respectively, which are less than the required outage probability of $T = 10\%$; thus, the outage constraints are always satisfied. This is while the Max SINR algorithm does not necessarily satisfy the outage constraints. Moreover, similar to the rate problem, the CDFs of rate resulted by the distributed algorithm always lie below the CDFs of rate from the Max SINR algorithm. The rate gain for the cell edge users is $\alpha = 1.4, 1.23$, and 1.1 for minimum thresholds of $\gamma = 1.2, 1$, and 0.8 bits/s, respectively.

Fig. 2.4 demonstrates the effectiveness of the distributed cell association algorithm for

the rate problem in a stochastic setting. The cell association problem $\mathbf{P_x}$ introduced in Section 2.3 can be solved by three different methods. First one is solving the problem directly as a linear program using the simplex method [77]. This method does not necessarily produce binary values for the association indices, however, provides an upper bound to all the other methods. We call this method the optimal method. The second method is obtained by rounding the solution of the optimal linear program method to the closest integer value, producing 0s and 1s for the association indices. We call this method the rounding method. Finally, we have the distributed algorithm introduced in this chapter. In Fig. 2.4, the rate gain $\alpha_a = \frac{r_a(\text{Probability})}{r_{\text{Max SINR}}(\text{Probability})}$ is plotted against the probability, where $a \in \{\text{Optimal}, \text{Rounding}, \text{Distributed}\}$. For instance, at probability 0.2, α of the optimal algorithm is the ratio of the rate for which 20% of the users experience rates below that rate when the problem is solved by the optimal algorithm, over the rate for which 20% of the users experience rates below that rate when the problem is solved by the Max SINR algorithm. It can be seen that the rate gains for the optimal and rounding methods are close, meaning that the solution of the optimal linear program is mostly composed of 0s and 1s. Also, the rate gains of the distributed algorithm is close to the rounding algorithm, which proves the effectiveness of our distributed algorithm. We have observed similar trends for the rate problem in a static setting, and outage problem in a stochastic setting.

2.5.2 The effect of number of femto BSs

The effects of number of femto BSs per macro BS on the performance of the distributed and Max SINR algorithms are demonstrated in Figures 2.5 and 2.6. In a stochastic setting, Fig. 2.5 shows the average sum utility of instantaneous rate for the rate problem (problem $\mathbf{P1_x}$) and rate thresholds of $\gamma = 1, 2$, and 3 bits/s, while Fig. 2.6 shows the logarithm of the probability of no users experiencing outage, $\log_{10}(1 - \widehat{P_{\text{out}}})$, for the outage problem (problem $\mathbf{P2_x}$) and rate thresholds of $\gamma = 0.8, 1$, and 1.2 bits/s and outage probability of $T = 10\%$. It can be seen that the distributed algorithm outperforms the Max SINR algorithm in all the cases. It is also observed that the performance of the distributed algorithm slightly worsens by increasing the number of femto BSs, which is attributed to introducing more interference in the network.

Moreover, for the rate problem in Fig. 2.5, the performance of the Max SINR algorithm first improves as the number of femto BSs increases, which is because more resources become available per unit area and the likelihood of having overloaded BSs decreases. As the number of femto BSs surpasses a threshold, the performance of Max SINR saturates then worsens, similar to the distributed algorithm, since the effect of more interference dominates the more

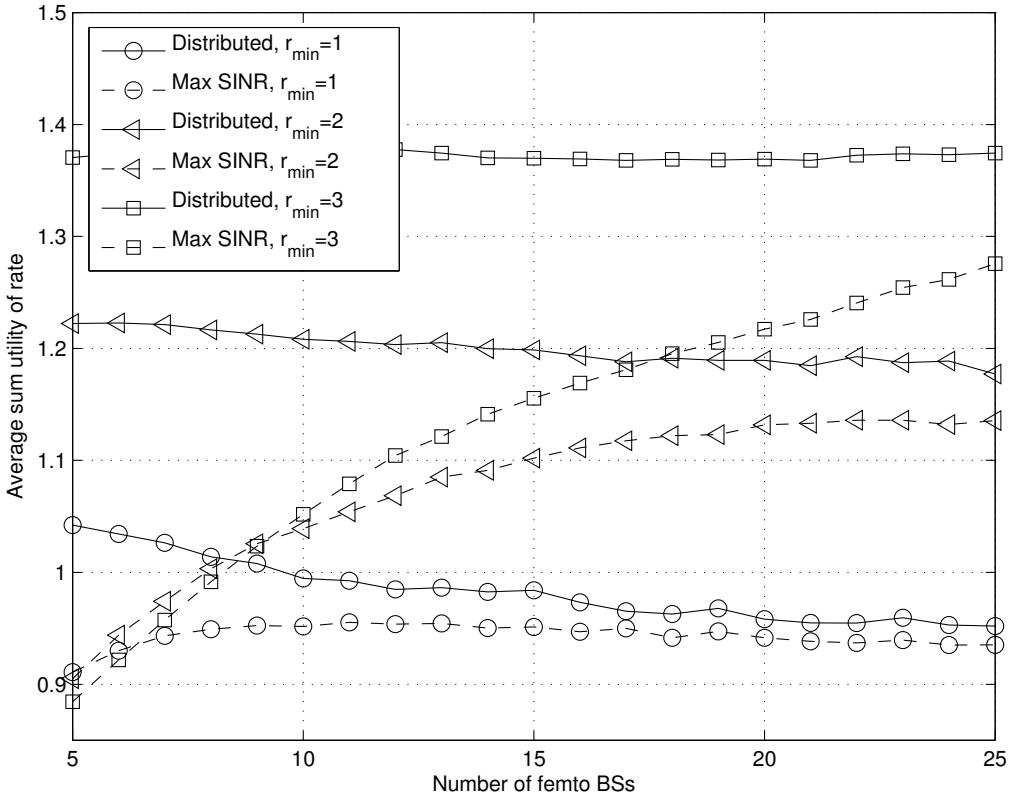

Figure 2.5: The average sum utility of instantaneous rate against number of femto BSs for the rate problem in a stochastic setting

availability of resources. As for the outage problem in Fig. 2.6, the performance of the Max SINR algorithm for the cases of $\gamma = 1$ and 1.2 bits/s shows a decreasing trend since the effect of more available RBs never dominates the interference. However, in the case of $\gamma = 0.8$ bits/s, first the interference worsens the performance and then the availability of more resources boosts the performance.

2.5.3 The effect of number of users

The effects of number of users per macro BS on the performance of the distributed and Max SINR algorithms are demonstrated in Figures 2.7 and 2.8. In a stochastic setting, Fig. 2.7 shows the average sum utility of instantaneous rate for the rate problem (problem $\mathbf{P1_x}$) and rate thresholds of $\gamma = 1, 2$, and 3 bits/s, while Fig. 2.8 shows the logarithm of the probability of no users experiencing outage, $\log_{10}(1 - \widehat{P_{\text{out}}})$, for the outage problem (problem $\mathbf{P2_x}$) and threshold rates of $\gamma = 0.8, 1$, and 1.2 bits/s and outage probability of $T = 10\%$. It can be

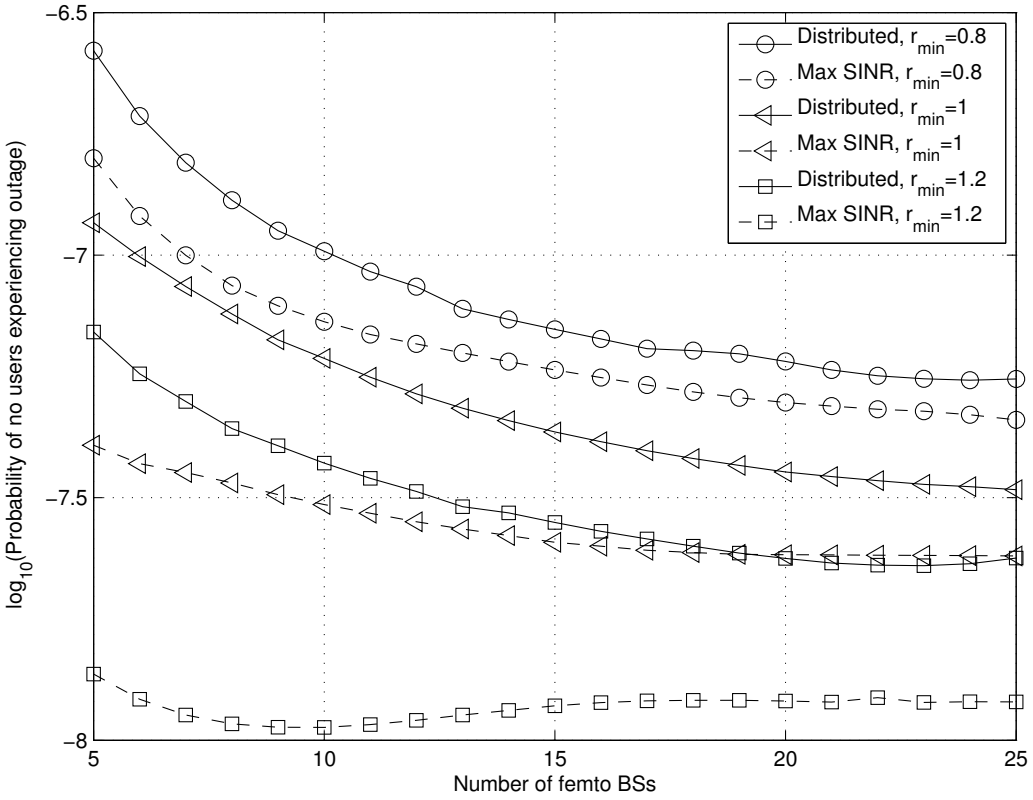

Figure 2.6: The probability of no users being in outage against number of femto BSs for the outage problem and outage probability of $T = 10\%$

seen that the distributed algorithm outperforms the Max SINR algorithm in all the cases.

For the rate problem, as it can be seen in Fig. 2.7, the distributed algorithm keeps the average sum utility around a constant value, which is because of the load balancing it achieves. The distributed algorithm provides each user with only enough number of RBs to satisfy the rate constraints. This is why the performance does not vary with the number of users, and increases with increasing the rate threshold. As for the outage problem in Fig. 2.8, $\log_{10}(1-\widehat{P_{\text{out}}})$ decreases almost linearly. This trend occurs because the distributed algorithm provides users with only enough number of RBs to keep the outage probability of each link slightly below the required outage probability. Besides, more users translates into more multiplicative terms in $1-\widehat{P_{\text{out}}} = \prod_{i\in\mathcal{U}}\prod_{j\in\mathcal{B}}\left(1-P_{ij}^{\text{out}}\right)^{x_{ij}}$, causing the logarithm of $1-\widehat{P_{\text{out}}}$ to decrease almost linearly. In an intuitive fashion, when there are more users in the system, the likelihood of at least one user going into outage increases. Therefore, the probability of no users experiencing outage decreases.

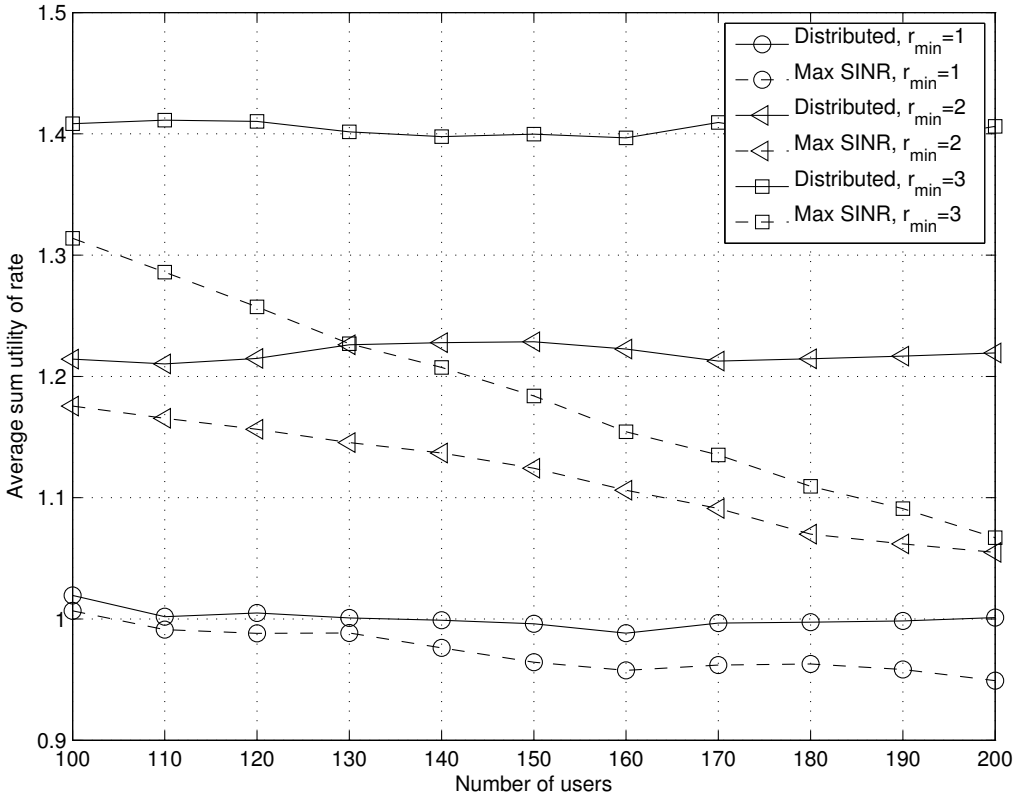

Figure 2.7: The average sum utility of instantaneous rate against number of users for the rate problem in a stochastic setting

As for the performance of the Max SINR algorithm, increasing the number of users leads to less availability of resources and decline of the performance in both rate and outage problems.

2.5.4 The effect of distributing the remaining RBs

By far, in all our simulations we have considered only the distributed cell association algorithm solving the optimization problem $\mathbf{P_x}$. The effect of distributing the remaining RBs after the cell association phase for the rate (solving $\mathbf{P1_{n},}_j$ on top of the cell association problem $\mathbf{P1_x}$) and outage (solving $\mathbf{P2_{n},}_j$ on top of the cell association problem $\mathbf{P2_x}$) problems is demonstrated in Figures 2.9 and 2.10, respectively. In Fig. 2.9, we can see the average sum utility of instantaneous rate for the distributed algorithm solving the cell association problem, and the distributed algorithm with the remaining RBs, against the rate threshold in a stochastic setting. In Fig. 2.10, we can see the logarithm of the probability of no

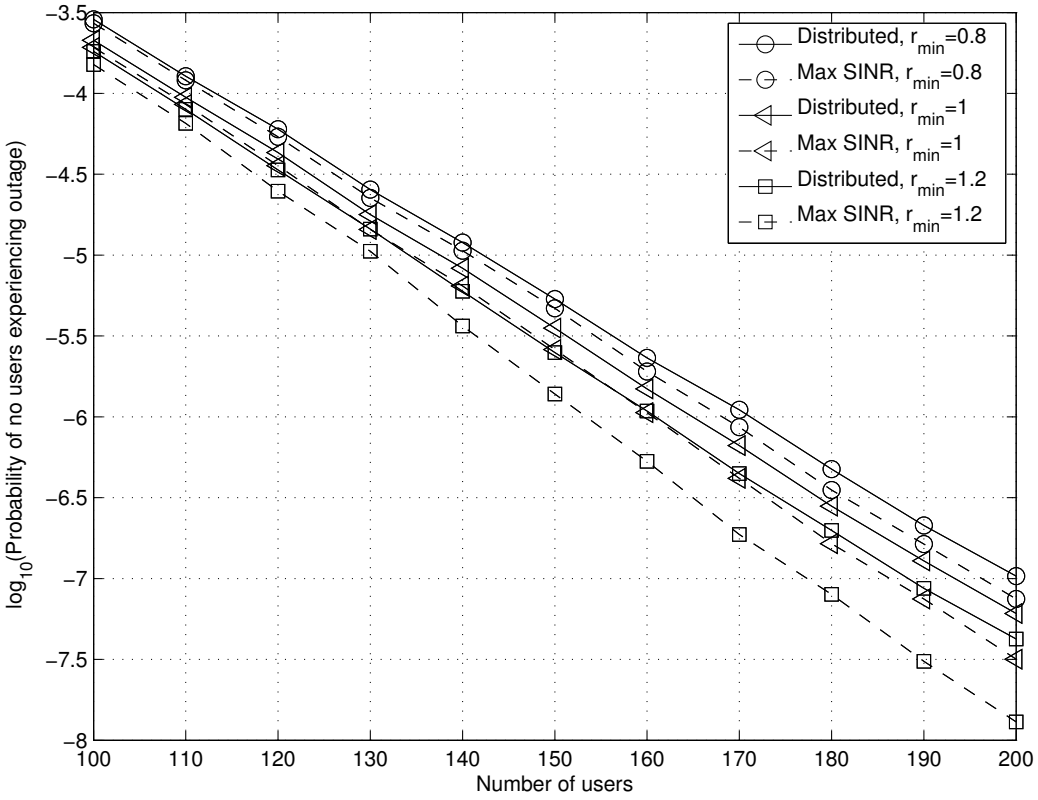

Figure 2.8: The probability of no users being in outage against number of users for the outage problem and outage probability of $T = 10\%$

users experiencing outage for the distributed algorithm , and the distributed algorithm with the remaining RBs, against the rate threshold and link outage probability of $T = 10\%$. In both figures, the curves corresponding to 150 and 200 users per macro BS are plotted. The first observation on these two figures is that the distributed algorithm with the remaining RBs significantly outperforms the results obtained through the distributed cell association algorithm only. Secondly, with lower number of users, the performance of the distributed algorithm with the remaining RBs improves. This is because for a given rate threshold, the cell association algorithm first provides users with only enough number of RBs to satisfy the QoS constraints. Therefore, less users require less overall number of RBs to have their QoS constraints satisfied, leaving more RBs unused. More unused RBs trivially translates into a stronger boost in the performance after distributing them among the users. Finally, by increasing the rate threshold, the performance of the distributed cell association only algorithm gets close to the performance of the distributed algorithm with the remanning

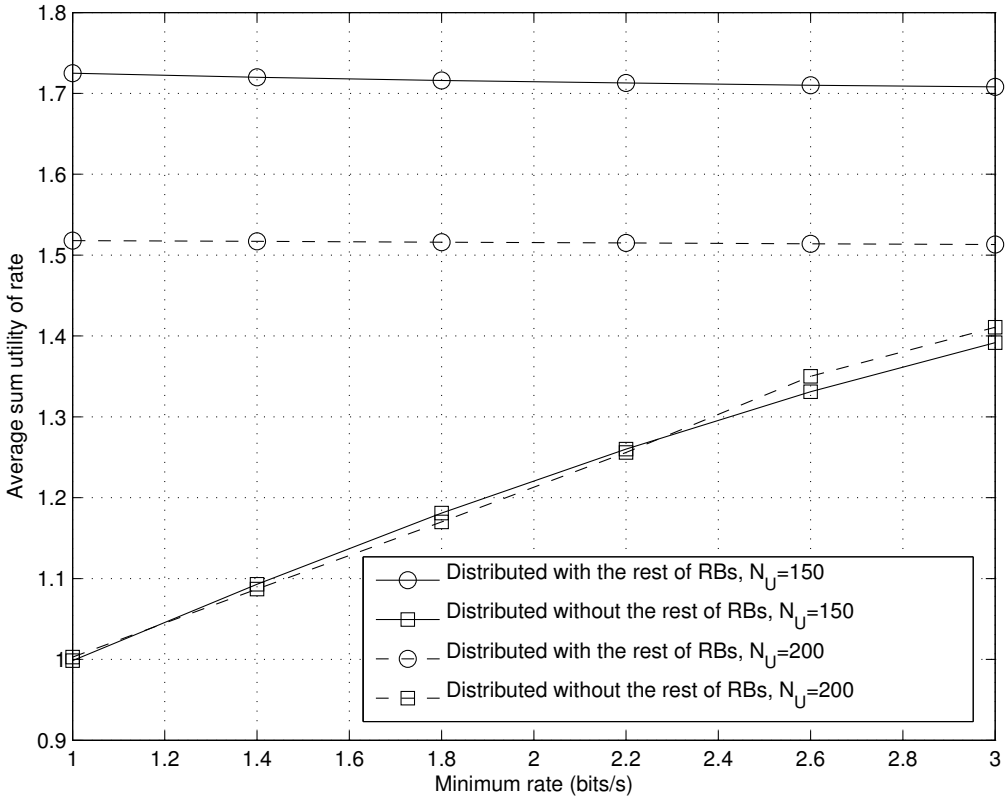

Figure 2.9: The average sum utility of instantaneous rate against minimum rate for the rate problem showing the effect of distributing the remaining RBs in a stochastic setting

RBs. This trend is seen since more RBs are required to satisfy QoS constraints with higher rate thresholds, leaving less overall unused RBs in the network. Distributing less unused RBs among users leads to a less improvement over distributed cell association algorithm.

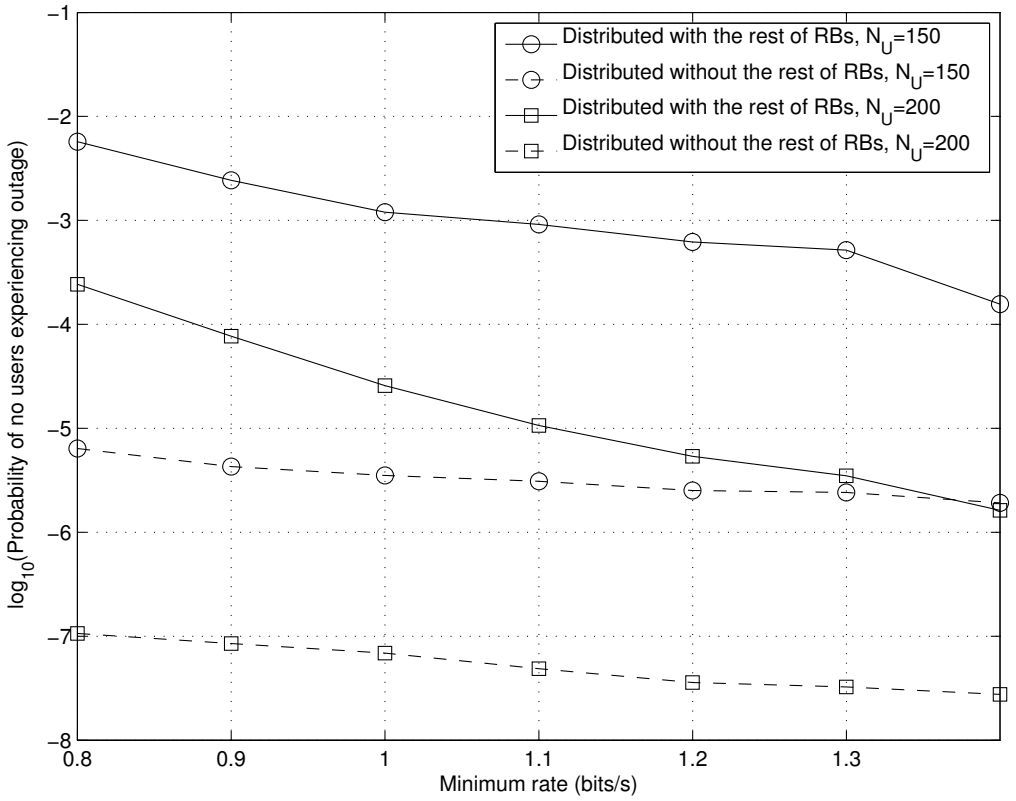

Figure 2.10: The probability of no users being in outage against minimum rate for the outage problem and outage probability of $T = 10\%$ showing the effect of distributing the remaining RBs

Chapter 3

Joint Downlink and Uplink Aware Cell Association in HetNets with QoS Provisioning

The accomplished works and research contributions in this chapter are briefly described in the following.

As an extension to Chapter 2, the main contribution of this chapter is considering both uplink and downlink in the cell association problem. In this chapter, we address a joint downlink and uplink cell association problem in a multi-tier HetNet in which BSs have finite number of RBs to distribute among the users in the downlink and uplink.

An optimization problem is defined to maximize the sum of weighted utility of long term data rates in downlink and uplink through cell association and RB allocation while maintaining QoS for the users. Separate QoS constraints are considered for downlink and uplink of a user. The QoS constraints are defined in the context of outage probability that is keeping the instantaneous rate above a certain threshold with a certain probability. Using outage QoS constraints renders the cell association scheme suitable for environments with high mobility and fast fading.

The optimization problem is broken into two phases: Cell association phase followed by distributing the rest of RBs phase. We are interested in providing a distributed scheme to the downlink and uplink aware cell association phase of the problem, while the RB distribution phase is kept optional for energy saving purposes. As users cannot measure the uplink attributes such as the uplink interference by listening to the reference signals of BSs, a limited amount of feedback is added to the reference signals of the BSs to inform the users of the uplink interference and make the distributed algorithm design possible. The amount of feedback introduced to the system is negligible compared to already existing reference signals in standards such as LTE-Advanced. Moreover, by assigning different weights to the downlink and uplink rates in the objective of the defined optimization problem, the proposed distributed scheme can be modified to be only downlink oriented, only uplink oriented, or both downlink and uplink aware. Comparing the proposed scheme with the

downlink oriented maximum SINR scheme, significant uplink rate gains are observed. Rate gains in the downlink are also considerable.

In RB distribution phase, the remaining RBs are distributed among the users to increase their rates. The RB distribution problem can be decoupled with respect to downlink and uplink. Therefore, the RB distribution problem is broken into downlink and uplink RB distribution sub-problems. Both of the sub-problems have a similar structure to that of the water-filling problem. Therefore, their optimal solution is obtained through KKT conditions.

It should be mentioned that interference co-ordination, resource partitioning, as well as frequency selectivity of wide channels are not considered to keep the system model as general as possible.

The rest of the chapter is organized as follows: In the next section, the chosen system model is described. Defining our optimization problem as well as outlining the solution approach are brought in Section 3.2. A base line cell association solution is presented in Section 3.3. The distributed cell association scheme and a solution to the RB distribution problem are presented in Section 3.4. Finally, We examine the performance of our proposed schemes in this chapter through numerical simulations in Section 3.5.

3.1 System model

The network of interest is a multi-tier HetNet composed of a set of BSs $\mathcal{B} = \{1, 2, \cdots, N_{\mathcal{B}}\}$ and a set of users $\mathcal{U} = \{1, 2, \cdots, N_{\mathcal{U}}\}$. An individual BS is indicated by $j \in \mathcal{B}$ and an individual user is denoted by $i \in \mathcal{U}$. All the BSs are connected through a high speed backhaul and negotiate with each other with negligible time delay. Furthermore, all BSs constantly transmit unique pilot signals from which users can estimate the average channel power gains between themselves and all the BSs in their range.

The transmitting power of BS j is assumed to be the constant $P_j^{\mathcal{B}}$ W while user i is capable of transmitting at $P_i^{\mathcal{U}}$ W of power. Depending on the available bandwidth and scheduling interval at BS j, BS j has N_j^{DL} available RBs to distribute among its associated users in the downlink and N_j^{UL} available RBs to distribute among its associated users in the uplink. n_{ij}^{DL} indicates the number of RBs given to user i by BS j to be used in downlink transmission, and n_{ij}^{UL} represents the number of RBs given to user i by BS j for uplink transmission. The number of RBs given to a user depends on the QoS level required by that user; higher number of RBs improves QoS.

Table 3.1: List of key parameters in Chapter 3

$\mathcal{U}$	Set of users
$\mathcal{B}$	Set of BSs
i	User $i \in \mathcal{U}$
j	BS $j \in \mathcal{B}$
N_j^{DL} / N_j^{UL}	Downlink/Uplink budget of BS j
n_{ij}^{DL} / n_{ij}^{UL}	#RBs given to user i from BS j in downlink/uplink
$P_j^{\mathcal{B}}$	Transmitting power of BS j
$P_i^{\mathcal{U}}$	Transmitting power of user i
$H_{ij} = G_{ij}F_{ij}$	Channel power gain between user i and BS j
G_{ij}	Large scale component of H_{ij}
F_{ij}	Small scale component of H_{ij}
$\lambda_{ij} = \frac{1}{G_{ij}}$	Exponential parameter of H_{ij}
$\mathrm{SINR}_{ij}^{\mathrm{DL}}$ / $\mathrm{SINR}_{ij}^{\mathrm{UL}}$	Instantaneous SINR at user i from BS j / at BS j from user i
$\overline{\mathrm{SINR}}_{ij}^{\mathrm{DL}}$ / $\overline{\mathrm{SINR}}_{ij}^{\mathrm{UL}}$	Long term SINR at user i from BS j / at BS j from user i
c_{ij}^{DL} / c_{ij}^{UL}	Instantaneous RB capacity at user i from BS j / at BS j from user i
$\bar{c}_{ij}^{\mathrm{DL}}$ / $\bar{c}_{ij}^{\mathrm{UL}}$	Long term RB capacity at user i from BS j / at BS j from user i
r_{ij}^{DL} / r_{ij}^{UL}	Instantaneous rate at user i from BS j / at BS j from user i
$\bar{r}_{ij}^{\mathrm{DL}}$ / $\bar{r}_{ij}^{\mathrm{UL}}$	Long term rate at user i from BS j / at BS j from user i
$\mathrm{PO}_{ij}^{\mathrm{DL}}$ / $\mathrm{PO}_{ij}^{\mathrm{UL}}$	Downlink/Uplink probability of outage on link $i-j$
γ_i^{DL} / γ_i^{UL}	Downlink/Uplink rate requirement of user i
T_i^{DL} / T_i^{UL}	Downlink/Uplink outage probability requirement of user i
$\bar{n}_{ij}^{\mathrm{DL}}$ / $\bar{n}_{ij}^{\mathrm{UL}}$	Minimum # of required RBs of user i from BS j in downlink/uplink
$\hat{\mathrm{PO}}_{ij}^{\mathrm{UP}}$	Worst case outage probability of user i connected to BS j in the uplink
$\hat{n}_{ij}^{\mathrm{UP}}$	Minimum # of RBs to satisfy the worst outage QoS constraint in uplink
$\hat{r}_{ij}^{\mathrm{UP}}$	Long term rate of user i associated with $\hat{n}_{ij}^{\mathrm{UP}}$

The positive channel power gain between BS j and user i is represented by H_{ij} as in

$$H_{ij} = G_{ij}F_{ij},\ \forall(i,j) \in \mathcal{U} \times \mathcal{B}, \tag{3.1}$$

where G_{ij} is the large scale slow fading component of the channel capturing the effects of path loss and shadowing, and F_{ij} represents the small scale fast fading component of the channel. In the above equation, $\cdot \times \cdot$ denotes the Cartesian product of two sets. It is assumed that G_{ij} remains constant during one association period. To model the small scale Rayleigh fading, it is assumed that F_{ij} fluctuates fast during an association period following an exponential probability distribution function with variance 1. According to these assumptions, H_{ij} is an exponentially distributed RV with expected value ($\mathrm{E}[H_{ij}]$) of G_{ij}. In other words, H_{ij} is an exponentially distributed RV with parameter λ_{ij}, where

$$\lambda_{ij} = \frac{1}{\mathrm{E}[H_{ij}]} = \frac{1}{G_{ij}},\ \forall(i,j) \in \mathcal{U} \times \mathcal{B}. \tag{3.2}$$

User i can estimate the exponential parameter of the channel λ_{ij} between itself and all the BSs in its range by listening to the pilot signals the BSs transmit.

The instantaneous SINR seen by user i from BS j (downlink) and seen by BS j from user i (uplink) are respectively defined as

$$\mathrm{SINR}_{ij}^{\mathrm{DL}} = \frac{P_j^{\mathcal{B}} H_{ij}}{\sum_{k \in \mathcal{B} \setminus \{j\}} P_k^{\mathcal{B}} H_{ik} + \Delta f N_0}, \tag{3.3}$$

$$\mathrm{SINR}_{ij}^{\mathrm{UL}} = \frac{P_i^{\mathcal{U}} H_{ij}}{\sum_{k \in \mathcal{U} \setminus \{i\}} P_k^{\mathcal{U}} H_{kj} + \Delta f N_0}, \tag{3.4}$$

where Δf, without loss of generality, is the bandwidth of one RB, N_0 is the noise spectral power, and $\cdot \setminus \cdot$ is the set minus operation.

The instantaneous achievable Shannon capacity is a logarithmic function of SINR. Therefore, the instantaneous achievable Shannon capacities on a single RB in downlink and uplink are

$$c_{ij}^{\mathrm{DL}} = \log_2(1 + \mathrm{SINR}_{ij}^{\mathrm{DL}}), \tag{3.5}$$

$$c_{ij}^{\mathrm{UL}} = \log_2(1 + \mathrm{SINR}_{ij}^{\mathrm{UL}}), \tag{3.6}$$

respectively.

Given that user i is connected to BS j, and BS j allocates n_{ij}^{DL} and n_{ij}^{UL} RBs to user i for its downlink and uplink transmissions, respectively, the instantaneous rates seen by that

user on the downlink and uplink are

$$r_{ij}^{\mathrm{DL}} = n_{ij}^{\mathrm{DL}} c_{ij}^{\mathrm{DL}}, \tag{3.7}$$

$$r_{ij}^{\mathrm{UL}} = n_{ij}^{\mathrm{UL}} c_{ij}^{\mathrm{UL}}. \tag{3.8}$$

The above equations are valid if we assume flat fading on the bandwidth of BSs from the users' point of view. The flat fading assumption is made to preserve simplicity in the system model. The study of the frequency selective fading scenario where users see different channel gains on different RBs (and in turn, different SINR levels and capacities on different RBs) is left for future work.

Associated with the instantaneous SINR, capacity, and rate, we define the long term SINR, capacity, and rate where only the large scale component of the channel power gains G_{ij} is taken into account and the fast fading small scale component F_{ij} is averaged out. Indicating the long term SINR, capacity, and rate by $\overline{\mathrm{SINR}}$, $\bar{c}$, and $\bar{r}$, respectively, these parameters for user i that is assumed to be connected to BS j in the downlink and uplink are

$$\overline{\mathrm{SINR}}_{ij}^{\mathrm{DL}} = \frac{P_j^{\mathcal{B}} G_{ij}}{\sum_{k \in \mathcal{B} \setminus \{j\}} P_k^{\mathcal{B}} G_{ik} + \Delta f N_0}, \tag{3.9}$$

$$\overline{\mathrm{SINR}}_{ij}^{\mathrm{UL}} = \frac{P_i^{\mathcal{U}} G_{ij}}{\sum_{k \in \mathcal{U} \setminus \{i\}} P_k^{\mathcal{U}} G_{kj} + \Delta f N_0}, \tag{3.10}$$

$$\bar{c}_{ij}^{\mathrm{DL}} = \log(1 + \overline{\mathrm{SINR}}_{ij}^{\mathrm{DL}}), \tag{3.11}$$

$$\bar{c}_{ij}^{\mathrm{UL}} = \log(1 + \overline{\mathrm{SINR}}_{ij}^{\mathrm{UL}}), \tag{3.12}$$

$$\bar{r}_{ij}^{\mathrm{DL}} = n_{ij}^{\mathrm{DL}} \bar{c}_{ij}^{\mathrm{DL}}, \tag{3.13}$$

$$\bar{r}_{ij}^{\mathrm{UL}} = n_{ij}^{\mathrm{UL}} \bar{c}_{ij}^{\mathrm{UL}}. \tag{3.14}$$

The outage event for user i on its downlink is defined as the event where the instantaneous downlink rate of that user drops below a certain threshold γ_i^{DL}. Likewise, the uplink outage event is the event where the instantaneous uplink rate of user i drops below a threshold γ_i^{UL}. We indicate the probability of outage on downlink by $\mathrm{PO}_{ij}^{\mathrm{DL}}$, while the probability of outage on the uplink is indicated by $\mathrm{PO}_{ij}^{\mathrm{UL}}$, where

$$\mathrm{PO}_{ij}^{\mathrm{DL}} = \Pr\{r_{ij}^{\mathrm{DL}} \leq \gamma_i^{\mathrm{DL}}\}, \tag{3.15}$$

$$\mathrm{PO}_{ij}^{\mathrm{UL}} = \Pr\{r_{ij}^{\mathrm{UL}} \leq \gamma_i^{\mathrm{UL}}\}. \tag{3.16}$$

Given the exponential parameters of the channel power gains λ_{ij} and the number of RBs

given to user i by BS j, $\mathrm{PO}_{ij}^{\mathrm{DL}}$ and $\mathrm{PO}_{ij}^{\mathrm{UL}}$ can be calculated analytically using the following formulas [68, 69]

$$\mathrm{PO}_{ij}^{\mathrm{DL}} = 1 - \left(e^{\frac{-\lambda_{ij}\Delta f N_0}{P_j^{\mathcal{B}}}\Gamma_{ij}^{\mathrm{DL}}} \right) \prod_{k\in\mathcal{B}\setminus\{j\}} \left(\frac{\frac{\lambda_{ik}}{P_k^{\mathcal{B}}}}{\frac{\lambda_{ij}}{P_j^{\mathcal{B}}}\Gamma_{ij}^{\mathrm{DL}} + \frac{\lambda_{ik}}{P_k^{\mathcal{B}}}} \right), \tag{3.17}$$

$$\mathrm{PO}_{ij}^{\mathrm{UL}} = 1 - \left(e^{\frac{-\lambda_{ij}\Delta f N_0}{P_i^{\mathcal{U}}}\Gamma_{ij}^{\mathrm{UL}}} \right) \prod_{k\in\mathcal{U}\setminus\{i\}} \left(\frac{\frac{\lambda_{kj}}{P_k^{\mathcal{U}}}}{\frac{\lambda_{ij}}{P_i^{\mathcal{U}}}\Gamma_{ij}^{\mathrm{UL}} + \frac{\lambda_{kj}}{P_k^{\mathcal{U}}}} \right), \tag{3.18}$$

where

$$\Gamma_{ij}^{\mathrm{DL}} = 2^{\frac{\gamma_i^{\mathrm{DL}}}{n_{ij}^{\mathrm{DL}}}} - 1, \tag{3.19}$$

$$\Gamma_{ij}^{\mathrm{UL}} = 2^{\frac{\gamma_i^{\mathrm{UL}}}{n_{ij}^{\mathrm{UL}}}} - 1. \tag{3.20}$$

We refer the reader to [68] for an easy to read proof validating the results in (3.17) and (3.18). Moreover, inspecting (3.17) and (3.18), it can be observed that $\mathrm{PO}_{ij}^{\mathrm{DL}}$ and $\mathrm{PO}_{ij}^{\mathrm{UL}}$ are strictly decreasing functions of n_{ij}^{DL} and n_{ij}^{UL}, respectively; more RBs improves the outage behaviour.

Each user requires a certain level of QoS on its downlink and a certain level of QoS on its uplink. We define the QoS class required by user i on downlink to be the pair $(\gamma_i^{\mathrm{DL}}, T_i^{\mathrm{DL}})$, where $\gamma_i^{\mathrm{DL}} > 0$ is the rate threshold and $0 < T_i^{\mathrm{DL}} < 1$ is the maximum outage probability needed by user i. User i wants its instantaneous rate to drop below γ_i^{DL} no more than T_i^{DL} fraction of time. Likewise, The QoS class required by user i on the uplink is defined by the pair $(\gamma_i^{\mathrm{UL}}, T_i^{\mathrm{UL}})$. The reason behind selecting the outage framework to define the QoS constraints is to tackle the wireless environments with fast fading. It is well-established in theory of communication that ensuring a minimum instantaneous rate to users is not achievable in environments with high mobility and fast fluctuations in the channel gains. However, it is possible to provide a certain rate level with a certain outage probability depending on the average channel gains.

Assuming that user i is connected to BS j, and BS j has allocated n_{ij}^{DL} and n_{ij}^{UL} RBs to user i to be used in downlink and uplink transmissions, respectively, the downlink and uplink outage QoS constraints of user i are

$$\mathrm{PO}_{ij}^{\mathrm{DL}} = \Pr\{r_{ij}^{\mathrm{DL}} \leq \gamma_i^{\mathrm{DL}}\} \leq T_i^{\mathrm{DL}}, \tag{3.21}$$

$$\mathrm{PO}_{ij}^{\mathrm{UL}} = \Pr\{r_{ij}^{\mathrm{UL}} \leq \gamma_i^{\mathrm{UL}}\} \leq T_i^{\mathrm{UL}}. \tag{3.22}$$

As it has been mentioned before, the $\mathrm{PO}_{ij}^{\mathrm{DL}}$ and $\mathrm{PO}_{ij}^{\mathrm{UL}}$ are strictly decreasing functions of number of allocated RBs n_{ij}^{DL} and n_{ij}^{UL}, respectively. Therefore, there is a lower bound on n_{ij}^{DL} and a lower bound on n_{ij}^{UL} above which the outage probability requirements of the user, $\mathrm{PO}_{ij}^{\mathrm{DL}} < T_i^{\mathrm{DL}}$ and $\mathrm{PO}_{ij}^{\mathrm{UL}} < T_i^{\mathrm{UL}}$, are satisfied. We indicate these two lower bounds by $\bar{n}_{ij}^{\mathrm{DL}}$ and $\bar{n}_{ij}^{\mathrm{UL}}$, respectively.

$$n_{ij}^{\mathrm{DL}} \geq \bar{n}_{ij}^{\mathrm{DL}}, \tag{3.23}$$

$$n_{ij}^{\mathrm{UL}} \geq \bar{n}_{ij}^{\mathrm{UL}}. \tag{3.24}$$

According to (3.23) and (3.24), if BS j is the serving BS of user i, BS j is obliged to allocate to user i at least $\bar{n}_{ij}^{\mathrm{DL}}$ RBs for downlink transmission and $\bar{n}_{ij}^{\mathrm{UL}}$ RBs for uplink transmission. Since n_{ij} can only assume natural numbers, finding these lower bounds can be done by incrementing the number of RBs one by one and checking whether the outage QoS is satisfied.

In the next section, it will be apparent how the joint uplink and downlink cell association problem is defined and formulated over the described system model in this section.

The key parameters that are used in this chapter are listed in Table 3.1.

3.2 Problem formulation

In order to define the cell association problem, we first introduce the $N_{\mathcal{U}} \times N_{\mathcal{B}}$ binary association indices matrix $\mathbf{x}$. $x_{ij} \in \{0, 1\}$ is the element on i^{th} row and j^{th} column of matrix $\mathbf{x}$. If $x_{ij} = 1$, user i is associated with BS j, otherwise $x_{ij} = 0$. We also introduce the $N_{\mathcal{U}} \times N_{\mathcal{B}}$ matrices $\mathbf{n}^{\mathrm{DL}}$ and $\mathbf{n}^{\mathrm{UL}}$. Matrices $\mathbf{n}^{\mathrm{DL}}$ and $\mathbf{n}^{\mathrm{UL}}$ contain n_{ij}^{DL} and n_{ij}^{UL} elements, respectively, which are the number of RBs that BS j allocates to user i in downlink and uplink.

Next step is to define the objective of the problem. We select the weighted sum of the utility of downlink and uplink long term data rates as the objective function to be maximized:

$$\sum_{i \in \mathcal{U}} \sum_{j \in \mathcal{B}} x_{ij} \big(w_i^{\mathrm{DL}} U_i(\bar{r}_{ij}^{\mathrm{DL}}) + w_i^{\mathrm{UL}} U_i(\bar{r}_{ij}^{\mathrm{UL}}) \big).$$

In the above equation, $U_i(\cdot)$ is an increasing and concave function that models the satisfaction level of user i from the rate it gets, whether the rate is in the downlink or uplink. w_i^{DL} is the weight that user i assigns to its satisfaction from the rate it gets in downlink. Similarly, w_i^{UL} is the weight that user i assigns to its satisfaction from the uplink rate. Without loss of generality, we can assume $w_i^{\mathrm{DL}} > 0$, $w_i^{\mathrm{UL}} > 0$, and $w_i^{\mathrm{DL}} + w_i^{\mathrm{UL}} = 1$. If the user is running downlink rate hungry applications on its end such as video streaming applications, then it is

reasonable to expect that the weight assigned to downlink $w_i^{\mathrm{DL}} = 1$, and in turn, $w_i^{\mathrm{UL}} = 0$. On the other hand, in applications that crave for uplink rate such as uploading a large file, $w_i^{\mathrm{UL}} = 1$. In the middle point of these two extremes, applications that require comparable rates on both downlink and uplink lead the user to set $w_i^{\mathrm{DL}} = w_i^{\mathrm{UL}} = 0.5$.

Finally, considering the finite resource budget of the BSs and also the outage QoS constraints introduced in (3.21) and (3.22), the joint uplink and downlink cell association with outage QoS provisioning problem ($\mathbf{P}$) is

$$\mathbf{P}: \underset{\mathbf{x},\mathbf{n}^{\mathrm{DL}},\mathbf{n}^{\mathrm{UL}}}{\text{maximize}} \sum_{i\in\mathcal{U}}\sum_{j\in\mathcal{B}} x_{ij}\big(w_i^{\mathrm{DL}}U_i(\bar{r}_{ij}^{\mathrm{DL}}) + w_i^{\mathrm{UL}}U_i(\bar{r}_{ij}^{\mathrm{UL}})\big) \tag{3.25}$$

$$\begin{aligned}
\text{subject to}\ \ & C_1: \sum_{i\in\mathcal{U}} x_{ij} n_{ij}^{\mathrm{DL}} \le N_j^{\mathrm{DL}},\ \forall j\in\mathcal{B},\\
& C_2: \sum_{i\in\mathcal{U}} x_{ij} n_{ij}^{\mathrm{UL}} \le N_j^{\mathrm{UL}},\ \forall j\in\mathcal{B},\\
& C_3: \sum_{j\in\mathcal{B}} x_{ij} \le 1,\ \forall i\in\mathcal{U},\\
& C_4: \prod_{j\in\mathcal{B}} \big(\mathrm{PO}_{ij}^{\mathrm{DL}}\big)^{x_{ij}} \le T_i^{\mathrm{DL}},\ \forall i\in\mathcal{U},\\
& C_5: \prod_{j\in\mathcal{B}} \big(\mathrm{PO}_{ij}^{\mathrm{UL}}\big)^{x_{ij}} \le T_i^{\mathrm{UL}},\ \forall i\in\mathcal{U},\\
& x_{ij}\in\{0,1\},\ \forall (i,j)\in\mathcal{U}\times\mathcal{B}, && (3.26)\\
& n_{ij}^{\mathrm{DL}}\in\{0,1,\ldots,N_j^{\mathrm{DL}}\}, \forall (i,j)\in\mathcal{U}\times\mathcal{B}, && (3.27)\\
& n_{ij}^{\mathrm{UL}}\in\{0,1,\ldots,N_j^{\mathrm{UL}}\}, \forall (i,j)\in\mathcal{U}\times\mathcal{B}. && (3.28)
\end{aligned}$$

In optimization problem $\mathbf{P}$, constraints C_1 and C_2 are resource budget constraints; they assure the number of RBs given to users does not exceed the BS budget in the downlink and uplink for all the BSs. The third constraint, C_3, allows the users to be connected to at most one BS at a given time. Constraints C_4 and C_5 are the outage QoS constraints in downlink and uplink, respectively. These two constraints are obtained by manipulating inequalities (3.21) and (3.22). Lastly, constraints (3.26), (3.27), and (3.28) keep the association indices binary, and the number of RBs given to users integers within the BSs' budgets.

Solving problem $\mathbf{P}$ optimally with low complexity is involved since it is a complicated mixed integer and combinatorial optimization problem over three sets of variables $\mathbf{x}$, $\mathbf{n}^{\mathrm{DL}}$, and $\mathbf{n}^{\mathrm{UL}}$. In order to reduce the complexity, we approach the problem in two phases. First, by fixing $\mathbf{n}^{\mathrm{DL}}$ and $\mathbf{n}^{\mathrm{UL}}$ elements we solve for $\mathbf{x}$, i.e., solving the cell association phase. Note that assigning $\mathbf{n}^{\mathrm{DL}}$ and $\mathbf{n}^{\mathrm{UL}}$ elements to arbitrary integers can violate the QoS constraints. However, $\mathbf{n}^{\mathrm{DL}}$ and $\mathbf{n}^{\mathrm{UL}}$ elements need to be assigned to integers that satisfy inequalities (3.23)

and (3.24). In the second phase, we set $\mathbf{x}$ to the result of the cell association phase and solve for $\mathbf{n}^{\mathrm{DL}}$ and $\mathbf{n}^{\mathrm{UL}}$, i.e., the RB distribution phase. In this chapter, we mostly address the cell association phase and let the RB distribution phase to be optional.

In order to devise a base line solution to the cell association problem, we let $\mathbf{n}^{\mathrm{DL}}$ and $\mathbf{n}^{\mathrm{UL}}$ to be the minimum number of required RBs by users to satisfy their QoS constraints, i.e., $n_{ij}^{\mathrm{DL}} = \bar{n}_{ij}^{\mathrm{DL}}$ and $n_{ij}^{\mathrm{UL}} = \bar{n}_{ij}^{\mathrm{UL}}$, $\forall (i,j) \in \mathcal{U} \times \mathcal{B}$. Then, we solve for $\mathbf{x}$. The centralized base line cell association solution is presented in the next section.

Later in the chapter, we will make it clear how the ability of users to estimate their minimum number of required RBs helps in devising a distributed cell association scheme. As mentioned in Section 3.1, user i can estimate the average channel gains between itself and all the BSs in its range by listening to the BSs' pilot signals. Average channel gains ($G_{ij} = 1/\lambda_{ij}$) and the QoS class that user i requires are enough for user i to be able to calculate the minimum required number of RBs in downlink ($\bar{n}_{ij}^{\mathrm{DL}}$) for all the BSs in its range using (3.17) and (3.21). However, $\bar{n}_{ij}^{\mathrm{UL}}$ cannot be estimated by user i given λ_{ij} between itself and all the BSs since the user cannot estimate the interference level created by other users at a given BS. Only the BS can measure the uplink interference levels. In order to devise a distributed scheme, we require the BSs to quantize the uplink interference levels with few number of bits and broadcast it along with their other reference signals. Low number of bits to represent the uplink interference level puts negligible message passing overhead over already existing reference signals of BSs. From this reference signal, the user conservatively estimates the minimum number of required uplink RBs to keep the *worst case QoS constraint* satisfied, compensating for the quantization error. Introducing this limited amount of feedback, we present a distributed cell association scheme in Section 3.4.

From another perspective, keeping the allocated number of RBs to users minimum helps preserving energy by spending less power. Power efficiency is more valuable to the users with their limited battery lives compared to the BSs. Also, reducing the consumed power contributes to leaving behind less carbon footprint that is harmful to nature [30]. Power saving concerns also motivates us to let the RB distribution phase (solving for $\mathbf{n}^{\mathrm{DL}}$ and $\mathbf{n}^{\mathrm{UL}}$) be optional. Moreover, it will be seen in Section 3.4 that after the cell association phase, the RB distribution phase in downlink and uplink can be done separately using the technique presented in Subsection 2.4.1 of this thesis.

3.3 Base line cell association solution

In this section, we provide a centralized solution to the cell association phase of problem $\mathbf{P}$. As mentioned in the previous section, we replace the downlink and uplink QoS constraints in $\mathbf{P}$ (C_4 and C_5) by $n_{ij}^{\mathrm{DL}} = \bar{n}_{ij}^{\mathrm{DL}}$ and $n_{ij}^{\mathrm{UL}} = \bar{n}_{ij}^{\mathrm{UL}}$, respectively, $\forall (i,j) \in \mathcal{U} \times \mathcal{B}$. After applying this change, an assignment problem that is NP-hard in $\mathbf{x}$ is resulted because of the resource budget constraints C_1 and C_2 [71]. Therefore, we propose to relax the binary constraint (3.26) to convert the integer program to a convex one. We replace (3.26) by $0 \leq x_{ij} \leq 1, \forall (i,j) \in \mathcal{U} \times \mathcal{B}$. We call the resulting problem the ideal cell association problem and indicate it by $\mathbf{P_x}$ as the following

$$\mathbf{P_x}: \underset{\mathbf{x}}{\text{maximize}} \sum_{i \in \mathcal{U}} \sum_{j \in \mathcal{B}} x_{ij} a_{ij} \tag{3.29}$$

$$\begin{aligned} \text{subject to } & \sum_{i \in \mathcal{U}} x_{ij} \bar{n}_{ij}^{\mathrm{DL}} \leq N_j^{\mathrm{DL}}, \ \forall j \in \mathcal{B}, \\ & \sum_{i \in \mathcal{U}} x_{ij} \bar{n}_{ij}^{\mathrm{UL}} \leq N_j^{\mathrm{UL}}, \ \forall j \in \mathcal{B}, \\ & \sum_{j \in \mathcal{B}} x_{ij} \leq 1, \ \forall i \in \mathcal{U}, \\ & 0 \leq x_{ij} \leq 1, \ \forall (i,j) \in \mathcal{U} \times \mathcal{B}, \end{aligned} \tag{3.30}$$

where

$$a_{ij} = \big(w_i^{\mathrm{DL}} U_i(\bar{r}_{ij}^{\mathrm{DL}}) + w_i^{\mathrm{UL}} U_i(\bar{r}_{ij}^{\mathrm{UL}}) \big).$$

The above problem is a linear program in $\mathbf{x}$ that can be solved efficiently using well-established methods such as the simplex method [77]. We call the solution obtained by solving the linear program *the ideal solution*. Note that the ideal solution may not result in binary association indices. This can be problematic since it indicates some users are connected partially to several BSs. In order to produce binary association indices, we round the ideal solution to the closest integer. We call this solution *the rounding solution*. The value of the objective function obtained by applying the rounding solution is upper bounded by the value obtained by plugging in the ideal solution. The rounding solution is used as a base line solution with which we compare our distributed solution presented in the next section.

Moreover, we have observed in our simulations that results of the ideal and rounding solutions are very close. The rounding solution is always within 5% error margin of the ideal solution, which indicates that the ideal solution is mostly composed of 0s and 1s.

3.4 Distributed cell association solution

In this section, we present a distributed solution to the cell association phase of problem **P**. As mentioned in Section 3.2, the ability of users to estimate the number of RBs to satisfy downline and uplink outage QoS constraints greatly helps in devising a distributed scheme. As for the downlink minimum required number of RBs, we have shown that the users can estimate the average channel gain between themselves and all the BSs in the range by listening to BSs' unique pilot signals. By applying the average channel gains and the required QoS class in the downlink determined by the pair $(\gamma_i^{\mathrm{DL}}, T_i^{\mathrm{DL}})$ in (3.17) and (3.21), users can estimate $\bar{n}_{ij}^{\mathrm{DL}}$. However, estimating $\bar{n}_{ij}^{\mathrm{UL}}$ is not possible at the user end, unless the BSs inform the users of the uplink interference level seen by the BS. In the next subsection, we require the BSs to quantize the uplink interference levels and broadcast them using few number of bits. The users then can estimate the worst case interference level associated with the broadcasted quantized interference level, and in turn, the minimum number of RBs required to have the uplink QoS satisfied assuming the worst case interference level.

3.4.1 Worst case uplink outage probability and the associated required number of RBs

We require the BSs to broadcast the quantized version of the measured uplink interference levels along with their other reference signals. Note that the interference at each BS (uplink interference) is created by the users that are in the vicinity of and not connected to the investigated BS. Therefore, it can be assumed that the interference level for all the users that are going to be connected to this BS is identical. Let the interference level at BS j be

$$I_j^{\mathrm{UL}} = \sum_{k \in U_j} P_k^{\mathcal{U}} H_{kj}, \tag{3.31}$$

where U_j is the set of interfering users at BS j. We also assume that there is a lower and upper bound on the uplink interference level as the following

$$I_j^{\mathrm{UL}} \in [I_{\min}^{\mathrm{UL}}, I_{\max}^{\mathrm{UL}}]. \tag{3.32}$$

If BS j uses M bits to quantize the interference level, there are $L = 2^M$ different levels in the interval $[I_{\min}^{\mathrm{UL}}, I_{\max}^{\mathrm{UL}}]$. Then, if BS j measures the interference level to be I_j^{UL}, it transmits

$l_j \in \{0, 1, \cdots, L-1\}$ as the quantized interference level, where

$$l_j = \Big\lfloor \frac{I_j^{\mathrm{UL}} - I_{\min}^{\mathrm{UL}}}{\frac{I_{\max}^{\mathrm{UL}} - I_{\min}^{\mathrm{UL}}}{L}} \Big\rfloor. \tag{3.33}$$

In the above equation, $\lfloor \cdot \rfloor$ represents the floor function that rounds the argument to the largest integer less than or equal to the argument.

Upon receiving the value of l_j from BS j by a user, the user assumes that the highest (worst) interference in the l_j^{th} level is happening. Indicating this interference level by $\hat{I}_j^{\mathrm{UL}}$, we obtain

$$\hat{I}_j^{\mathrm{UL}} = I_{\min}^{\mathrm{UL}} + (l_j + 1)(\frac{I_{\max}^{\mathrm{UL}} - I_{\min}^{\mathrm{UL}}}{L}). \tag{3.34}$$

Replacing the term $\sum_{k \in B \setminus i} P_k^{\mathcal{U}} H_{kj}$ by $\hat{I}_j^{\mathrm{UL}}$ in (3.4), and in turn, modifying (3.6), (3.8), (3.10), (3.12) and (3.14), the worst case uplink outage probability that is indicated by $\hat{\mathrm{OP}}_{ij}^{\mathrm{UL}}$ can be defined as

$$\hat{\mathrm{PO}}_{ij}^{\mathrm{UL}} = \Pr\Big\{ n_{ij}^{\mathrm{UL}} \log_2\Big(\frac{P_i^{\mathcal{U}} H_{ij}}{\hat{I}_j^{\mathrm{UL}} + \Delta f N_0}\Big) \leq \gamma_i^{\mathrm{UL}} \Big\}. \tag{3.35}$$

In the above definition, the only RV is H_{ij} which is an exponentially distributed RV with parameter λ_{ij} that is measurable by the user. Therefore, the user can calculate the worst case outage probability as

$$\hat{\mathrm{PO}}_{ij}^{\mathrm{UL}} = 1 - e^{-\frac{\lambda_{ij}}{P_i^{\mathcal{U}}}(\Gamma_{ij}^{\mathrm{UL}}(\hat{I}_{ij}^{\mathrm{UL}} + \Delta f N_0))}, \tag{3.36}$$

where $\Gamma_{ij}^{\mathrm{UL}}$ is given in (3.20). Now, the new uplink outage QoS constraint determined by the pair $(\gamma_i^{\mathrm{UL}}, T_i^{\mathrm{UL}})$ is

$$\big(\hat{\mathrm{PO}}_{ij}^{\mathrm{UL}} = \Pr\{r_{ij}^{\mathrm{UL}} \leq \gamma_i^{\mathrm{UL}}\}\big) \leq T_i^{\mathrm{UL}}. \tag{3.37}$$

By applying (3.36) in (3.37), user i can estimate the minimum number of required RBs to satisfy the worst case uplink QoS constraint. Indicating this number by $\hat{n}_{ij}^{\mathrm{UL}}$, we have

$$\hat{n}_{ij}^{\mathrm{UL}} = \Big\lceil \frac{\gamma_i^{\mathrm{UL}}}{\log_2\big(1 + \frac{P_i^{\mathcal{U}}/\lambda_{ij}}{\hat{I}_j^{\mathrm{UL}} + \Delta f N_0} \log(\frac{1}{1 - T_i})\big)} \Big\rceil. \tag{3.38}$$

In the above equation, $\lceil \cdot \rceil$ represents the ceiling function that rounds the argument to the

smallest integer greater than or equal to the argument.

It should be noted that $\hat{n}_{ij}^{\mathrm{UL}} \geq \bar{n}_{ij}^{\mathrm{UL}}$, since in the worst case, the user assumes a higher level of uplink interference than what it actually is.

3.4.2 Cell association solution

As outlined in Section 3.2, we replace the downlink and uplink QoS constraints in $\mathbf{P}$ (C_4 and C_5) by $n_{ij}^{\mathrm{DL}} = \bar{n}_{ij}^{\mathrm{DL}}$ and $n_{ij}^{\mathrm{UL}} = \hat{n}_{ij}^{\mathrm{UL}}$, respectively, $\forall (i,j) \in \mathcal{U} \times \mathcal{B}$. $\bar{n}_{ij}^{\mathrm{DL}}$ and $\hat{n}_{ij}^{\mathrm{UL}}$ are the minimum number of RBs that user i needs from BS j to have the downlink QoS and uplink worst case QoS constraints satisfied while they are calculatable at the user end. Similar to the previous section, we relax the association constraints in $\mathbf{P}$ by replacing (3.26) with $0 \leq x_{ij} \leq 1, \forall (i,j) \in \mathcal{U} \times \mathcal{B}$. We relax the association constraints so that the combinatorial nature of the problem transforms into a continuous and convex one. Then the Lagrange dual decomposition method can be applied to search for a distributed scheme solving the resulting problem. The resulting cell association problem is indicated by $\hat{\mathbf{P}}_{\mathbf{x}}$ as in the following

$$\hat{\mathbf{P}}_{\mathbf{x}} : \underset{\mathbf{x}}{\text{maximize}} \sum_{i \in \mathcal{U}} \sum_{j \in \mathcal{B}} x_{ij} \hat{a}_{ij} \tag{3.39}$$

$$\text{subject to} \quad \sum_{i \in \mathcal{U}} x_{ij} \bar{n}_{ij}^{\mathrm{DL}} \leq N_j^{\mathrm{DL}}, \ \forall j \in \mathcal{B}, \tag{3.40}$$

$$\sum_{i \in \mathcal{U}} x_{ij} \hat{n}_{ij}^{\mathrm{UL}} \leq N_j^{\mathrm{UL}}, \ \forall j \in \mathcal{B}, \tag{3.41}$$

$$\sum_{j \in \mathcal{B}} x_{ij} \leq 1, \ \forall i \in \mathcal{U}, \tag{3.42}$$

$$0 \leq x_{ij} \leq 1, \ \forall (i,j) \in \mathcal{U} \times \mathcal{B}, \tag{3.43}$$

where

$$\hat{a}_{ij} = \left(w_i^{\mathrm{DL}} U_i(\bar{r}_{ij}^{\mathrm{DL}}) + w_i^{\mathrm{UL}} U_i(\hat{r}_{ij}^{\mathrm{UL}}) \right). \tag{3.44}$$

In the above equation, $\hat{r}_{ij}^{\mathrm{UL}}$ is the long term uplink rate that user i receives assuming the worst case uplink interference level $\hat{I}_{ij}^{\mathrm{UL}}$ and worst case minimum number of required uplink RBs $\hat{n}_{ij}^{\mathrm{UL}}$.

Similar to problem $\mathbf{P}_{\mathbf{x}}$ in the previous section, problem $\hat{\mathbf{P}}_{\mathbf{x}}$ is a linear optimization problem; therefore, it is also convex [72]. Moreover, it can be shown that Slater's condition holds for $\hat{\mathbf{P}}_{\mathbf{x}}$. Slater's condition is the necessary and sufficient condition for the strong duality property to hold [72]. The strong duality property of $\mathbf{P}_{\mathbf{x}}$ implies that the optimum value

of the Lagrange dual problem is identical to the optimum value of the original problem. Because of the strong duality property of problem $\hat{\mathbf{P}}_{\mathbf{x}}$, and also in an attempt to devise a distributed scheme, we choose to solve this problem using Lagrange dual decomposition method [73].

The Lagrangian of $\hat{\mathbf{P}}_{\mathbf{x}}$ is defined by keeping the constraints (3.42) and (3.43), and taking constraints (3.40) and (3.41) into the objective function. We also introduce $N_{\mathcal{B}} \times 1$ vectors μ^{DL} and μ^{UL} that contain the Lagrange multipliers associated with the downlink and uplink resource constraints of the BSs indicated by μ_j^{DL} and μ_j^{UL}. The Lagrangian of $\hat{\mathbf{P}}_{\mathbf{x}}$ is given by

$$\begin{aligned}\mathcal{L}(\mathbf{x},&\mu^{\mathrm{DL}},\mu^{\mathrm{UL}}) = \\ &\sum_{i\in\mathcal{U}}\sum_{j\in\mathcal{B}} x_{ij}\hat{a}_{ij} - \sum_{j\in\mathcal{B}}\mu_j^{\mathrm{DL}}\big(\sum_{i\in\mathcal{U}} x_{ij}\bar{n}_{ij}^{\mathrm{DL}} - N_j^{\mathrm{DL}}\big) \\ +&\sum_{i\in\mathcal{U}}\sum_{j\in\mathcal{B}} x_{ij}\hat{a}_{ij} - \sum_{j\in\mathcal{B}}\mu_j^{\mathrm{UL}}\big(\sum_{i\in\mathcal{U}} x_{ij}\hat{n}_{ij}^{\mathrm{UL}} - N_j^{\mathrm{DUL}}\big).\end{aligned} \tag{3.45}$$

Then, the Lagrange dual function of $\hat{\mathbf{P}}_{\mathbf{x}}$ is obtained from the Lagrangian as in the following

$$\begin{aligned}g(\mu^{\mathrm{DL}},\mu^{\mathrm{UL}}) = \sup_{\mathbf{x}} \quad &\sum_{i\in\mathcal{U}}\sum_{j\in\mathcal{B}} x_{ij}(\hat{a}_{ij} - \mu_j^{\mathrm{DL}}\bar{n}_{ij}^{\mathrm{DL}} - \mu_j^{\mathrm{UL}}\hat{n}_{ij}^{\mathrm{UL}}) \\ &+ \sum_{j\in\mathcal{B}}\mu_j^{\mathrm{DL}}N_j^{\mathrm{DL}} + \sum_{j\in\mathcal{B}}\mu_j^{\mathrm{UL}}N_j^{\mathrm{UL}} \qquad (3.46)\end{aligned}$$

$$\text{subject to} \;\; 0 \le x_{ij} \le 1, \;\forall (i,j) \in \mathcal{U}\times\mathcal{B}, \tag{3.47}$$

$$\sum_{j\in\mathcal{B}} x_{ij} \le 1, \;\forall i \in \mathcal{U}. \tag{3.48}$$

The Lagrange dual function $g(\mu^{\mathrm{DL}},\mu^{\mathrm{UL}})$ can be decoupled with respect to users; therefore, it can be written in the following form

$$\begin{aligned}g(\mu^{\mathrm{DL}},\mu^{\mathrm{UL}}) = &\sum_{i\in\mathcal{U}} g_i(\mu^{\mathrm{DL}},\mu^{\mathrm{UL}}) \\ &+ \sum_{j\in\mathcal{B}}\mu_j^{\mathrm{DL}}N_j^{\mathrm{DL}} + \sum_{j\in\mathcal{B}}\mu_j^{\mathrm{UL}}N_j^{\mathrm{UL}},\end{aligned} \tag{3.49}$$

where for all users $i \in \mathcal{U}$ we have

$$\begin{aligned}g_i(\mu^{\mathrm{DL}},\mu^{\mathrm{UL}}) = \sup_{x_{ij}, j\in\mathcal{B}} \quad &\sum_{j\in\mathcal{B}} x_{ij}\mathrm{QI}_{ij} \qquad (3.50) \\ \text{subject to} \;\; &0 \le x_{ij} \le 1, \; j \in \mathcal{B},\end{aligned}$$

$$\sum_{j\in\mathcal{B}} x_{ij} \leq 1.$$

In the above equation, QI_{ij} is called the qualification index of BS j from user i's point of view, and it is given by

$$\mathrm{QI}_{ij} = \hat{a}_{ij} - \mu_j^{\mathrm{DL}}\bar{n}_{ij}^{\mathrm{DL}} - \mu_j^{\mathrm{UL}}\hat{n}_{ij}^{\mathrm{UL}}, \quad \forall (i,j) \in \mathcal{U}\times\mathcal{B}. \tag{3.51}$$

If we require the BSs to broadcast their Lagrange multipliers in uplink and downlink, μ^{DL} and μ^{UL}, along with the quantized uplink interference level and other already existing reference signals, user i can calculate all the terms in QI_{ij}. Then, $g_i(\mu^{\mathrm{DL}}, \mu^{\mathrm{UL}})$ in (3.50) can be solved at the user end. Accordingly, the unique solution to the user's problem is

$$x_{ij} = \begin{cases} 1 & \text{if } j = j^* \\ 0 & \text{if } j \neq j^* \end{cases}, \ \forall i \in \mathcal{U}, \tag{3.52}$$

where

$$j^* = \underset{j\in\mathcal{B}}{\mathrm{argmax}}(\mathrm{QI}_{ij}), \ \forall i \in \mathcal{U}. \tag{3.53}$$

This procedure automatically produces binary association indices. Therefore, no additional rounding is required.

As for the Lagrange multipliers, we use the gradient descent method [72]. Therefore, we update the Lagrange multipliers for all BSs $j \in \mathcal{B}$ according to the following

$$\begin{aligned} \mu_j^{\mathrm{DL}}(t+1) &= \left[\mu_j^{\mathrm{DL}}(t) - \beta(t)\big(N_j^{\mathrm{DL}} - \sum_{i\in\mathcal{U}} x_{ij}\bar{n}_{ij}^{\mathrm{DL}}\big)\right]^+, \\ \mu_j^{\mathrm{UL}}(t+1) &= \left[\mu_j^{\mathrm{UL}}(t) - \beta(t)\big(N_j^{\mathrm{UL}} - \sum_{i\in\mathcal{U}} x_{ij}\hat{n}_{ij}^{\mathrm{UL}}\big)\right]^+, \end{aligned} \tag{3.54}$$

where the terms $\big(N_j^{\mathrm{DL}} - \sum_{i\in\mathcal{U}} x_{ij}\bar{n}_{ij}^{\mathrm{DL}}\big)$ and $\big(N_j^{\mathrm{UL}} - \sum_{i\in\mathcal{U}} x_{ij}\hat{n}_{ij}^{\mathrm{UL}}\big)$ are the partial derivatives of the Lagrangian with respect to the downlink and uplink Lagrange multipliers, respectively. In addition, the operator $[\cdot]^+$ returns the maximum of the argument in the operator and 0, and $\beta(t)$ is a step size that satisfies the following two conditions

$$\lim_{t\to\infty} \beta(t) = 0 \quad , \text{ and } \quad \sum_{t=1}^{\infty} \beta(t) = \infty. \tag{3.55}$$

The above conditions assure the convergence of the gradient descent method if the association indices are continuous variables of the form $0 \leq x_{ij} \leq 1$, as indicated by proposition 6.3.4 in [74]. Nevertheless, $\beta(t) = 0.5/t$ is used in our simulations, and in all cases the distributed scheme converged in less than 50 iterations; most of the times the convergence was reached in less than 25 iterations.

3.4.3 Distributed cell association scheme design

In this subsection, we describe the designed cell association scheme based on the analysis in the previous subsection.

Step 1: Initialization All BSs $j \in \mathcal{B}$ initialize their associated Lagrange multipliers, μ_j^{DL} and μ_j^{UL}, and broadcast them in the network. The BSs also measure the uplink interference levels and quantize them to obtain l_j. Each BS j broadcasts l_j along with μ_j^{DL}, μ_j^{UL}, and other reference signals.

Step 2: User request All Users $i \in \mathcal{U}$ listen to BSs and acquire λ_{ij}, μ_j^{DL}, μ_j^{UL}, and l_j for all BSs in their range. From these, users calculate $\bar{n}_{ij}^{\mathrm{DL}}$, $\hat{n}_{ij}^{\mathrm{UL}}$, and QI_{ij} for all the BSs in their range. Then, each user i sends an association request to the BS with the best QI_{ij} (BS j^* in (3.53)). The association request contains the required number of RBs in downlink and uplink, $\bar{n}_{ij}^{\mathrm{DL}}$, $\hat{n}_{ij}^{\mathrm{UL}}$.

Step3: User admission BSs receive the users' requests. If BSs can accommodate all the requests they receive without violating the resource budget constraints, an admission message will be sent to the users. Now, the users are connected to their desired BSs.

Step 4: BS Lagrange multiplier update BSs update their Lagrange multipliers according to (3.54). BSs also update the uplink interference level according to their new measurements. Each BS j broadcasts the new μ_j^{DL}, μ_j^{UL}, and l_j in the network. The scheme continues by going to step 2.

Few remarks on the scheme are as follows:

Remark 1 By inspecting (3.44) and (3.51), it can be seen that each user tends to send an association request to the BS that provides the best utility of rate with the lower required number of RBs. Users also tend to associate with BSs that have lower Lagrange multipliers (Lagrange multipliers can be interpreted as the price of connecting to a given BS). By inspecting (3.54), it can be seen that BS j increases its price if the load on BS j increases. As a result, users are guided towards less populated BSs in the network. These mechanisms achieve some levels of load balancing.

Remark 2 In this scheme, users receive only enough number of RBs to have their QoS constraints satisfied. This is in particular important in reducing the energy consumption.

Remark 3 In step 3, some BSs may not have enough RBs to accommodate all their user requests. This case is discussed in the next subsection.

3.4.4 Feasibility problem and admission control

In the distributed cell association scheme, the users determine the BS to which they want to connect through (3.53). This is while the users do not have any information on how many other users are requesting to connect to that BS, and how many available RBs are left for the BS to allocate to its users. As a consequence, BSs may violate their resource constraints in downlink or uplink (constraints (3.40) or (3.41)) upon admitting all the requests they receive. In other words, the association indices $\mathbf{x}$ is infeasible under such conditions. Apart from the fact that the infeasibility of the solution indicates a systematic problem, it also affects the convergence of the gradient descent method from a mathematical point of view. Therefore, at any instance where the solution is infeasible, it needs to be brought back to the feasible set. This motivates us to use the gradient projection method [75] instead of the gradient descent method.

In this chapter, we use a heuristic to project the association solution back to the feasible set. We add this heuristic as an intermediate step in step 2 of the distributed scheme described in the previous subsection. Firstly, we require the users to modify their request messages that they send to the BS with the best qualification index QI_{ij^*}, where j^* is given in (3.53). The users sort the BSs in their range according to their qualification index QI_{ij} in descending order. The request that user i sends to BS j^* contains this sorted list of BSs according to their QI_{ij}. The request also contains the number of RBs in downlink and uplink required from each BS in the list.

BSs process the requests received from the users. If BS j has enough RBs in the downlink and uplink to accommodate all the user requests, those users will be admitted to BS j. Otherwise, if the uplink resource budget is violated, BS j forwards the request of users that consume the highest number of uplink RBs to the indicated second best BS in the lists until the uplink resource constraint is satisfied. The second best BS checks whether it can accommodate all the user requests it has received. If not, the second best BS forwards the request of the users consuming the highest number of RBs to the next best BS according to the list in the users' requests. The procedure continues until all users are accommodated. The same procedure is performed if the downlink resource budget is violated. If both resource constraints in downlink and uplink are violated, the BS separately processes the downlink and uplink and forwards the requests to the next best BS according to the lists provided in the users' requests.

This intermediate step achieves further load balancing by avoiding some BSs to get overpopulated.

In the next subsection, we briefly address distributing the rest of the RBs available at the BSs.

3.4.5 RB distribution phase

The cell association phase of problem $\mathbf{P}$ has been addressed in Sections 3.3 and 3.4. In this subsection, we use the association indices $\mathbf{x}$ from the distributed cell association phase solution and solve for $\mathbf{n}^{\mathrm{DL}}$ and $\mathbf{n}^{\mathrm{UL}}$ to distribute the remaining RBs and further improve the users' rates. If we define $\mathcal{U}_j$ as the set of users connected to BS j, the RB distribution problem at each BS $j \in \mathcal{B}$, which is indicated by $\mathbf{P}_{\mathbf{n},j}$, can be written as

$$\mathbf{P}_{\mathbf{n},j}: \underset{\tilde{n}_{ij}^{\mathrm{DL}},\tilde{n}_{ij}^{\mathrm{UL}},i\in\mathcal{U}_j}{\text{maximize}} \sum_{i\in\mathcal{U}_j} \left(w_i^{\mathrm{DL}} U_i(n_{ij}^{\mathrm{DL}}\bar{c}_{ij}^{\mathrm{DL}}) + w_i^{\mathrm{UL}} U_i(n_{ij}^{\mathrm{UL}}\bar{c}_{ij}^{\mathrm{UL}})\right) \tag{3.56}$$

$$\text{subject to} \quad \sum_{i\in\mathcal{U}_j} n_{ij}^{\mathrm{DL}} \le N_j^{\mathrm{DL}}, \tag{3.57}$$

$$\sum_{i\in\mathcal{U}_j} n_{ij}^{\mathrm{UL}} \le N_j^{\mathrm{UL}}, \tag{3.58}$$

$$n_{ij}^{\mathrm{DL}} = \bar{n}_{ij}^{\mathrm{DL}} + \tilde{n}_{ij}^{\mathrm{DL}}, \quad \forall i \in \mathcal{U}_j, \tag{3.59}$$

$$n_{ij}^{\mathrm{UL}} = \hat{n}_{ij}^{\mathrm{UL}} + \tilde{n}_{ij}^{\mathrm{UL}}, \quad \forall i \in \mathcal{U}_j. \tag{3.60}$$

In problem $\mathbf{P}_{\mathbf{n},j}$, $\bar{n}_{ij}^{\mathrm{DL}}$ and $\hat{n}_{ij}^{\mathrm{UL}}$ are the number of already allocated RBs by the distributed cell association scheme in downlink and uplink, respectively. However, $\tilde{n}_{ij}^{\mathrm{DL}}$ and $\tilde{n}_{ij}^{\mathrm{UL}}$ are the extra RBs that are allocated to the users connected to BS j through solving $\mathbf{P}_{\mathbf{n},j}$. Moreover, It is implicitly assumed that $\tilde{n}_{ij}^{\mathrm{DL}}$ and $\tilde{n}_{ij}^{\mathrm{UL}}$ are integer values that satisfy $\bar{n}_{ij}^{\mathrm{DL}} \le \tilde{n}_{ij}^{\mathrm{DL}} \le N_j^{\mathrm{DL}}$ and $\hat{n}_{ij}^{\mathrm{UL}} \le \tilde{n}_{ij}^{\mathrm{UL}} \le N_j^{\mathrm{UL}}$. It is also implicitly assumed that w_i^{DL} and w_i^{UL} are not zero. It can be seen that problem $\mathbf{P}_{\mathbf{n},j}$ can be decoupled with respect to uplink and downlink. Therefore, problem $\mathbf{P}_{\mathbf{n},j}$ is broken into two sub-problems for each BS $j \in \mathcal{B}$: downlink RB distribution problem ($\mathbf{P}_{\mathbf{n},j}^{\mathrm{DL}}$), and uplink RB distribution problem ($\mathbf{P}_{\mathbf{n},j}^{\mathrm{UL}}$):

$$\mathbf{P}_{\mathbf{n},j}^{\mathrm{DL}}: \underset{\tilde{n}_{ij}^{\mathrm{DL}},i\in\mathcal{U}_j}{\text{maximize}} \sum_{i\in\mathcal{U}_j} w_i^{\mathrm{DL}} U_i(n_{ij}^{\mathrm{DL}}\bar{c}_{ij}^{\mathrm{DL}}) \tag{3.61}$$

$$\text{subject to} \quad \sum_{i\in\mathcal{U}_j} n_{ij}^{\mathrm{DL}} \le N_j^{\mathrm{DL}}, \tag{3.62}$$

$$n_{ij}^{\mathrm{DL}} = \bar{n}_{ij}^{\mathrm{DL}} + \tilde{n}_{ij}^{\mathrm{DL}}, \quad \forall i \in \mathcal{U}_j, \tag{3.63}$$

$$\mathbf{P}^{\mathrm{UL}}_{\mathbf{n},j}: \underset{\tilde{n}^{\mathrm{UL}}_{ij}, i\in\mathcal{U}_j}{\text{maximize}} \sum_{i\in\mathcal{U}_j} w^{\mathrm{UL}}_i U_i(n^{\mathrm{UL}}_{ij}\bar{c}^{\mathrm{UL}}_{ij}) \tag{3.64}$$

$$\text{subject to} \sum_{i\in\mathcal{U}_j} n^{\mathrm{UL}}_{ij} \leq N^{\mathrm{UL}}_j, \tag{3.65}$$

$$n^{\mathrm{UL}}_{ij} = \hat{n}^{\mathrm{UL}}_{ij} + \tilde{n}^{\mathrm{UL}}_{ij}, \quad \forall i \in \mathcal{U}_j. \tag{3.66}$$

If we assume that $\tilde{n}^{\mathrm{DL}}_{ij}$ and $\tilde{n}^{\mathrm{UL}}_{ij}$ are continuous variables, it can be shown that both $\mathbf{P}^{\mathrm{DL}}_{\mathbf{n},j}$ and $\mathbf{P}^{\mathrm{UL}}_{\mathbf{n},j}$ are convex optimization problems for which strong duality property holds since the objective functions are composed of concave utility functions and the constraints are affine [72]. In fact, both $\mathbf{P}^{\mathrm{DL}}_{\mathbf{n},j}$ and $\mathbf{P}^{\mathrm{UL}}_{\mathbf{n},j}$ have a similar structure to that of water-filling problem. Therefore, $\tilde{n}^{\mathrm{DL}}_{ij}$ and $\tilde{n}^{\mathrm{UL}}_{ij}$ can be found using KKT conditions [72]. After writing the KKT conditions for $\mathbf{P}^{\mathrm{DL}}_{\mathbf{n},j}$, the number of extra RBs in downlink are

$$\tilde{n}^{\mathrm{DL}}_{ij} = \left[\frac{1}{\bar{c}^{\mathrm{DL}}_{ij}}(U_i^{'})^{-1}\Big(\frac{\nu^{\mathrm{DL}}}{w^{\mathrm{DL}}_i \bar{c}^{\mathrm{DL}}_{ij}}\Big) - \bar{n}^{\mathrm{DL}}_{ij}\right]^{+}, \ \forall i \in \mathcal{U}_j, \tag{3.67}$$

where ν^{DL} is the unique solution of the following equation

$$\sum_{i\in\mathcal{U}_j} \max\left\{\frac{1}{\bar{c}^{\mathrm{DL}}_{ij}}(U_i^{'})^{-1}\Big(\frac{\nu^{\mathrm{DL}}}{w^{\mathrm{DL}}_i \bar{c}^{\mathrm{DL}}_{ij}}\Big), \bar{n}^{\mathrm{DL}}_{ij}\right\} = N^{\mathrm{DL}}_j. \tag{3.68}$$

In addition, $(U_i^{'})^{-1}(\cdot)$ is the inverse of the derivative of $U_i(\cdot)$ with respect to $\tilde{n}^{\mathrm{DL}}_{ij}$. The solution of the above equation is unique since $U_i(\cdot)$s are concave and strictly increasing functions, hence, $(U_i^{'})^{-1}(\cdot)$ and its weighted sum is a strictly increasing (monotonic) function of ν^{DL}. This equation can be solved efficiently using a numerical search method. The resulting $\tilde{n}^{\mathrm{DL}}_{ij}$ is then rounded to the closest integer less than or equal to $\tilde{n}^{\mathrm{DL}}_{ij}$ in order to have integer number of RBs.

The number of extra RBs for the uplink users at each BS can be obtained in a similar manner.

3.5 Numerical simulation results

In this section, the joint uplink and downlink distributed cell association scheme described in Section 3.4 is examined through numerical simulations. We consider three tires of BSs. In 1000 m×1000 m cells, we fix 1 macro BS at the centre of the cell and randomly locate 5 micro BSs, 10 femto BSs, and 200 users in each cell, unless otherwise stated. The transmitting power of macro BSs, micro BSs, femto BSs, and users are set to 46, 35, 20, and 20 dBm,

respectively. The large scale path loss between users and macro BSs is modelled as $PL(d) = 34 + 40\log_{10}(d)$, where d is the distance in meters. The large scale path loss between users and micro or femto BSs is $PL(d) = 37 + 30\log_{10}(d)$. Furthermore, shadowing effect comes on top of the large scale path loss as a lognormal RV with 8 dB of standard deviation, while exponentially distributed RVs with unit variance represent the Rayleigh small scale fading. Considering that RBs in LTE standard are 180 kHz wide in frequency domain, the thermal noise power is set to -111.45 dBm. The RB budget in both downlink and uplink is 400, 200, and 100 for macro, micro and femto BSs, respectively. Finally, we assume that a proportionally fair scheduler is implemented at the BSs with scheduling interval of 1 second. In the following, the developed schemes refer to the distributed and base line schemes, while downlink oriented scheme refers to the developed schemes with $w_{\mathrm{DL}} = 1$ or the maximum SINR scheme, and uplink oriented scheme refers to either of developed schemes with $w_{\mathrm{UL}} = 1$.

3.5.1 Rate cumulative distribution functions

As mentioned in [44], the rate distribution is a more meaningful metric compared to SINR or spectral efficiency distribution to compare different schemes in HetNets. Therefore, we show the cumulative distribution function (CDF) of the instantaneous rates in downlink and uplink in Figures 3.1 and 3.2. In these two figures, the rate threshold and outage probability requirement of all users in the downlink and uplink is set to $\gamma^{\mathrm{DL}} = 1.2$ bits/s and $\gamma^{\mathrm{UL}} = 0.6$ bits/s and $T = 10\%$. Moreover, The number of uplink interference quantization bits is set to $M = 8$.

In Figures 3.1 and 3.2, the downlink and uplink rate CDF is plotted for 7 cases. The downlink and uplink rate CDF of the distributed and base line cell association schemes with $w_{\mathrm{DL}}, w_{\mathrm{UL}} = 1, 0.5$, and 0 comprises 6 curves, and the downlink and uplink rate CDF of the maximum SINR scheme is the seventh case. In the case of $w_{\mathrm{DL}} = 0$, we disregard the downlink resource constraints to let the developed schemes focus only on the uplink. Therefore, the downlink resource constraints can be violated for some BSs. Similarly, since admission control is not considered in maximum SINR scheme, some BSs may allocate more RBs than their budget to users in downlink and have the downlink resource constraints violated. In these cases, the BS scheduler needs to schedule some users in the next scheduling intervals, leading to some reduction in the perceived data rate by the users. This rate reduction is taken into account in our simulations. The same arguments hold for uplink data rates in the developed schemes with $w_{\mathrm{UL}} = 0$, and maximum SINR scheme.

As it can be seen in Fig. 3.1, the distributed and base line schemes with $w_{\mathrm{DL}} = 1$ and 0.5 result in downlink rate CDFs that lie below the curve resulted from maximum SINR

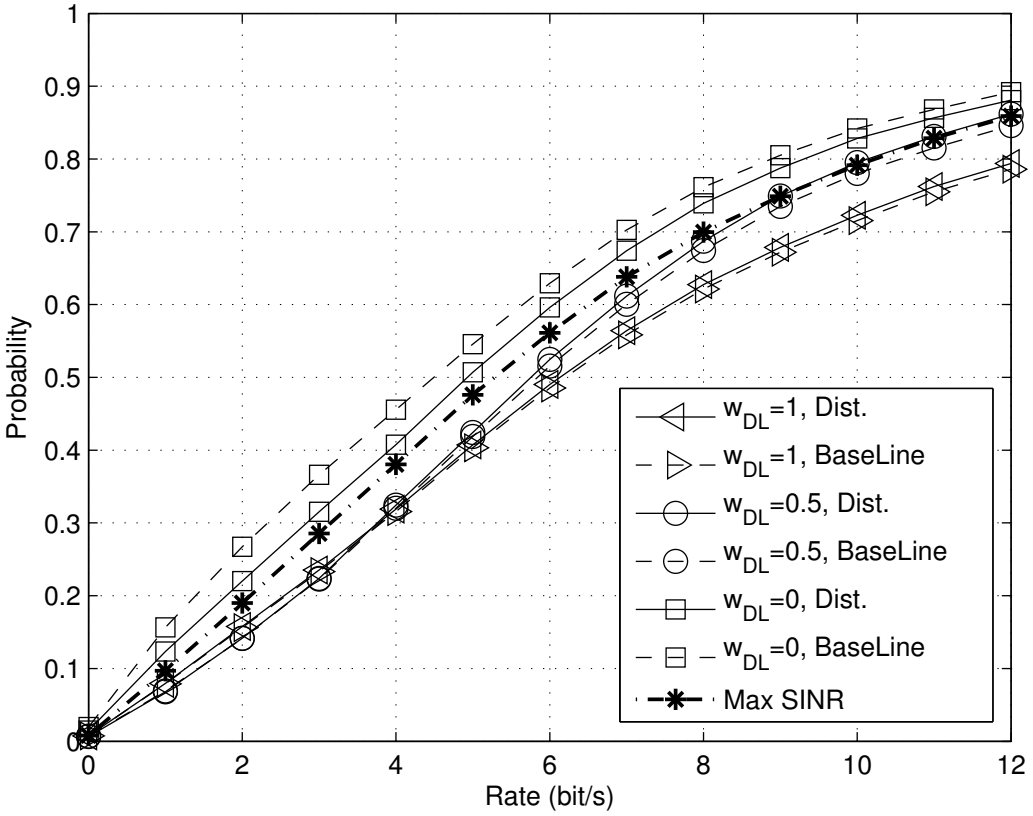

Figure 3.1: Downlink rate CDFs for the developed schemes with various w_{DL} and maximum SINR scheme, where $\gamma^{\mathrm{DL}} = 1.2$ bits/s, $\gamma^{\mathrm{UL}} = 0.6$ bits/s, $T = 10\%$, and $M = 8$

scheme. This implies that the developed schemes outperform maximum SINR scheme in the downlink when $w_{\mathrm{DL}} = 1$ and 0.5. However, with $w_{\mathrm{DL}} = 0$, both distributed and base line schemes perform worse than the maximum SINR since developed schemes in this case are uplink oriented ($w_{\mathrm{UL}} = 1$ when $w_{\mathrm{DL}} = 0$), while maximum SINR is a downlink oriented scheme. Furthermore, since the developed schemes are only downlink oriented with $w_{\mathrm{DL}} = 1$, we observe a better downlink performance compared to the case of $w_{\mathrm{DL}} = 0.5$ in which the developed schemes are both uplink and downlink aware. Another observation on this figure is that the performance of the distributed and base line schemes in downlink is very close with $w_{\mathrm{DL}} = 1$. As $w_{\mathrm{DL}} = 1$ results in identical optimization problems for the distributed and base line schemes in downlink, the closeness of the curves obtained from the distributed and base line schemes shows the precision. The performance obtained from distributed and base line schemes in downlink for $w_{\mathrm{DL}} = 0.5$ are also close to each other since no quantization has been introduced in the downlink.

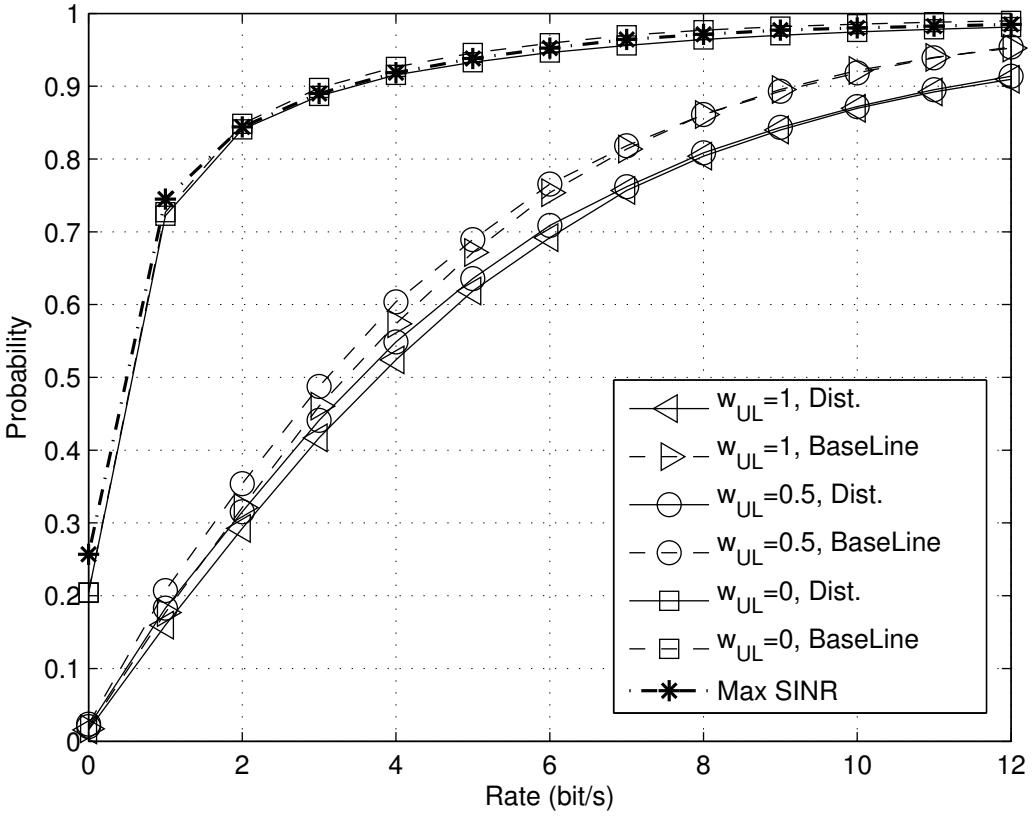

Figure 3.2: Uplink rate CDFs for the developed schemes with various w_{UL} and maximum SINR scheme, where $\gamma^{\mathrm{DL}} = 1.2$ bits/s, $\gamma^{\mathrm{UL}} = 0.6$ bits/s, $T = 10\%$, and $M = 8$

In Fig. 3.2, we can see the uplink counterpart of Fig. 3.1. Similar to downlink, the developed schemes with $w_{\mathrm{UL}} = 1$ show the best performance, which are followed by the performance of the developed schemes with $w_{\mathrm{UL}} = 0.5$, while the worst uplink performance belongs to maximum SINR scheme. Also, maximum SINR performs worse in uplink compared to its downlink counterpart since this scheme is downlink oriented. The performance of the distributed and base line schemes with $w_{\mathrm{UL}} = 0$ is somewhat the same as in maximum SINR scheme. However, as opposed to the downlink case, the distributed scheme shows higher rates than those of the base line scheme for the cases of $w_{\mathrm{UL}} = 1$ and 0.5. This is because in the distributed scheme, the users see the worst case uplink interference resulted from the quantization process. Assuming worst uplink interference, users request for more RBs to satisfy the worst case uplink QoS constraints.

From another perspective, by zooming in at the left bottom corner of Figures 3.1 and 3.2, we can verify whether the outage QoS constraints are satisfied. We also can compare

the rate of cell edge users. As for the QoS in downlink, the outage probabilities resulted from the distributed and base line schemes with minimum rate of $\gamma^{\mathrm{DL}} = 1.2$ bits/s are 9.3% and 8.1% for the cases of $w_{\mathrm{DL}} = 1$ and 0.5, respectively, which are less than the required outage probability of $T = 10\%$. This is while the maximum SINR scheme cannot satisfy the downlink QoS constraints. As for the QoS in uplink, the outage probabilities of 10%, 11% , 12%, and 14% are observed for the schemes of distributed with $w_{\mathrm{UL}} = 1$ and 0.5, and base line with $w_{\mathrm{UL}} = 1$ and 0.5, respectively, for $\gamma^{\mathrm{UL}} = 0.6$ bits/s. The outage QoS constraints are only satisfied for the uplink oriented distributed scheme. This is because the interference level that is reported by the BSs in the uplink is for the time that the new users in the network are not associated yet. After the association process, the uplink interference levels change depending on the association pattern. The new pattern and resulting interference levels change the outage probabilities which cannot be known beforehand at the user end. However, the conservative nature of the distributed scheme leads users closer to satisfying the QoS constraints. In fact, by studying Fig. 3.3, we will see that by decreasing the number of quantization bits we can make the scheme more conservative and get closer to the required QoS by the users at the expense of consuming more RBs. It is worth mentioning that the uplink rates resulted from maximum SINR scheme drop below the required rate threshold with probability of around 50%. We define the cell edge users as the users that experience the lowest 10% rates. In the downlink, the rate gains of up to 1.5 is observed for $\gamma^{\mathrm{DL}} = 1.2$ bits/s. In our simulations, we have observed that this rate gain increases by increasing the minimum rate threshold γ^{DL}. In the uplink, on the other hand, the gain is more significant. As it can be seen in Fig. 3.2, users experience rates below the minimum value of the rates set in our the simulations (0.1 bits/s) with probability of more than 20%. Therefore, with the current definition of cell edge users, very large uplink rate gains are resulted. If we modify the definition of cell edge users to users with the worst 40% rates, the uplink rate gain is around 7 for $\gamma^{\mathrm{UL}} = 0.6$ bits/s. According to our simulations, this gain also increases by increasing γ^{UL}.

Fig. 3.3 shows the effects of number of uplink quantization bits M and uplink minimum rate threshold γ^{UL} on the uplink rate CDFs. CDF curves for $M = 8$, and 10, $\gamma^{\mathrm{UL}} = 0.5$, and 0.7 bits/s, distributed, base line, and maximum SINR schemes, and $w_{\mathrm{UL}} = 1$ are demonstrated. The depth of quantization M reduces the gap between base line and distributed schemes performance, implying that reducing the number of quantization bits provides higher rates to users at the expense of spending more RBs. Decreasing M also increases the likelihood of satisfying the uplink QoS constraints. Moreover, increasing minimum uplink rate threshold γ^{UL} increases the gap between developed schemes and maximum SINR scheme, implying that higher rates are provided to users by increasing γ^{UL}. This is while SINR

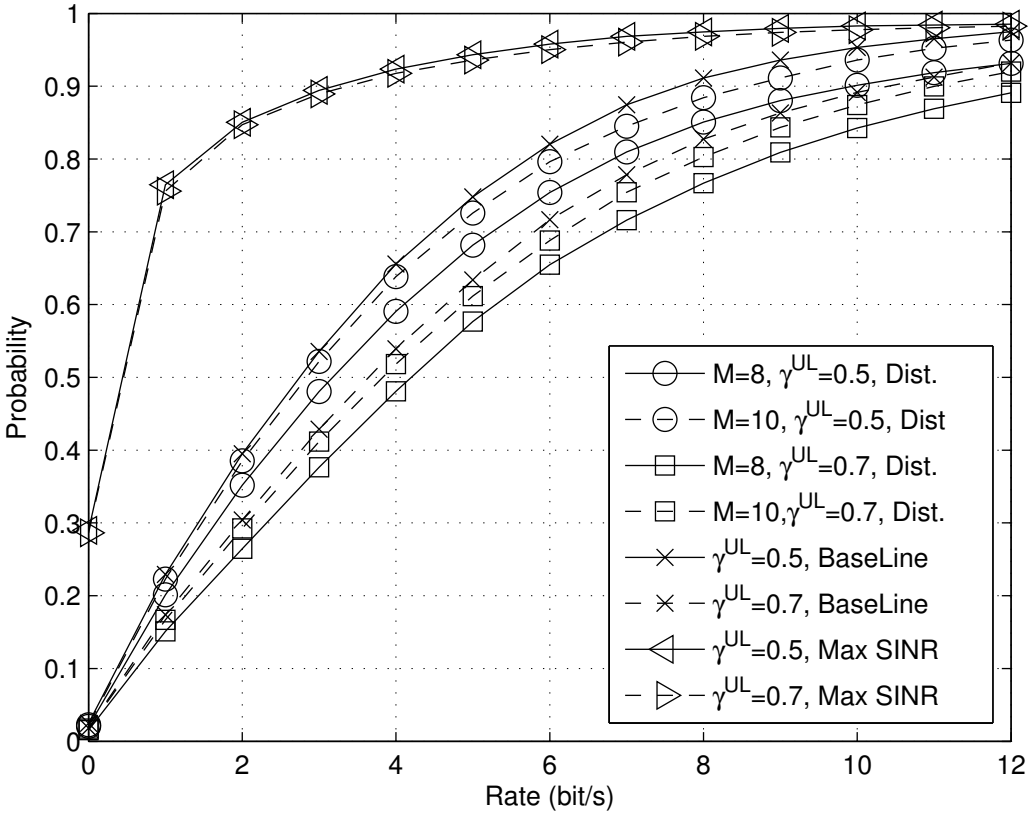

Figure 3.3: Uplink rate CDFs for the distributed scheme with various M and γ^{UL}, and base line and maximum SINR schemes with various γ^{UL}, where $w_{\mathrm{UL}} = 1$

scheme does not respond to minimum uplink rate threshold since maximum SINR does not take into account γ^{UL} in finding the cell association pattern. We have observed through simulations that minimum rate threshold plays a similar role in downlink rates for the developed schemes as well as the maximum SINR scheme. In downlink, maximum SINR scheme responds to changing γ^{DL} since it is downlink oriented and γ^{DL} is considered. However, a figure containing downlink CDF curves for various γ^{DL} is not included here.

3.5.2 The effect of number of femto BSs

Figures 3.4 and 3.5 show the effect of number of femto BSs on the sum utility of rates in downlink and uplink, respectively. The logarithmic utility function of $U(x) = \log(1 + x)$ is used in the simulations. In Fig. 3.4, the utility of rate curves in downlink are shown for the schemes of distributed with $w_{\mathrm{DL}} = 1, 0.5$, and 0, base line with $w_{\mathrm{DL}} = 1, 0.5$, and 0.5, and maximum SINR. Fig. 3.5 contains utility of rate curves in uplink for the same schemes as

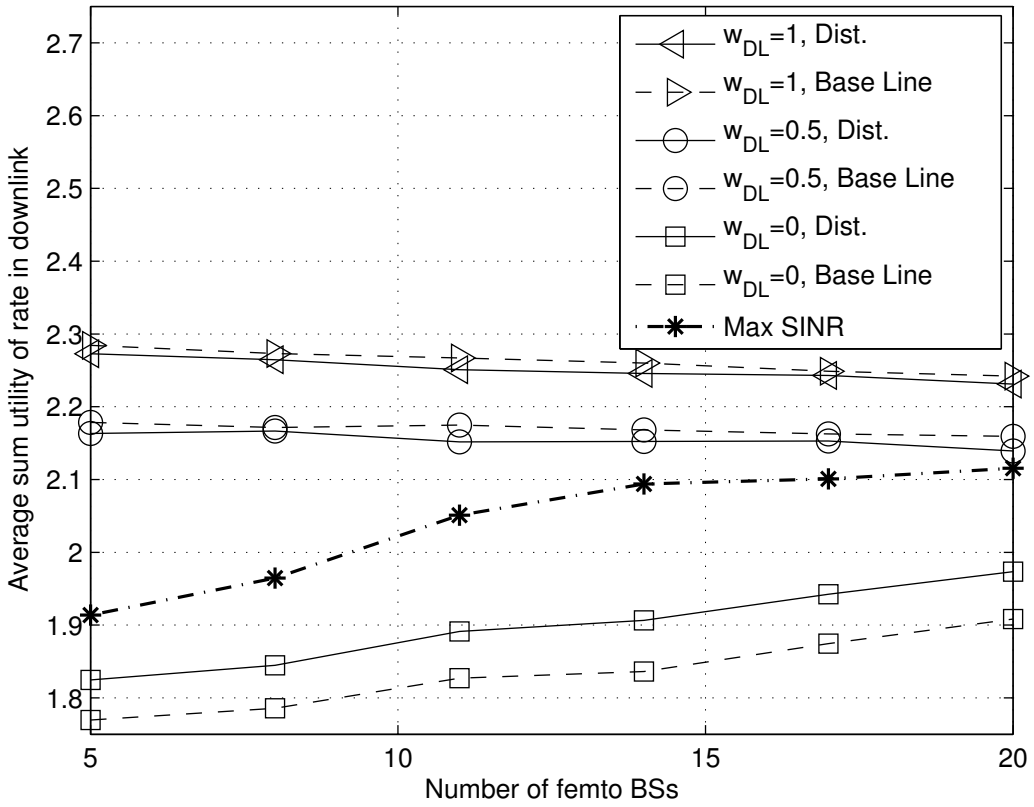

Figure 3.4: Downlink average utility of rate against number of femto BSs for the developed schemes with various w_{DL} and maximum SINR scheme, where $\gamma^{\mathrm{DL}} = 1.2$ bits/s, $\gamma^{\mathrm{UL}} = 0.6$ bits/s, $T = 10\%$, and $M = 10$

in Fig. 3.4.

In Fig. 3.4, as expected from previous figures, the downlink oriented versions of the developed schemes show the best performances, followed by the performances of developed schemes with $w_{\mathrm{DL}} = 0.5$. Maximum SINR curve falls between the curves from the developed schemes with $w_{\mathrm{DL}} = 1$ and 0.5, and the uplink oriented version of the developed schemes. Moreover, increasing the number of femto BSs enhances the performance of maximum SINR and developed schemes with $w_{\mathrm{DL}} = 0$, due to more availability of RBs in the network. The downlink aware versions of the developed schemes also show a slightly worse performance with increasing the number of BSs, which is due to introducing more interference in the downlink by increasing the number of BSs. Similar trends are observed for uplink in Fig. 3.5, except that the uplink aware versions of the developed schemes keep the utility around a constant. This is because increasing the number of BSs does not change the interference levels in uplink. In addition, as expected, the distributed scheme outperforms the base line

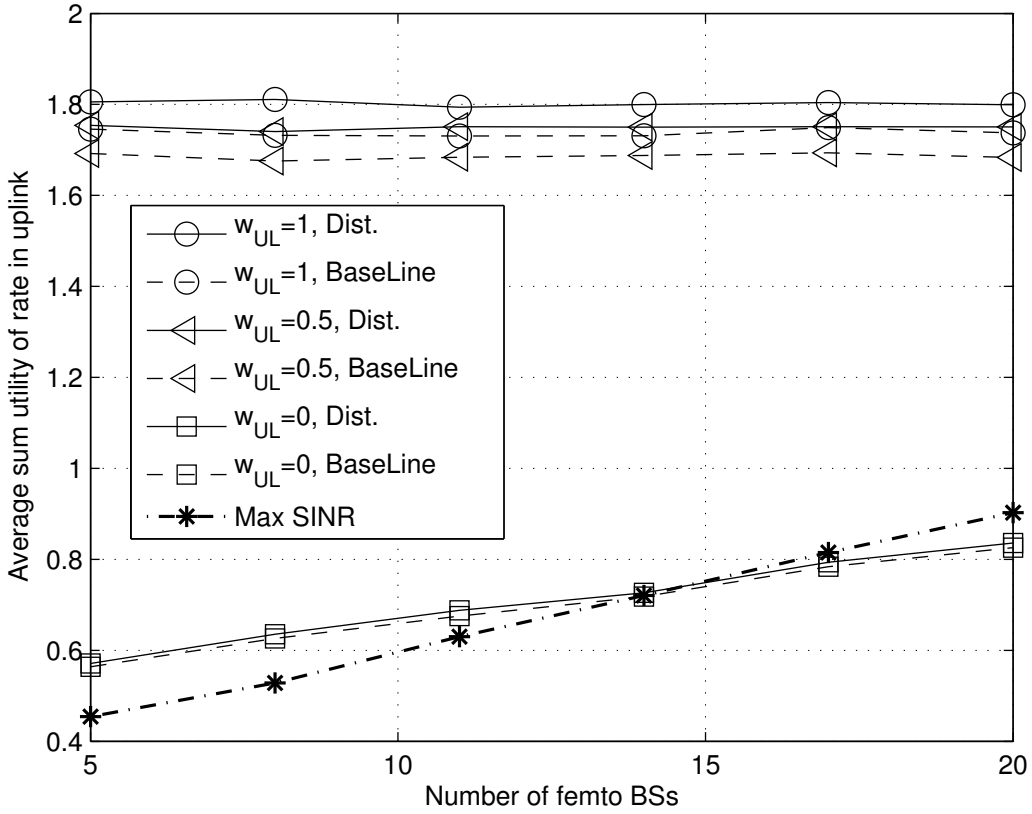

Figure 3.5: Uplink average utility of rate against number of femto BSs for the developed schemes with various w_{UL} and maximum SINR scheme, where $\gamma^{\mathrm{DL}} = 1.2$ bits/s, $\gamma^{\mathrm{UL}} = 0.6$ bits/s, $T = 10\%$, and $M = 10$

scheme at the expense of consuming more RBs.

3.5.3 The effect of number of users

Figures 3.6 and 3.7 show the effect of number of users on the sum utility of rates in downlink and uplink, respectively. The logarithmic utility function of $U(x) = \log(1+x)$ is used in the simulations. In Fig. 3.6, the utility of rate curves in downlink are shown for the schemes of distributed with $w_{\mathrm{DL}} = 1, 0.5$, and 0, base line with $w_{\mathrm{DL}} = 1, 0.5$, and 0.5, and maximum SINR. Fig. 3.6 contains utility of rate curves in uplink for the same schemes as in Fig. 3.7. As expected, the developed schemes with proper weights outperform the maximum SINR scheme in both downlink and uplink. However, increasing the number of users in the network worsens the downlink performance of the developed schemes with $w_{\mathrm{DL}} = 0$, and maximum SINR scheme. This is because more users require more RBs, which increases the likelihood

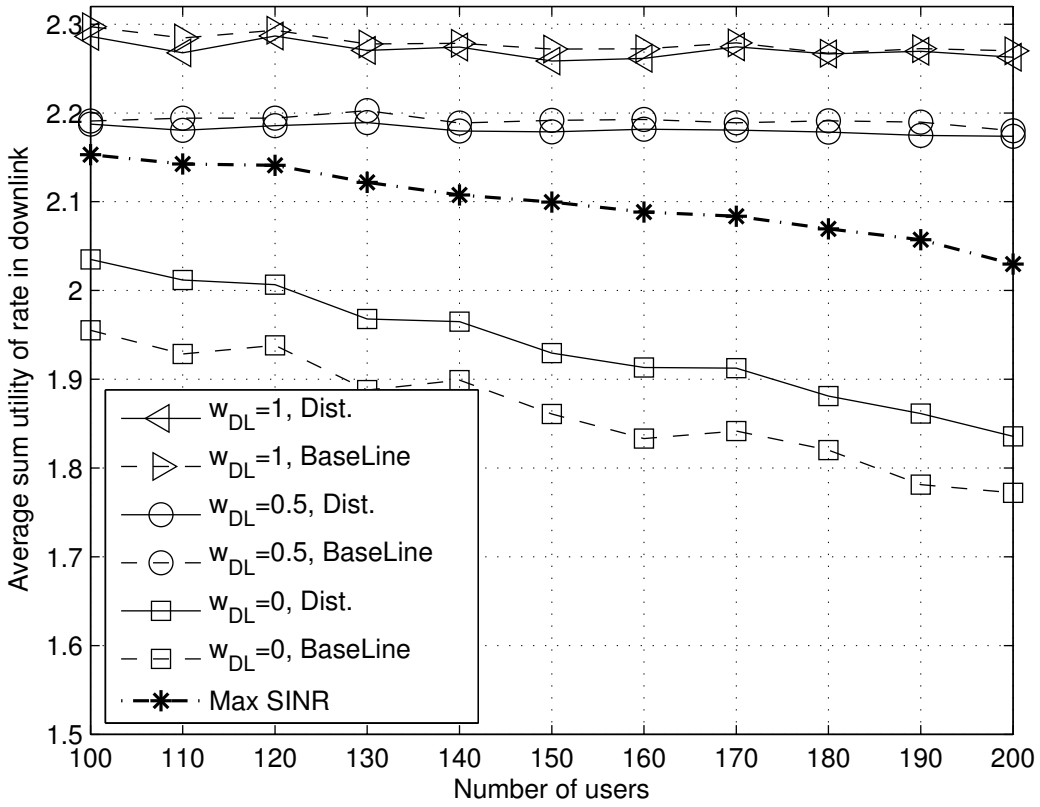

Figure 3.6: Downlink average utility of rate against number of users for the developed schemes with various w_{DL} and maximum SINR scheme, where $\gamma^{\mathrm{DL}} = 1.2$ bits/s, $\gamma^{\mathrm{UL}} = 0.6$ bits/s, $T = 10\%$, and $M = 10$

of having overloaded BSs in the downlink of developed schemes with $w_{\mathrm{DL}} = 0$ and maximum SINR scheme. However, the downlink aware versions of the developed schemes keep the utility in the downlink around a constant. In the uplink, the same trend is observed for the developed schemes with $w_{\mathrm{UL}} = 0$ as well as the maximum SINR scheme. However, the uplink aware versions of the developed schemes also show a slightly worse performance with increasing the number of users, which is due to introducing more interference in the uplink by increasing the number of users.

3.5.4 The effect of distributing the remaining RBs

By far, in all our simulations, we have considered only the base line and distributed cell association algorithms solving the optimization problems $\mathbf{P_x}$ and $\hat{\mathbf{P}}_{\mathbf{x}}$. The effect of distributing the remaining RBs after the cell association phase for downlink (solving $\mathbf{P}^{\mathrm{DL}}_{\mathbf{n},j}$ on top of the

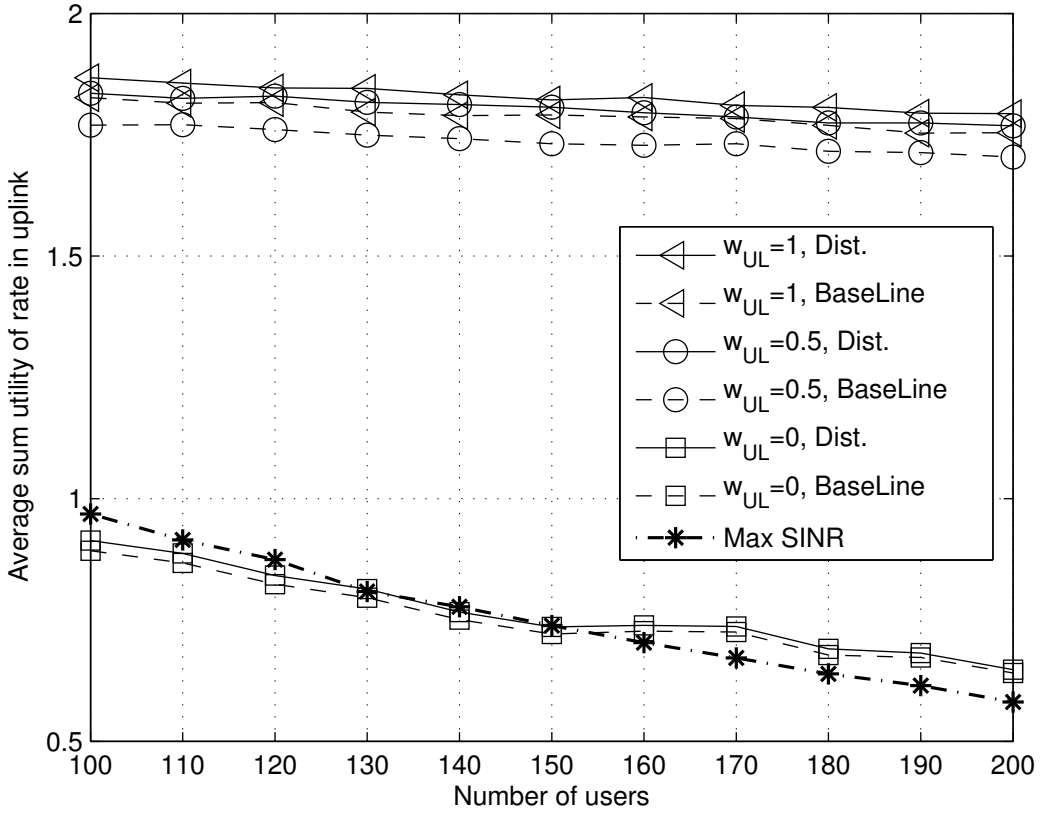

Figure 3.7: Uplink average utility of rate against number of users for the developed schemes with various w_{UL} and maximum SINR scheme, where $\gamma^{\mathrm{DL}} = 1.2$ bits/s, $\gamma^{\mathrm{UL}} = 0.6$ bits/s, $T = 10\%$, and $M = 10$

cell association problem $\mathbf{P_x}$ or $\hat{\mathbf{P}}_\mathbf{x}$) and uplink (solving $\mathbf{P}^{\mathrm{UL}}_{\mathbf{n},j}$ on top of the cell association problem $\mathbf{P_x}$ or $\hat{\mathbf{P}}_\mathbf{x}$) problems is demonstrated in Figures 3.8 and 3.9, respectively. In Fig. 3.8, the downlink average utility of rate against minimum downlink rate threshold γ^{DL} for the developed schemes with $w_{\mathrm{DL}} = 1$ and $T = 10\%$ are shown. In Fig. 3.9, the uplink average utility of rate against minimum uplink rate threshold γ^{UL} for the developed schemes with $w_{\mathrm{UL}} = 1$, $T = 10\%$, and $M = 10$ are plotted. The first observation on these two figures is that the developed algorithms with the remaining RBs significantly outperform the results obtained through the base line and distributed cell association schemes. Furthermore, by increasing the rate threshold, the performance of the base line and distributed cell association schemes get close to the performance of these schemes with the remaining RBs. This trend is seen since more RBs are required to satisfy QoS constraints with higher rate thresholds, leaving less overall unused RBs in the network. Distributing less unused RBs among users leads to a less improvement over cell association schemes.

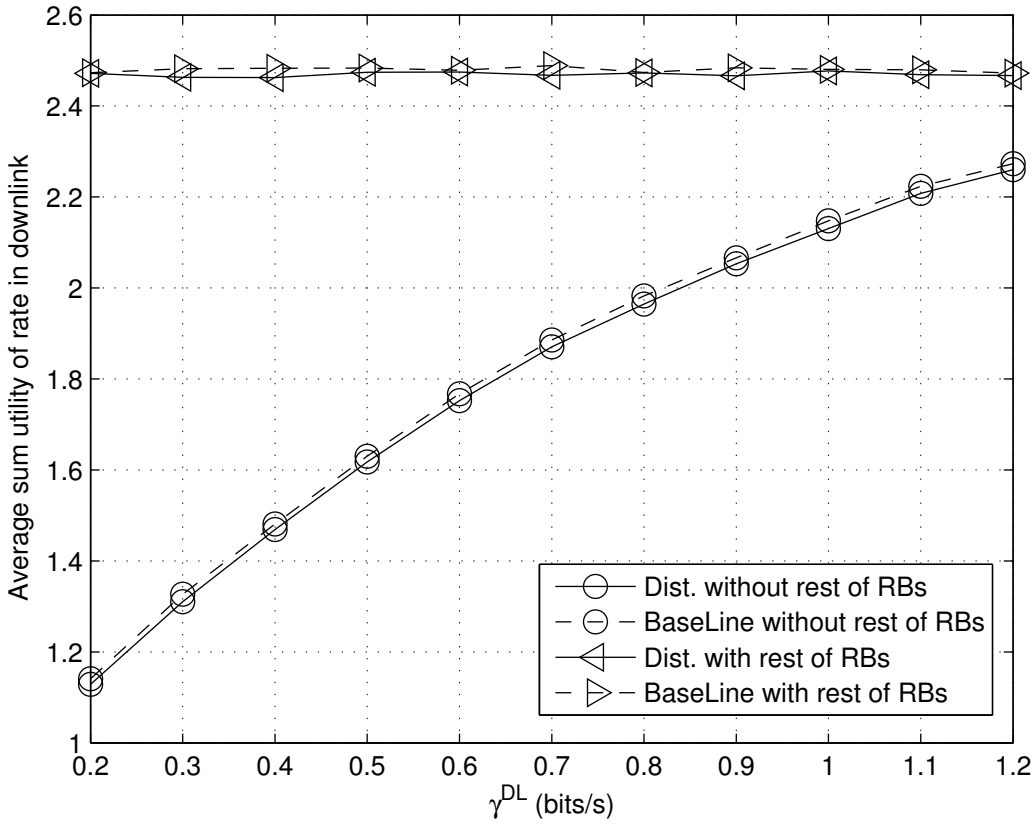

Figure 3.8: Downlink average utility of rate against minimum downlink rate threshold for the developed schemes with $w_{\mathrm{DL}} = 1$ and $T = 10\%$, showing the effect of distributing the rest of RBs in downlink

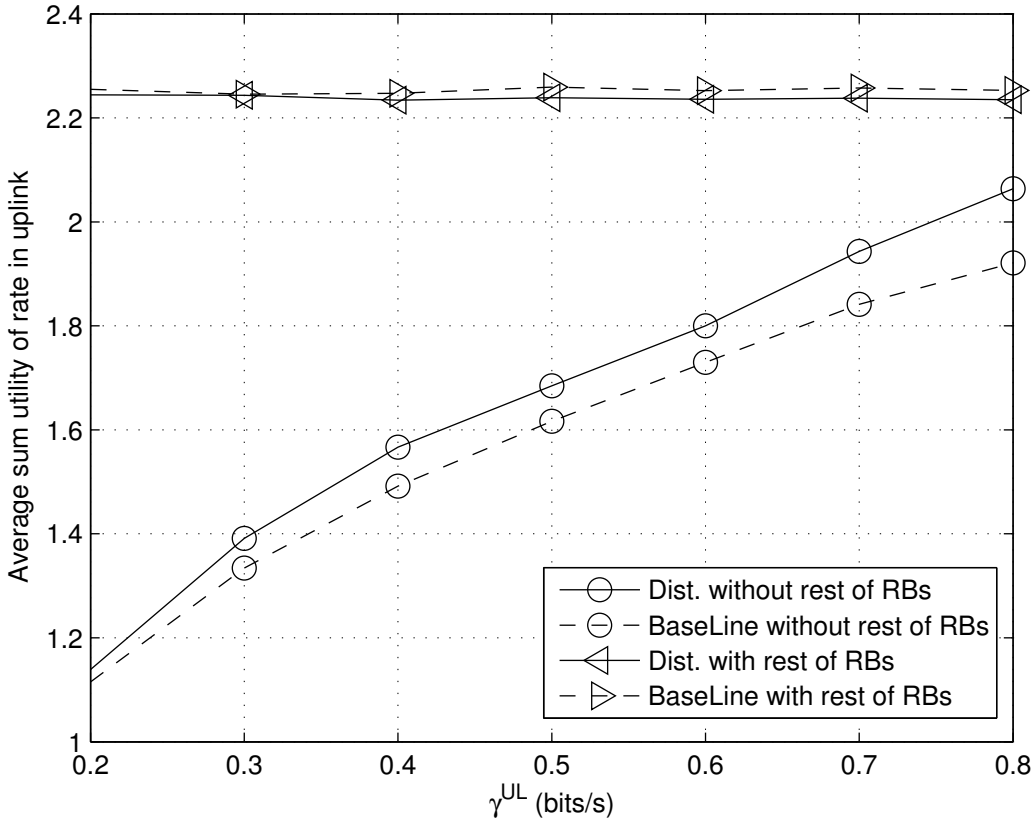

Figure 3.9: Uplink average utility of rate against minimum uplink rate threshold for the developed schemes with $w_{\mathrm{UL}} = 1$, $T = 10\%$, $M = 10$, showing the effect of distributing the rest of RBs in uplink

Chapter 4

Outage Capacity Analysis for OFDM Decode-and-Forward Systems in Frequency Selective Rayleigh Fading Channels

In this chapter, we investigate a DF two-hop relaying system consisting of one source, one relay and one destination, in which OFDM is used in Rayleigh frequency selective channels. The contributions of this chapter are:

- We present an outage probability analysis based on approximating the probability distribution function (PDF) of the total capacity by a Gaussian distribution.
- Tight approximations on the outage probability assuming correlated OFDM subcarriers as well as arbitrary number of bits on each OFDM subcarrier are found.
- As a special case, i.i.d. OFDM subcarriers are also addressed where a closed form solution to the variance of the total capacity is obtained, leading us to even tighter approximations on the outage probability.

The following notations are used in this chapter. We use $|\cdot|$ to denote magnitude of a complex argument, and $\delta(\cdot)$ and $U(\cdot)$ to represent the unit impulse and step functions. The Cartesian product of two sets is represented by $(\cdot)\times(\cdot)$, and defined as the set of all ordered pairs whose first element is a member of the left argument, and the second element is a member of the right argument. Moreover, $\bar{\cdot}$ and $\mathrm{E}[\cdot]$ indicate the expected value, $\mathrm{var}(\cdot)$ symbolizes the variance, $\mathrm{cov}(\cdot,\cdot)$ indicates the covariance of the two arguments, while the PDF of X is denoted by $f_X(\cdot)$, and $\mathcal{N}(0,\sigma^2)$ and $\mathcal{CN}(0,\sigma^2)$ denote the normal, and complex normal PDFs with zero mean and variance σ^2. Vectors and matrices are represented by bold letters, the i^{th} element of vector $\mathbf{V}$ is denoted by $\mathbf{V}(i)$, $\mathrm{diag}(\cdot)$ is a matrix with elements on the main diagonal taken from the elements of the input vector and zeros elsewhere, and $\mathrm{trace}(\cdot)$ is a scalar obtained by adding up the elements on the main diagonal of the input matrix.

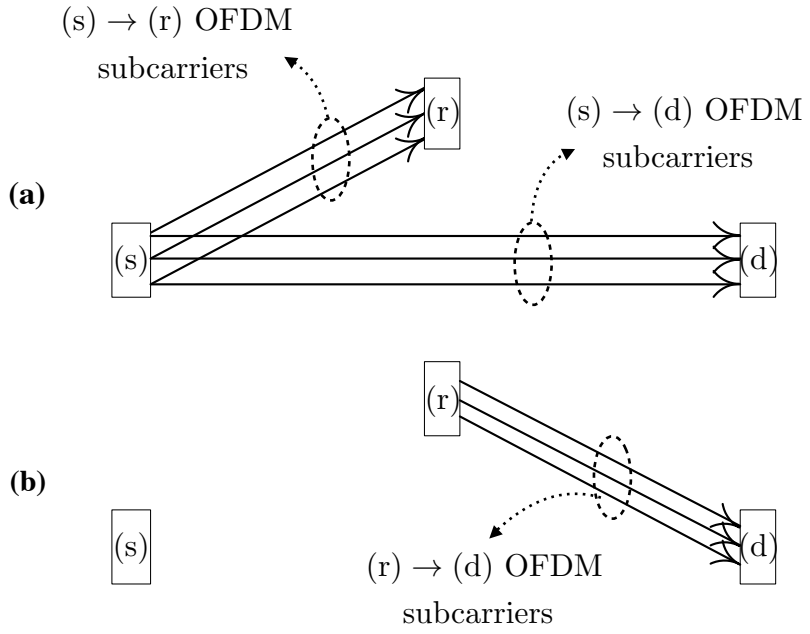

Figure 4.1: System model (a) First time slot (b) Second time slot

The rest of the chapter is organized as follows. In the next section, the used system model is described. The outage probability analysis is presented in Section 4.2, and the simulation results are provided in Section 4.3.

4.1 System model

In a wireless OFDM network operating on frequency selective channels, a source node (s) wishes to transmit data to a destination node (d) using the help of a relay node (r), all equipped with only one antenna. The total bandwidth is divided into N_{sc} frequency subcarriers such that each subcarrier has a frequency flat response. The power budget at source is indicated by P_{s}, and similarly, P_{r} denotes the power budget available at relay. Assuming equal power distribution among all the OFDM subcarriers, $p_{\text{s}_n} = P_{\text{s}}/N_{\text{sc}}$, $p_{\text{r}_n} = P_{\text{r}}/N_{\text{sc}}$, where p_{s_n} and p_{r_n} represent the power on the n^{th} subcarrier at (s) and (r), respectively. We assume perfect time and frequency synchronization along with a cyclic prefix that is long enough to overcome the channel delay spread. We adopt the two time slot protocol as in [27], where source broadcasts in the first time slot to the relay and destination, and second time slot is dedicated to the relay to transmit the source's data it received in the previous time slot. The system setup is illustrated in Fig. 4.1.

We define the channel impulse responses between the (s) → (r), (r) → (d), and (s) → (d)

as $h_{\mathrm{sr}}(\tau)$, $h_{\mathrm{rd}}(\tau)$, and $h_{\mathrm{sd}}(\tau)$, respectively. Representing the number of channel taps on (s) $\rightarrow$ (r), (r) $\rightarrow$ (d), and (s) $\rightarrow$ (d) channels by L_{sr}, L_{rd}, and L_{sd}, these channels can be mathematically modeled as

$$\begin{aligned} h_{\mathrm{sr}}(\tau) &= \sum_{l=0}^{L_{\mathrm{sr}}-1} \mathbf{h}_{\mathrm{sr}}(l)\delta(\tau - l \cdot T_c), \\ h_{\mathrm{rd}}(\tau) &= \sum_{l=0}^{L_{\mathrm{rd}}-1} \mathbf{h}_{\mathrm{rd}}(l)\delta(\tau - l \cdot T_c), \\ h_{\mathrm{sd}}(\tau) &= \sum_{l=0}^{L_{\mathrm{ds}}-1} \mathbf{h}_{\mathrm{sd}}(l)\delta(\tau - l \cdot T_c), \end{aligned} \tag{4.1}$$

where T_c indicates coherence time, and the channel tap coefficients are taken from the following L_{sr}, L_{rd} and L_{sd} element random vectors

$$\begin{aligned} \mathbf{h}_{\mathrm{sr}} &= [\mathbf{h}_{\mathrm{sr}}(1)\ \mathbf{h}_{\mathrm{sr}}(2)\ \ \ldots\ \ \mathbf{h}_{\mathrm{sr}}(L_{\mathrm{sr}})]^T, \\ \mathbf{h}_{\mathrm{rd}} &= [\mathbf{h}_{\mathrm{rd}}(1)\ \mathbf{h}_{\mathrm{rd}}(2)\ \ \ldots\ \ \mathbf{h}_{\mathrm{rd}}(L_{\mathrm{rd}})]^T, \\ \mathbf{h}_{\mathrm{sd}} &= [\mathbf{h}_{\mathrm{sd}}(1)\ \mathbf{h}_{\mathrm{sd}}(2)\ \ \ldots\ \ \mathbf{h}_{\mathrm{sd}}(L_{\mathrm{sd}})]^T. \end{aligned} \tag{4.2}$$

It is assumed that the channel taps on a particular physical channel are statistically independent, zero mean, and complex normally distributed RVs. Therefore, channel tap coefiicent vectors $\mathbf{h}_{\mathrm{sr}}$, $\mathbf{h}_{\mathrm{rd}}$, and $\mathbf{h}_{\mathrm{sd}}$ are modeled as complex normal vectors with covariance matrices $\mathbf{\Gamma}_{\mathrm{sr}}$, $\mathbf{\Gamma}_{\mathrm{rd}}$, and $\mathbf{\Gamma}_{\mathrm{sd}}$, as follows

$$\mathbf{h}_{\mathrm{sr}} \sim \mathcal{CN}(0, \mathbf{\Gamma}_{\mathrm{sr}}),\ \ \mathbf{h}_{\mathrm{rd}} \sim \mathcal{CN}(0, \mathbf{\Gamma}_{\mathrm{rd}}),\ \ \mathbf{h}_{\mathrm{sd}} \sim \mathcal{CN}(0, \mathbf{\Gamma}_{\mathrm{sd}}), \tag{4.3}$$

where

$$\begin{aligned} \mathbf{\Gamma}_{\mathrm{sr}} &= \mathrm{diag}\left[\mathrm{var}\left(\mathbf{h}_{\mathrm{sr}}(1)\right)\ \ \ldots\ \ \mathrm{var}\left(\mathbf{h}_{\mathrm{sr}}(L_{\mathrm{sr}})\right)\right], \\ \mathbf{\Gamma}_{\mathrm{rd}} &= \mathrm{diag}\left[\mathrm{var}\left(\mathbf{h}_{\mathrm{rd}}(1)\right)\ \ \ldots\ \ \mathrm{var}\left(\mathbf{h}_{\mathrm{rd}}(L_{\mathrm{rd}})\right)\right], \\ \mathbf{\Gamma}_{\mathrm{sd}} &= \mathrm{diag}\left[\mathrm{var}\left(\mathbf{h}_{\mathrm{sd}}(1)\right)\ \ \ldots\ \ \mathrm{var}\left(\mathbf{h}_{\mathrm{sd}}(L_{\mathrm{sd}})\right)\right]. \end{aligned} \tag{4.4}$$

Having defined the channels in time domain, the Rayleigh OFDM subcarrier gains in frequency domain can be modeled as N_{sc} element vectors, which are obtained by performing N_{sc}-point discrete Fourier transform (N_{sc}-DFT) on channel tap coefficient vectors,

$$\mathbf{H}_{\mathrm{sr}} = [\mathbf{H}_{\mathrm{sr}}(1)\ \mathbf{H}_{\mathrm{sr}}(2)\ \ \ldots\ \ \mathbf{H}_{\mathrm{sr}}(N_{\mathrm{sc}})]^T = N_{\mathrm{sc}}\text{-DFT}\{\mathbf{h}_{\mathrm{sr}}\},$$

$$\begin{aligned}\mathbf{H}_{\mathrm{rd}} &= [\mathbf{H}_{\mathrm{rd}}(1)\ \mathbf{H}_{\mathrm{rd}}(2)\ \ldots\ \mathbf{H}_{\mathrm{rd}}(N_{\mathrm{sc}})]^T = N_{\mathrm{sc}}\text{-DFT}\{\mathbf{h}_{\mathrm{rd}}\},\\ \mathbf{H}_{\mathrm{sd}} &= [\mathbf{H}_{\mathrm{sd}}(1)\ \mathbf{H}_{\mathrm{sd}}(2)\ \ldots\ \mathbf{H}_{\mathrm{sd}}(N_{\mathrm{sc}})]^T = N_{\mathrm{sc}}\text{-DFT}\{\mathbf{h}_{\mathrm{sd}}\}.\end{aligned} \tag{4.5}$$

The OFDM subcarrier power gain vectors on (s)→(r), (r)→(d), and (s)→(d) channels are indicated by $\mathbf{X}$, $\mathbf{Y}$, and $\mathbf{Z}$, respectively. These random vectors are formally defined by

$$\begin{aligned}\mathbf{X} &= [|\mathbf{H}_{\mathrm{sr}}(1)|^2\ \ldots\ |\mathbf{H}_{\mathrm{sr}}(N_{\mathrm{sc}})|^2],\\ \mathbf{Y} &= [|\mathbf{H}_{\mathrm{rd}}(1)|^2\ \ldots\ |\mathbf{H}_{\mathrm{rd}}(N_{\mathrm{sc}})|^2],\\ \mathbf{Z} &= [|\mathbf{H}_{\mathrm{sd}}(1)|^2\ \ldots\ |\mathbf{H}_{\mathrm{sd}}(N_{\mathrm{sc}})|^2].\end{aligned} \tag{4.6}$$

Here, we can deduce that elements of $\mathbf{X}$, $\mathbf{Y}$, and $\mathbf{Z}$ are exponentially distributed RVs, since the subcarrier gains in frequency domain are Rayleigh distributed [67]. Moreover, elements of $\mathbf{X}$ are identical RVs, thus all associated with exponential parameter λ_{sr}. The same argument holds for $\mathbf{Y}$ and $\mathbf{Z}$ and their corresponding exponential parameter λ_{rd} and λ_{sd}. Hence, the elements of $\mathbf{X}$, $\mathbf{Y}$ and $\mathbf{Z}$ are taken from the following exponential distributions

$$\begin{aligned}f_{\mathbf{X}(n)}(x) &= \lambda_{\mathrm{sr}} e^{-\lambda_{\mathrm{sr}} x}\cdot U(x),\ \forall n \in \{1,\ldots,N_{\mathrm{sc}}\},\\ f_{\mathbf{Y}(n)}(y) &= \lambda_{\mathrm{rd}} e^{-\lambda_{\mathrm{rd}} x}\cdot U(x),\ \forall n \in \{1,\ldots,N_{\mathrm{sc}}\},\\ f_{\mathbf{Z}(n)}(z) &= \lambda_{\mathrm{sd}} e^{-\lambda_{\mathrm{sd}} x}\cdot U(x),\ \forall n \in \{1,\ldots,N_{\mathrm{sc}}\},\end{aligned} \tag{4.7}$$

where the parameters of these exponential RVs can be obtained as follows

$$\lambda_{\mathrm{sr}} = \frac{1}{\mathrm{trace}[\mathbf{\Gamma}_{\mathrm{sr}}]}\quad,\quad \lambda_{\mathrm{rd}} = \frac{1}{\mathrm{trace}[\mathbf{\Gamma}_{\mathrm{rd}}]}\quad,\quad \lambda_{\mathrm{sd}} = \frac{1}{\mathrm{trace}[\mathbf{\Gamma}_{\mathrm{sd}}]}\ . \tag{4.8}$$

Furthermore, the covariances $\mathrm{cov}(\mathbf{X}(n_1),\mathbf{X}(n_2))$, $\mathrm{cov}(\mathbf{Y}(n_1),\mathbf{Y}(n_2))$, and $\mathrm{cov}(\mathbf{Z}(n_1),\mathbf{Z}(n_2))$, can be easily obtained to be [78–80]

$$\begin{aligned}\mathrm{cov}(\mathbf{X}(n_1),\mathbf{X}(n_2)) &= \Big|\sum_{l=0}^{L_{\mathrm{sr}}-1}\mathrm{var}\left(\mathbf{h}_{\mathrm{sr}}(l)\right)e^{-\hat{j}2\pi l\frac{n_1-n_2}{N_{\mathrm{sc}}}}\Big|^2,\\ \mathrm{cov}(\mathbf{Y}(n_1),\mathbf{Y}(n_2)) &= \Big|\sum_{l=0}^{L_{\mathrm{rd}}-1}\mathrm{var}\left(\mathbf{h}_{\mathrm{rd}}(l)\right)e^{-\hat{j}2\pi l\frac{n_1-n_2}{N_{\mathrm{sc}}}}\Big|^2,\\ \mathrm{cov}(\mathbf{Z}(n_1),\mathbf{Z}(n_2)) &= \Big|\sum_{l=0}^{L_{\mathrm{sd}}-1}\mathrm{var}\left(\mathbf{h}_{\mathrm{sd}}(l)\right)e^{-\hat{j}2\pi l\frac{n_1-n_2}{N_{\mathrm{sc}}}}\Big|^2,\end{aligned} \tag{4.9}$$

where $\hat{j}$ is the imaginary unit $\sqrt{-1}$. Furthermore, note that $\mathrm{cov}(\mathbf{X}(n_1),\mathbf{Y}(n_2)) = 0$, since

they are obtained from two independent events (One represents the (s)→(r) channel, and the other represents the (r)→(d) channel.) The same results hold for $\mathrm{cov}(\mathbf{X}(n_1), \mathbf{Z}(n_2))$, and $\mathrm{cov}(\mathbf{Y}(n_1), \mathbf{Z}(n_2))$.

Having defined all these parameters, the capacity on the n^{th} OFDM subcarrier is [27]

$$C(n) = \frac{1}{2}\log\Big(1 + \min\big\{\mathbf{X}(n)\frac{P_{\mathrm{s}}}{N_{\mathrm{sc}}\sigma_{\mathrm{r}}^2}, \mathbf{Y}(n)\frac{P_{\mathrm{r}}}{N_{\mathrm{sc}}\sigma_{\mathrm{d}}^2} + \mathbf{Z}(n)\frac{P_{\mathrm{s}}}{N_{\mathrm{sc}}\sigma_{\mathrm{d}}^2}\big\}\Big), \tag{4.10}$$

where σ_{r}^2 and σ_{d}^2 are noise variances at (r) and (d). Then, the total capacity is

$$C = \frac{1}{N_{\mathrm{sc}}}\sum_{n=1}^{N_{\mathrm{sc}}} C(n). \tag{4.11}$$

4.2 Outage probability analysis

In order to characterize the outage probability, the probability distribution of the total capacity from (4.11) is needed. As it can be observed in equation (4.11), the total capacity is a summation over subcarrier capacities ($C(n)$) which are identical, but correlated RVs (See (4.9) and (4.10).) If these RVs were i.i.d., the central limit theorem would assert that the total capacity follows a Gaussian distribution. However, although these RVs are correlated, still approximating the total capacity by a Gaussian RV seems to be practical. As a matter of fact, we have observed in our simulation results that Gaussian approximation indeed represents the total capacity tightly, even with small number of OFDM subcarriers such as $N_{\mathrm{sc}} = 8$.

A Gaussian RV is completely characterized by its mean and variance, which are addressed in the rest of this section. In order to proceed, let us define another set of RVs as

$$\mathbf{V}(n) = \min\big\{\mathbf{X}(n)\frac{P_{\mathrm{s}}}{N_{\mathrm{sc}}\sigma_{\mathrm{r}}^2}, \mathbf{Y}(n)\frac{P_{\mathrm{r}}}{N_{\mathrm{sc}}\sigma_{\mathrm{d}}^2} + \mathbf{Z}(n)\frac{P_{\mathrm{s}}}{N_{\mathrm{sc}}\sigma_{\mathrm{d}}^2}\big\}, \quad \forall n \in \{1, 2, \ldots, N_{\mathrm{sc}}\}. \tag{4.12}$$

Given the probability distribution functions (PDF) of $\mathbf{X}(n)$, $\mathbf{Y}(n)$, and $\mathbf{Z}(n)$ from (4.7), the PDF of $\mathbf{V}(n)$ can be obtained to be

$$f_{\mathbf{V}(n)}(v) = \left[\alpha_{\mathrm{sd}}\Big(\frac{\alpha_{\mathrm{sr}} + \alpha_{\mathrm{rd}}}{\alpha_{\mathrm{sd}} - \alpha_{\mathrm{rd}}}\Big)e^{-(\alpha_{\mathrm{sr}}+\alpha_{\mathrm{rd}})v} - \alpha_{\mathrm{rd}}\Big(\frac{\alpha_{\mathrm{sr}} + \alpha_{\mathrm{sd}}}{\alpha_{\mathrm{sd}} - \alpha_{\mathrm{rd}}}\Big)e^{-(\alpha_{\mathrm{sr}}+\alpha_{\mathrm{sd}})v}\right]U(v), \tag{4.13}$$

where

$$\alpha_{\mathrm{sr}} = \frac{\lambda_{\mathrm{sr}} \cdot N_{\mathrm{sc}}\sigma_{\mathrm{r}}^2}{P_{\mathrm{s}}}, \;\; \alpha_{\mathrm{rd}} = \frac{\lambda_{\mathrm{rd}} \cdot N_{\mathrm{sc}}\sigma_{\mathrm{d}}^2}{P_{\mathrm{s}}}, \;\; \alpha_{\mathrm{sd}} = \frac{\lambda_{\mathrm{sd}} \cdot N_{\mathrm{sc}}\sigma_{\mathrm{d}}^2}{P_{\mathrm{s}}}. \tag{4.14}$$

Note that $f_{\mathbf{V}(n)}(v)$ cannot be evaluated from (4.13) if $\alpha_{\mathrm{rd}} = \alpha_{\mathrm{sd}}$, which happens rarely due to the random nature of wireless fading channels. Besides this, by substituting (4.12) into (4.10) we have

$$\mathrm{E}[C] = \frac{1}{N_{\mathrm{sc}}} \sum_{n=1}^{N_{\mathrm{sc}}} \mathrm{E}[C(n)] = \mathrm{E}[C(n)] \Rightarrow \mathrm{E}[C] = \int_0^{\infty} \frac{1}{2} \log(1+v) f_{\mathbf{V}(n)}(v) \mathrm{d}v. \tag{4.15}$$

And finally, by calculating the above integral, the expected value of the total capacity is

$$\mathrm{E}[C] = \frac{1}{2} \log_2(e) \Bigg[e^{(\alpha_{\mathrm{sr}}+\alpha_{\mathrm{sd}})} \Big(\frac{\alpha_{\mathrm{rd}}}{\alpha_{\mathrm{sd}} - \alpha_{\mathrm{rd}}} \Big) \mathrm{Ei}\big(-(\alpha_{\mathrm{sr}} + \alpha_{\mathrm{sd}}) \big) - e^{(\alpha_{\mathrm{sr}}+\alpha_{\mathrm{rd}})} \Big(\frac{\alpha_{\mathrm{sd}}}{\alpha_{\mathrm{sd}} - \alpha_{\mathrm{rd}}} \Big) \mathrm{Ei}\big(-(\alpha_{\mathrm{sr}} + \alpha_{\mathrm{rd}}) \big) \Bigg], \tag{4.16}$$

in which $\mathrm{Ei}(\cdot)$ is the exponential integral and defined as $\mathrm{Ei}(x) = \int_{-\infty}^{x} \frac{\exp(t)}{t} \mathrm{d}t$ [81].

The next step is calculating the variance of total capacity:

$$\sigma_C^2 = \mathrm{E}[(C - \bar{C})^2] = \mathrm{E}[C^2] - \bar{C}^2 = \frac{1}{N_{\mathrm{sc}}^2} \sum_{n_1=1}^{N_{\mathrm{sc}}} \sum_{n_2=1}^{N_{\mathrm{sc}}} \mathrm{E}[C(n_1)C(n_2)] - \bar{C}^2. \tag{4.17}$$

According to above equation, calculating $\mathrm{E}[C(n_1)C(n_2)]$ is crucial, however not quite straightforward, considering that the joint PDF of any two OFDM subcarrier gain in (s)→(r), (r)→(d), or (s)→(d) link (e.g., $|\mathbf{H}_{\mathrm{sr}}(n_1)|$ and $|\mathbf{H}_{\mathrm{sr}}(n_2)|$) follows a bivariate Rayleigh distribution (joint PDF of two correlated Rayleigh RVs) obtained in [82, 83]. Therefore, we use the Delta method [84] to approximate the variance of total capacity.

The Delta method, in summary, is a way to approximate the variance and covariance of functions of RVs through using the Taylor series expansion up to the first degree around the mean value of the RVs. To illustrate the concept, we use the Delta method to approximate the variance of g which is a function of two random variables, t and u, with expected values of μ_t and μ_u, respectively. The Taylor series expansion of $g(t, u)$ up to the first degree around the expected values of the arguments is

$$g(t, u) \approx g(\mu_t, \mu_u) + \frac{\partial g}{\partial t}(t - \mu_t) + \frac{\partial g}{\partial u}(u - \mu_u), \tag{4.18}$$

where $\frac{\partial g}{\partial u}$ denotes the partial derivative of function g with respect to u. Taking the variance

of both sides of the above equation yields

$$\mathrm{var}\left(g(t,u)\right) \approx \left(\frac{\partial g}{\partial t}\right)^2 \mathrm{var}(t) + \left(\frac{\partial g}{\partial u}\right)^2 \mathrm{var}(u) + 2\frac{\partial g}{\partial t}\frac{\partial g}{\partial u}\,\mathrm{cov}(t,u). \tag{4.19}$$

Now, we apply the Delta method to approximate the variance of total capacity as follows

$$\begin{aligned}\sigma_C^2 \approx \sum_{n_1=1}^{N_{\mathrm{sc}}}\sum_{n_2=1}^{N_{\mathrm{sc}}}\Bigg[&\frac{\partial C}{\partial \mathbf{X}(n_1)}\frac{\partial C}{\partial \mathbf{X}(N_2)}\,\mathrm{cov}(\mathbf{X}(n_1),\mathbf{X}(n_2)) \\ &+ \frac{\partial C}{\partial \mathbf{Y}(n_1)}\frac{\partial C}{\partial \mathbf{Y}(N_2)}\,\mathrm{cov}(\mathbf{Y}(n_1),\mathbf{Y}(n_2)) + \frac{\partial C}{\partial \mathbf{Z}(n_1)}\frac{\partial C}{\partial \mathbf{Z}(N_2)}\,\mathrm{cov}(\mathbf{Z}(n_1),\mathbf{Z}(n_2))\Bigg],\end{aligned} \tag{4.20}$$

where $\frac{\partial C}{\partial \mathbf{X}(n)}$ denotes the partial derivative of total capacity C from (4.11) and (4.10) with respect to $\mathbf{X}(n)$. The derivatives are evaluated at $\mathrm{E}[\mathbf{X}(n)]$, $\mathrm{E}[\mathbf{Y}(n)]$, and $\mathrm{E}[\mathbf{Z}(n)]$, and thus given by

$$\begin{aligned}\frac{\partial C}{\partial \mathbf{X}(n)} &= \beta\begin{cases}\frac{a_x}{1+a_x\mathrm{E}[\mathbf{X}(n)]} & a_x\mathrm{E}[\mathbf{X}(n)] \le a_y\mathrm{E}[\mathbf{Y}(n)] + a_z\mathrm{E}[\mathbf{Z}(n)] \\ 0 & \text{otherwise}\end{cases}, \\ \frac{\partial C}{\partial \mathbf{Y}(n)} &= \beta\begin{cases}0 & a_x\mathrm{E}[\mathbf{X}(n)] \le a_y\mathrm{E}[\mathbf{Y}(n)] + a_z\mathrm{E}[\mathbf{Z}(n)] \\ \frac{a_y}{1+a_y\mathrm{E}[\mathbf{Y}(n)]+a_z\mathrm{E}[\mathbf{Z}(n)]} & \text{otherwise}\end{cases}, \\ \frac{\partial C}{\partial \mathbf{Z}(n)} &= \beta\begin{cases}0 & a_x\mathrm{E}[\mathbf{X}(n)] \le a_y\mathrm{E}[\mathbf{Y}(n)] + a_z\mathrm{E}[\mathbf{Z}(n)] \\ \frac{a_z}{1+a_y\mathrm{E}[\mathbf{Y}(n)]+a_z\mathrm{E}[\mathbf{Z}(n)]} & \text{otherwise}\end{cases},\end{aligned} \tag{4.21}$$

in which

$$\beta = \frac{\log_2(e)}{2N_{\mathrm{sc}}},\ a_x = \frac{P_{\mathrm{s}}}{N_{\mathrm{sc}}\sigma_{\mathrm{r}}^2},\ a_y = \frac{P_{\mathrm{r}}}{N_{\mathrm{sc}}\sigma_{\mathrm{d}}^2},\ a_z = \frac{P_{\mathrm{s}}}{N_{\mathrm{sc}}\sigma_{\mathrm{d}}^2}. \tag{4.22}$$

By substituting (4.9) and (4.21) into (4.20), the approximation of the variance is obtained. Having obtained both the mean and variance of the total capacity in (4.16) and (4.20), the total capacity now can be described as $C \sim \mathcal{N}(\bar{C}, \sigma_C^2)$. Hence, the outage probability is

$$P_{\mathrm{out}} = \Pr[C < \gamma] = 1 - Q\left(\frac{\gamma - \bar{C}}{\sigma_C}\right), \tag{4.23}$$

where γ is the threshold rate, and $Q(\cdot)$ is the standard Q-function. Clearly, the ϵ outage capacity (i.e. the maximum capacity that can be supported with probability of failure equal

to ϵ) can be written as

$$C_\epsilon = \sigma_C Q^{-1}(1-\epsilon) + \bar{C}, \tag{4.24}$$

where $Q^{-1}(\cdot)$ is the inverse of Q-function.

4.2.1 Special case: i.i.d. OFDM subcarriers

In this subsection, we address the case where the OFDM subcarrier gains are independent as well as identical. As one possibility, this case happens when channel taps have equal fading powers, and the number of channel taps is equal to the number of OFDM subcarriers. Here, the central limit theorem strictly applies, and we expect the capacity to be a Gaussian RV. The mean does not change and it is given by equation (4.16). As for the variance, since the $C(n)$s are independent (i.e. $\mathrm{E}[C(n_1)C(n_2)] = \mathrm{E}[C(n_1)]\mathrm{E}[C(n_2)]$,), manipulating (4.17) results in

$$\sigma_C^2 = \mathrm{E}[(C-\bar{C})^2] = \frac{1}{N_{\mathrm{sc}}}\sigma_{C(n)}^2 = \frac{1}{N_{\mathrm{sc}}}\big(\mathrm{E}[C(n)^2] - \bar{C(n)}^2\big) \tag{4.25}$$

Then, from equations (4.12) and (4.13) and (4.15)

$$\sigma_C^2 = \frac{1}{N_{\mathrm{sc}}}\int_0^\infty \big(\frac{1}{2}\log(1+v)\big)^2 f_{\mathbf{V}(n)}(v)\mathrm{d}v - \frac{\bar{C}^2}{N_{\mathrm{sc}}}. \tag{4.26}$$

Calculating the above integral,

$$\sigma_C^2 = \frac{(\log_2(e))^2}{2N_{\mathrm{sc}}}\left[Ae^a \mathrm{G}_{2,3}^{3,0}\left(\alpha_{\mathrm{sr}}+\alpha_{\mathrm{rd}}\middle|\begin{matrix}0,0\\-1,-1,-1\end{matrix}\right) - Be^b \mathrm{G}_{2,3}^{3,0}\left(\alpha_{\mathrm{sr}}+\alpha_{\mathrm{sd}}\middle|\begin{matrix}0,0\\-1,-1,-1\end{matrix}\right)\right] - \frac{\bar{C}^2}{N} \tag{4.27}$$

where G is Meijer G-function [81], and

$$A = \alpha_{\mathrm{sd}}\Big(\frac{\alpha_{\mathrm{sr}}+\alpha_{\mathrm{rd}}}{\alpha_{\mathrm{sd}}-\alpha_{\mathrm{rd}}}\Big)\ ,\ a = \alpha_{\mathrm{sr}}+\alpha_{\mathrm{rd}}, \quad B = \alpha_{\mathrm{rd}}\Big(\frac{\alpha_{\mathrm{sr}}+\alpha_{\mathrm{sd}}}{\alpha_{\mathrm{sd}}-\alpha_{\mathrm{rd}}}\Big)\ ,\ b = \alpha_{\mathrm{sr}}+\alpha_{\mathrm{sd}}. \tag{4.28}$$

After calculating the mean and variance of the total capacity, the probability of outage is similarly given by (4.23).

4.3 Numerical simulation results

We performed simulations to examine the accuracy of the analytical outage probability obtained in the previous section. It is assumed that all the three nodes are on a straight line where (r) node is located in the middle of (s) and (d) nodes. Furthermore, number of channel taps on all the three channels is L, i.e., $L_{\mathrm{sr}} = L_{\mathrm{rd}} = L_{\mathrm{sd}} = L$. Without loss of generality, the (s)→(r) and (r)→(d) channel power delay profiles are normalized to 1, and all the channel taps on these two channels are identical RVs, i.e., var($\mathbf{h}_{\mathrm{sr}}$) and var($\mathbf{h}_{\mathrm{rd}}$) are taken from $\mathcal{CN}(0, \frac{1}{L})$. Assuming path loss exponent of 4, the (s)→(d) channel taps are taken from $\mathcal{CN}(0, \frac{1}{16 \cdot L})$. In addition, the threshold rate is assumed to be $\gamma = 1$ bit/s/Hz, the number of OFDM subcarriers is $N_{\mathrm{sc}} = 32$, noise variances σ_{r}^2 and σ_{d}^2 are set to 1, and the SNR is the transmit SNR per OFDM subcarrier.

Fig. 4.2 and Fig. 4.3 show the analytical and simulated outage probability versus SNR assuming equal power budgets at (s) and (r) ($P_{\mathrm{r}} = P_{\mathrm{s}}$), and reduced power budget at (r) ($P_{\mathrm{r}} = 0.1 \cdot P_{\mathrm{s}}$), respectively. Results for different number of channel taps are illustrated. As it can be seen, the outage probability obtained by our analysis and simulation are almost identical in all the cases, demonstrating the precision of our analysis. Moreover, in both figures, the lowest curves correspond to the special case of i.i.d. OFDM subcarrier power gains, where the numerically evaluated and analytical results precisely agree. This is because the exact variance obtained in (4.27) is used to evaluate the outage probability. We also observe that by increasing the number of channel taps the outage performance improves, which is the result of a better frequency diversity. Another fact that stands out by comparing Fig. 4.2 and Fig. 4.3 is that when the power budget at (r) node is reduced, the outage performance drops. Intuitively, by reducing the power budget at (r), lower levels of overall power are available, which translates into lower SNRs, and worse probabilities of outage.

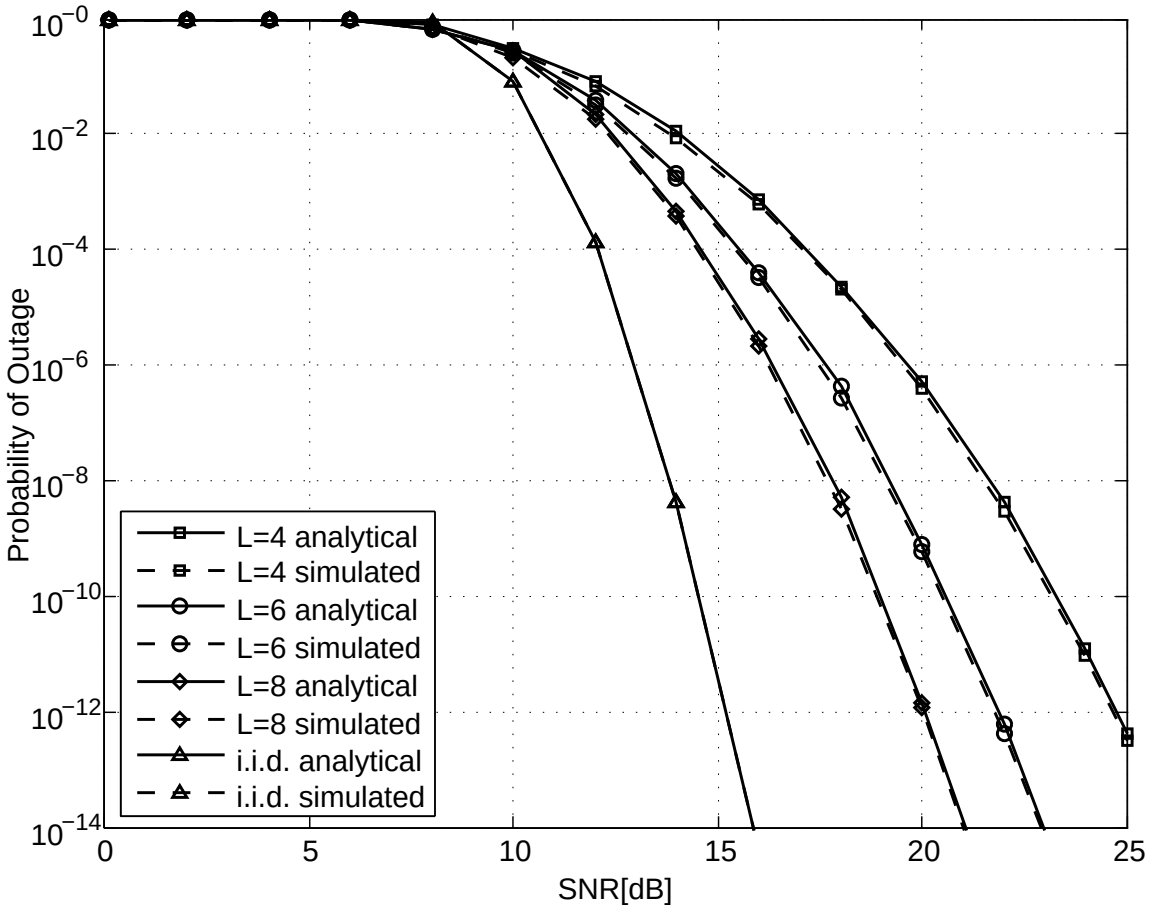

Figure 4.2: Outage probability against transmitted SNR when $P_R = P_S$ for $L = 4, 6, 8$ and i.i.d. subcarriers

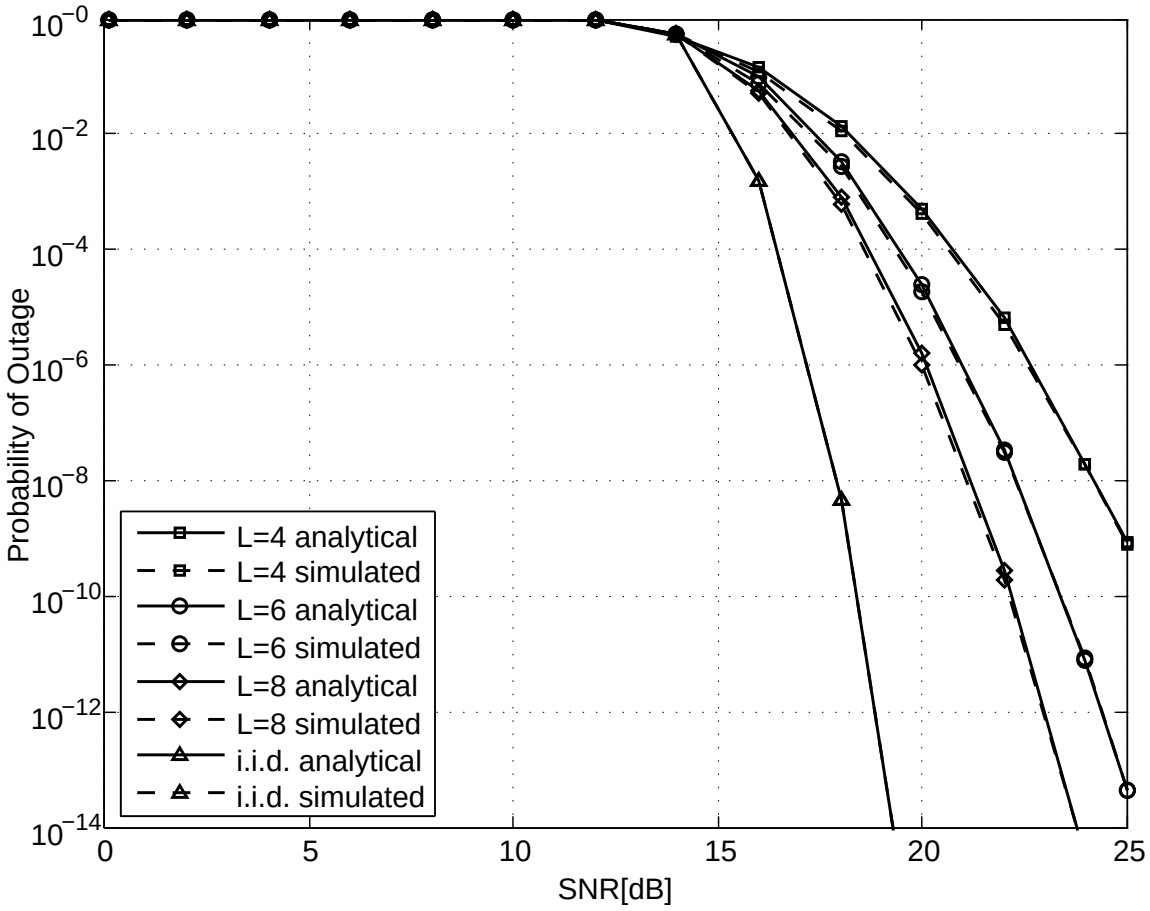

Figure 4.3: Outage probability against transmitted SNR when $P_R = 0.1 \cdot P_S$ for $L = 4, 6, 8$ and i.i.d. subcarriers

Chapter 5

Outage Probability Analysis for Multi-User Single-Relay OFDMA Decode-and-Forward Networks in Frequency Selective Rayleigh Fading Channels

This chapter is an extension to Chapter 4. In this chapter, we study an uplink multi-user single-relay DF OFDMA system, where a Rayleigh frequency selective channel model is adopted. We provide analytical approximations for the global outage probability in the sense that the outage event occurs when at least one link goes into outage.

In calculating the global outage probability of a multi-user single-relay OFDMA DF network, the contributions of this chapter are:

- Realizing that the link capacities are correlated RVs. The statistical correlation between the link capacities is created by the relay-destination channel that is common to all the links.
- Fitting a multi-variate normal distribution to the link capacities and characterizing the parameters of the fitted distribution.
- Proposing a method to approximate the correlation among link capacities.
- Obtaining the global outage probability in which the correlation of the link capacities, correlation between OFDM subcarriers, and arbitrary number of bits on each OFDM subcarrier are considered.

Before proceeding further, the used notations in this chapter are clarified. We use $|\cdot|$ to denote magnitude of a complex argument, and $\delta(\cdot)$ to represent unit impulse function. Vectors are represented by $\overrightarrow{\cdot}$ and matrices by bold letters, the i^{th} element of vector $\overrightarrow{V}$

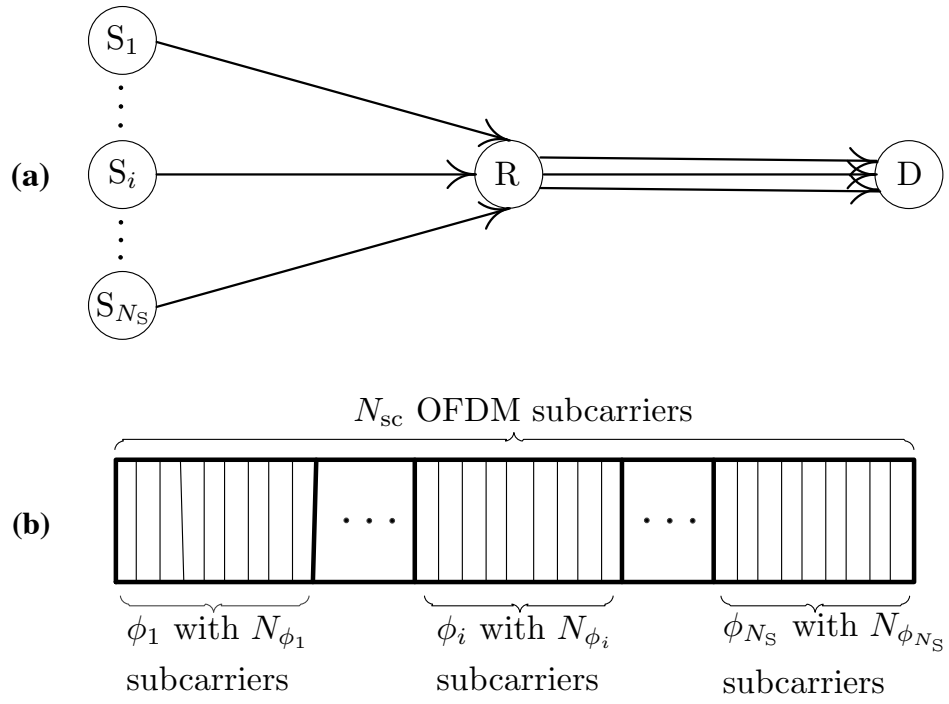

Figure 5.1: System model (a) System configuration (b) OFDMA setup

is denoted by $\overrightarrow{V}(i)$, diag($\overrightarrow{\cdot}$) is a matrix with elements on the main diagonal taken from the elements of the input vector and zeros elsewhere, and trace($\cdot$) is a scalar obtained by adding up the elements on the main diagonal of the input matrix. Besides, E[$\cdot$] symbolizes the expected value, var($\cdot$) indicates the variance, cov($\cdot,\cdot$) indicates the covariance between the two arguments, while $\mathcal{N}(\overrightarrow{\mu},\mathbf{Q})$ and $\mathcal{CN}(\overrightarrow{\mu},\mathbf{Q})$ denote the multi-variate normal, and complex normal PDFs with mean vector $\overrightarrow{\mu}$ and covariance matrix $\mathbf{Q}$. Finally, $G(\overrightarrow{\gamma},\overrightarrow{\mu},\mathbf{Q})$ represents the multi-variate normal CDF, which is the probability of a set of jointly normal distributed RVs with mean vector $\overrightarrow{\mu}$ and covariance matrix $\mathbf{Q}$ being less than the elements of vector $\overrightarrow{\gamma}$.

The rest of the chapter is organized as follows. The system model is described in the next section. The global outage probability analysis is presented in Section 5.2. Simulation results are provided in Section 5.3 to verify the validity of our proposed global outage analysis.

5.1 System model

In an uplink cooperative configuration, where the wireless channels suffer from Rayleigh multi-path fading, N_{S} sources ($\mathrm{S}_i, i \in \{1,\ldots,N_{\mathrm{S}}\}$) are to communicate with one destination

(D) through a single relay (R). In order to combat multi-path fading, OFDMA arrangement with N_{sc} available subcarriers is adopted, where these subcarriers are partitioned into N_{S} non-overlapping and not necessarily adjacent subcarrier subsets ($\phi_i, i \in \{1, \ldots, N_{\text{S}}\}$), each with N_{ϕ_i} subcarriers (i.e., $\sum_{i=1}^{N_{\text{S}}} N_{\phi_i} = N_{\text{sc}}$). Each subcarrier subset ϕ_i is assigned to a single source S_i, or equivalently to a single S_i-R-D link, to establish N_{S} links in frequency domain. The R operates under the well-known two time slot DF scheme. In the 1st time slot, sources S_i broadcast on their assigned subcarrier subsets ϕ_i, each with a power budget of P_{S_i}, spreading their budgets evenly among their available subcarriers (i.e., source S_i allocates $P_{\text{S}_i}/N_{\phi_i}$ to its available subcarriers). Then, the 2nd time slot follows where R decodes the messages, re-encodes them, and forwards the messages of each source S_i on its allocated subcarrier subset ϕ_i. R also allocates its power budget equally among all the subcarriers, putting $P_{\text{R}}/N_{\text{sc}}$ on each subcarrier. The system model and the OFDMA setup is illustrated in Fig. 5.1. The line of sight between the source and destination is not shown in Fig. 5.1, not to impair the readability of the figure. Also, as an illustrative example, assume that there are 2 sources and 4 available OFDM subcarriers. Let us say subcarriers 1 and 3 are allocated to S_1, and subcarriers 2 and 4 are given to S_2. In other words, $\phi_1 = \{1, 3\}$, and $\phi_2 = \{2, 4\}$. In the 1st time slot, S_1 transmits its OFDM symbols on 1st and 3rd subcarriers, while S_2 transmits on 2nd and 4th, both distributing their powers equally among the two subcarriers allocated to them. In the 2nd time slot, R decodes the information on 1st and 3rd subcarriers as S_1's information, and re-encodes them and relays them on the same subcarriers in ϕ_1. The relay treats the information received from S_2 in the same manner and forwards them on ϕ_2. The power allocated to all the 4 subcarriers at R are also equal.

Indicating by T_c the coherence time, the channel tap vectors on r-t channels by $\overrightarrow{h}_{rt}$, and the number of channel taps in these vectors by L_{rt}, the Rayleigh faded channels in our network are represented as

$$h_{\text{S}_i\text{R}}(\tau) = \sum_{l=0}^{L_{\text{S}_i\text{R}}-1} \overrightarrow{h}_{\text{S}_i\text{R}}(l)\delta(\tau - lT_c), \tag{5.1}$$

$$h_{\text{RD}}(\tau) = \sum_{l=0}^{L_{\text{RD}}-1} \overrightarrow{h}_{\text{RD}}(l)\delta(\tau - lT_c), \tag{5.2}$$

$$h_{\text{S}_i\text{D}}(\tau) = \sum_{l=0}^{L_{\text{S}_i\text{D}}-1} \overrightarrow{h}_{\text{S}_i\text{D}}(l)\delta(\tau - lT_c). \tag{5.3}$$

The channel tap vectors are modelled as zero mean complex normal vectors with covariance matrices $\mathbf{\Gamma}_{\text{S}_i\text{R}}$, $\mathbf{\Gamma}_{\text{RD}}$, and $\mathbf{\Gamma}_{\text{S}_i\text{D}}$. $\mathbf{\Gamma}_{\text{S}_i\text{R}}$, $\mathbf{\Gamma}_{\text{RD}}$, and $\mathbf{\Gamma}_{\text{S}_i\text{D}}$ have non-zero elements only on the main

diagonal which indicates the statistical independence of the channel taps on each physical channel:

$$\begin{aligned}
\overrightarrow{h}_{\mathrm{S}_i\mathrm{R}} &\sim \mathcal{CN}(0, \mathbf{\Gamma}_{\mathrm{S}_i\mathrm{R}}),\\
\overrightarrow{h}_{\mathrm{RD}} &\sim \mathcal{CN}(0, \mathbf{\Gamma}_{\mathrm{RD}}),\\
\overrightarrow{h}_{\mathrm{S}_i\mathrm{D}} &\sim \mathcal{CN}(0, \mathbf{\Gamma}_{\mathrm{S}_i\mathrm{D}}),
\end{aligned} \tag{5.4}$$

and

$$\begin{aligned}
\mathbf{\Gamma}_{\mathrm{S}_i\mathrm{R}} &= \mathrm{diag}\left[\mathrm{var}\left(\overrightarrow{h}_{\mathrm{S}_i\mathrm{R}}(1)\right) \ \ldots \ \mathrm{var}\left(\overrightarrow{h}_{\mathrm{S}_i\mathrm{R}}(L_{\mathrm{S}_i\mathrm{R}})\right)\right],\\
\mathbf{\Gamma}_{\mathrm{RD}} &= \mathrm{diag}\left[\mathrm{var}\left(\overrightarrow{h}_{\mathrm{RD}}(1)\right) \ \ldots \ \mathrm{var}\left(\overrightarrow{h}_{\mathrm{RD}}(L_{\mathrm{RD}})\right)\right],\\
\mathbf{\Gamma}_{\mathrm{S}_i\mathrm{D}} &= \mathrm{diag}\left[\mathrm{var}\left(\overrightarrow{h}_{\mathrm{S}_i\mathrm{D}}(1)\right) \ \ldots \ \mathrm{var}\left(\overrightarrow{h}_{\mathrm{S}_i\mathrm{D}}(L_{\mathrm{S}_i\mathrm{D}})\right)\right],
\end{aligned} \tag{5.5}$$

The OFDM subcarrier gains in the frequency domain are related to time domain channel tap vectors through N_{sc} point discrete Fourier transform (N_{sc}- DFT), thus we have

$$\begin{aligned}
\overrightarrow{H}_{\mathrm{S}_i\mathrm{R}} &= [\overrightarrow{H}_{\mathrm{S}_i\mathrm{R}}(1), \ldots, \overrightarrow{H}_{\mathrm{S}_i\mathrm{R}}(N_{\mathrm{sc}})] = N_{\mathrm{sc}}\text{- DFT}\{\overrightarrow{h}_{\mathrm{S}_i\mathrm{R}}\},\\
\overrightarrow{H}_{\mathrm{RD}} &= [\overrightarrow{H}_{\mathrm{RD}}(1), \ldots, \overrightarrow{H}_{\mathrm{RD}})] = N_{\mathrm{sc}}\text{- DFT}\{\overrightarrow{h}_{\mathrm{RD}}\},\\
\overrightarrow{H}_{\mathrm{S}_i\mathrm{D}} &= [\overrightarrow{H}_{\mathrm{S}_i\mathrm{D}}(1), \ldots, \overrightarrow{H}_{\mathrm{S}_i\mathrm{D}}(N_{\mathrm{sc}})] = N_{\mathrm{sc}}\text{- DFT}\{\overrightarrow{h}_{\mathrm{S}_i\mathrm{D}}\},
\end{aligned} \tag{5.6}$$

and in turn, the N_{sc} element OFDM subcarrier power gain vectors on S_i-R, R-D, and S_i-D physical channels are[4]

$$\begin{aligned}
\overrightarrow{X}_i &= [|\overrightarrow{H}_{\mathrm{S}_i\mathrm{R}}(1)|^2, \ldots, |\overrightarrow{H}_{\mathrm{S}_i\mathrm{R}}(N_{\mathrm{sc}})|^2],\\
\overrightarrow{Y} &= [|\overrightarrow{H}_{\mathrm{RD}}(1)|^2, \ldots, |\overrightarrow{H}_{\mathrm{RD}}(N_{\mathrm{sc}})|^2],\\
\overrightarrow{Z}_i &= [|\overrightarrow{H}_{\mathrm{S}_i\mathrm{D}}(1)|^2, \ldots, |\overrightarrow{H}_{\mathrm{S}_i\mathrm{D}}(N_{\mathrm{sc}})|^2].
\end{aligned} \tag{5.7}$$

It can easily be shown that all the subcarrier power gains on a given physical channel (e.g., $\overrightarrow{X}_i(n), n \in \{1, \ldots, N_{\mathrm{sc}}\}$) are identical exponentially distributed RVs. Thus, we associate all the elements in $\overrightarrow{X}_i$ with exponential distribution parameter $\lambda_{\mathrm{S}_i\mathrm{R}}$, elements of $\overrightarrow{Y}$ with λ_{RD},

[4]In this chapter, where not indicated, indices i can take any value in $\{1, \ldots, N_{\mathrm{S}}\}$, indices n, n_1, and n_2 refer to OFDM subcarriers, and can take values in $\{1, \ldots, N_{\mathrm{sc}}\}$.

and elements of $\overrightarrow{Z}_i$ with $\lambda_{\mathrm{S}_i\mathrm{D}}$. The exponential distribution parameters are calculated to be

$$\lambda_{\mathrm{S}_i\mathrm{R}} = \frac{1}{\mathrm{trace}[\mathbf{\Gamma}_{\mathrm{S}_i\mathrm{R}}]}\ ,\ \lambda_{\mathrm{RD}} = \frac{1}{\mathrm{trace}[\mathbf{\Gamma}_{\mathrm{RD}}]}\ ,\ \lambda_{\mathrm{S}_i\mathrm{D}} = \frac{1}{\mathrm{trace}[\mathbf{\Gamma}_{\mathrm{S}_i\mathrm{D}}]}. \tag{5.8}$$

We represent $\mathrm{cov}\left(\overrightarrow{X}_i(n_1), \overrightarrow{X}_i(n_2)\right)$, $\mathrm{cov}\left(\overrightarrow{Y}(n_1), \overrightarrow{Y}(n_2)\right)$, and $\mathrm{cov}\left(\overrightarrow{Z}_i(n_1), \overrightarrow{Z}_i(n_2)\right)$, by $\Theta_{\overrightarrow{X}_i}(n_1, n_2)$,$\Theta_{\overrightarrow{Y}}(n_1, n_2)$, and $\Theta_{\overrightarrow{Z}_i}(n_1, n_2)$, respectively. Due to the random nature of wireless channels, OFDM subcarrier power gains on separate physical channels are statistically independent (e.g., $\mathrm{cov}\left(\overrightarrow{X}_i(n_1), \overrightarrow{Y}(n_2)\right) = 0$, or $\mathrm{cov}\left(\overrightarrow{X}_i(n_1), \overrightarrow{X}_j(n_2)\right) = 0$ for $i \neq j$). However, the OFDM subcarrier gains on a specific physical channel are correlated as follows [78]

$$\begin{aligned}
\Theta_{\overrightarrow{X}_i}(n_1, n_2) &= \Big| \sum_{l=0}^{L_{\mathrm{S}_i\mathrm{R}}-1} \mathrm{var}\left(\overrightarrow{h}_{\mathrm{S}_i\mathrm{R}}(l)\right) e^{-\hat{j}2\pi l \frac{n_1-n_2}{N_{\mathrm{sc}}}} \Big|^2, \\
\Theta_{\overrightarrow{Y}}(n_1, n_2) &= \Big| \sum_{l=0}^{L_{\mathrm{RD}}-1} \mathrm{var}\left(\overrightarrow{h}_{\mathrm{RD}}(l)\right) e^{-\hat{j}2\pi l \frac{n_1-n_2}{N_{\mathrm{sc}}}} \Big|^2, \\
\Theta_{\overrightarrow{Z}_i}(n_1, n_2) &= \Big| \sum_{l=0}^{L_{\mathrm{S}_i\mathrm{D}}-1} \mathrm{var}\left(\overrightarrow{h}_{\mathrm{S}_i\mathrm{D}}(l)\right) e^{-\hat{j}2\pi l \frac{n_1-n_2}{N_{\mathrm{sc}}}} \Big|^2,
\end{aligned} \tag{5.9}$$

where $\hat{j}$ is the imaginary unit $\sqrt{-1}$.

Furthermore, by requiring the relay to fully decode the messages, the capacity of the S_i-R-D link on the n^{th} OFDM subcarrier, where $n \in \phi_i$ is [27]

$$C_i(n) \ = \ \frac{1}{2}\log\left(1 + \min\left\{\overrightarrow{X}_i(n)\frac{P_{\mathrm{S}_i}}{N_{\phi_i}\sigma^2_{\mathrm{R}}}, \overrightarrow{Y}(n)\frac{P_{\mathrm{R}}}{N_{\mathrm{sc}}\sigma^2_{\mathrm{D}}} + \overrightarrow{Z}_i(n)\frac{P_{\mathrm{S}_i}}{N_{\phi_i}\sigma^2_{D}}\right\}\right),\ n \in \phi_i, \tag{5.10}$$

where σ^2_R and σ^2_D are the noise variances at R and D, respectively. The overall capacity of S_i-R-D is obtained by summing the capacities on the subcarriers in ϕ_i:

$$C_i = \frac{1}{N_{\phi_i}} \sum_{n \in \phi_i} C_i(n). \tag{5.11}$$

Coming back to our illustrative example, $C_1 = 0.5[C_1(1) + C_1(3)]$, and $C_2 = 0.5[C_2(2) + C_2(4)]$. Note that C_1 is a function of $\overrightarrow{X}_1(1)$, $\overrightarrow{X}_1(3)$, $\overrightarrow{Z}_1(1)$, $\overrightarrow{Z}_1(3)$, $\overrightarrow{Y}(1)$, and $\overrightarrow{Y}(3)$, while C_2 is a function of $\overrightarrow{X}_2(2)$, $\overrightarrow{X}_2(4)$, $\overrightarrow{Z}_2(2)$, $\overrightarrow{Z}_2(4)$, $\overrightarrow{Y}(2)$, and $\overrightarrow{Y}(4)$. According to the second equation in (5.9), $\overrightarrow{Y}(1)$ and $\overrightarrow{Y}(3)$ are correlated with $\overrightarrow{Y}(2)$ and $\overrightarrow{Y}(4)$, thus C_1 and C_2 are also correlated RVs.

We indicate the outage probability of a single link S_i-R-D by $P_{\mathrm{out}}(i)$ and define it as the

probability of the event where the capacity of the link drops below a certain threshold γ_i :

$$P_{\text{out}}(i) = \Pr[C_i < \gamma_i]. \tag{5.12}$$

Finally, the global outage event is defined as the case where at least one link goes into outage. We indicate the probability of this event by $\widehat{P_{\text{out}}}$ and mathematically define it as

$$\widehat{P_{\text{out}}} = \Pr[C_1 < \gamma_1 \text{ or} \dots C_i < \gamma_i \text{ or} \dots C_{N_{\text{S}}} < \gamma_{N_{\text{S}}}]. \tag{5.13}$$

The purpose of this chapter is to characterize $\widehat{P_{\text{out}}}$.

5.2 Global outage probability

In Chapter 4, a tight approximation for the S_i-R-D link outage probability defined in (5.12) is provided by fitting a normal probability distribution to the link capacity given in (5.11). The approximation is based on the fact that the link capacity is a summation over OFDM subcarrier capacities given in (5.10), which are identical but correlated RVs through (5.9). If these RVs were also statistically independent, central limit theorem would readily yield the Gaussian distribution to the link capacity. However, regardless of the existing correlation, the central limit theorem has been applied and a tight approximation has been resulted.

On the other hand, if the link capacities were statistically independent, one could easily show that

$$\widehat{P_{\text{out}}} = 1 - \prod_{i=1}^{N_{\text{S}}} \big(1 - P_{\text{out}}(i)\big). \tag{5.14}$$

However, the link capacities are also correlated RVs through the correlation of the OFDM subcarriers on the R-D channel. The information received at R from S_is on independent channels is transmitted on a common physical channel to D, and the nonzero cov $\big(\overrightarrow{Y}(n_1), \overrightarrow{Y}(n_2)\big)$ makes C_is correlated. In order to tackle this issue, we approximate the joint probability distribution of C_is by a multi-variate normal distribution. To fully represent a multi-variate normal distribution, obtaining the mean vector $\overrightarrow{\mu}_{N_{\text{S}}}$ and the covariance matrix $\mathbf{Q}_{N_{\text{S}} \times N_{\text{S}}}$ are sufficient. The elements of $\overrightarrow{\mu}_{N_{\text{S}}}$ which are the mean values of link capacities are obtained in Chapter 4 as follows

$$\overrightarrow{\mu}_{N_{\text{S}}}(i) = \text{E}[C_i] = \frac{1}{2}\log_2(e)\Bigg[e^{(\alpha_{\text{S}_i\text{R}} + \alpha_{\text{S}_i\text{D}})}\Big(\frac{\alpha_{\text{RD}}}{\alpha_{\text{S}_i\text{D}} - \alpha_{\text{RD}}}\Big)\text{Ei}\big(-(\alpha_{\text{S}_i\text{R}} + \alpha_{\text{S}_i\text{D}})\big)$$

$$- e^{(\alpha_{\mathrm{S}_i\mathrm{R}}+\alpha_{\mathrm{RD}})}\Big(\frac{\alpha_{\mathrm{S}_i\mathrm{D}}}{\alpha_{\mathrm{S}_i\mathrm{D}}-\alpha_{\mathrm{RD}}}\Big)\mathrm{Ei}\big(-(\alpha_{\mathrm{S}_i\mathrm{R}}+\alpha_{\mathrm{RD}})\big)\Big], \quad (5.15)$$

where $\mathrm{Ei}(\cdot)$ is the exponential integral and defined as $\mathrm{Ei}(x)=\int_{-\infty}^{x}\frac{\exp(t)}{t}\mathrm{d}t$ [81], and

$$\alpha_{\mathrm{S}_i\mathrm{R}}=\frac{\lambda_{\mathrm{S}_i\mathrm{R}}N_{\phi_i}\sigma_{\mathrm{R}}^2}{P_{\mathrm{S}_i}}\ ,\ \alpha_{\mathrm{RD}}=\frac{\lambda_{\mathrm{RD}}N_{\mathrm{sc}}\sigma_{\mathrm{D}}^2}{P_{\mathrm{R}}}\ ,\ \alpha_{\mathrm{S}_i\mathrm{D}}=\frac{\lambda_{\mathrm{S}_i\mathrm{D}}N_{\phi_i}\sigma_{\mathrm{D}}^2}{P_{\mathrm{S}_i}}. \quad (5.16)$$

The elements on the main diagonal of $\mathbf{Q}_{N_\mathrm{S}\times N_\mathrm{S}}$ which are the variances of C_is are also calculated in Chapter 4. The Delta method [84] is used to approximate the variance of the link capacities, due to non-existence of closed form solution for the variances. After the necessary modifications, the main diagonal elements of $\mathbf{Q}_{N_\mathrm{S}\times N_\mathrm{S}}$ are

$$\mathbf{Q}_{N_\mathrm{S}\times N_\mathrm{S}}(i,i)=\sigma_{C_i}^2\approx\sum_{n_1\in\phi_i}\sum_{n_2\in\phi_i}\Bigg[\frac{\partial C_i}{\partial\overrightarrow{X}_i(n_1)}\frac{\partial C_i}{\partial\overrightarrow{X}_i(n_2)}\Theta_{\overrightarrow{X}_i}(n_1,n_2) \quad (5.17)$$

$$+\frac{\partial C_i}{\partial\overrightarrow{Y}(n_1)}\frac{\partial C_i}{\partial\overrightarrow{Y}(n_2)}\Theta_{\overrightarrow{Y}}(n_1,n_2) \quad (5.18)$$

$$+\frac{\partial C_i}{\partial\overrightarrow{Z}_i(n_1)}\frac{\partial C_i}{\partial\overrightarrow{Z}_i(n_2)}\Theta_{\overrightarrow{Z}_i}(n_1,n_2)\Bigg], \quad (5.19)$$

where $\frac{\partial C_i}{\partial\overrightarrow{X}_i(n)}$, $\frac{\partial C_i}{\partial\overrightarrow{Y}(n)}$, and $\frac{\partial C_i}{\partial\overrightarrow{Z}_i(n_1)}$ denote the partial derivatives of the link capacity C_i from (5.11) and (5.10) with respect to $\overrightarrow{X}_i(n)$, $\overrightarrow{Y}(n)$ and $\overrightarrow{Z}_i(n)$, respectively, and these derivatives are evaluated at $\mathrm{E}[\overrightarrow{X}_i(n)]$, $\mathrm{E}[\overrightarrow{Y}(n)]$, and $\mathrm{E}[\overrightarrow{Z}_i(n)]$ as the following

$$\frac{\partial C_i}{\partial\overrightarrow{X}_i(n)}=\beta\begin{cases}\frac{a_{x,i}}{1+a_{x,i}\mathrm{E}[\overrightarrow{X}_i(n)]} & a_{x,i}\mathrm{E}[\overrightarrow{X}_i(n)]\le a_y\mathrm{E}[\overrightarrow{Y}(n)]+a_{z,i}\mathrm{E}[\overrightarrow{Z}_i(n)]\\ 0 & \text{otherwise}\end{cases}, \quad (5.20)$$

$$\frac{\partial C_i}{\partial\overrightarrow{Y}(n)}=\beta\begin{cases}0 & a_{x,i}\mathrm{E}[\overrightarrow{X}_i(n)]\le a_y\mathrm{E}[\overrightarrow{Y}(n)]+a_{z,i}\mathrm{E}[\overrightarrow{Z}_i(n)]\\ \frac{a_y}{1+a_y\mathrm{E}[\overrightarrow{Y}(n)]+a_{z,i}\mathrm{E}[\overrightarrow{Z}_i(n)]} & \text{otherwise}\end{cases},$$

$$\frac{\partial C_i}{\partial\overrightarrow{Z}_i(n)}=\beta\begin{cases}0 & a_{x,i}\mathrm{E}[\overrightarrow{X}_i(n)]\le a_y\mathrm{E}[\overrightarrow{Y}(n)]+a_{z,i}\mathrm{E}[\overrightarrow{Z}_i(n)]\\ \frac{a_{z,i}}{1+a_y\mathrm{E}[\overrightarrow{Y}(n)]+a_{z,i}\mathrm{E}[\overrightarrow{Z}_i(n)]} & \text{otherwise}\end{cases},$$

and

$$\beta=\frac{\log_2(e)}{2N_{\phi_i}}, a_{x,i}=\frac{P_{\mathrm{S}_i}}{N_{\phi_i}\sigma_{\mathrm{R}}^2}, a_y=\frac{P_{\mathrm{R}}}{N_{\mathrm{sc}}\sigma_{\mathrm{D}}^2}, a_{z,i}=\frac{P_{\mathrm{S}_i}}{N_{\phi_i}\sigma_{\mathrm{D}}^2}. \quad (5.21)$$

The rest of the elements of $\mathbf{Q}_{N_\mathrm{S}\times N_\mathrm{S}}$ which represent the covariance between C_i and C_j for $i \neq j$ are also challenging to calculate. Therefore, we again use the Delta method to approximate these elements:

$$\mathbf{Q}_{N_\mathrm{S}\times N_\mathrm{S}}(i,j) = \mathrm{E}[(C_i - \overrightarrow{\mu}_{N_\mathrm{S}}(i))(C_j - \overrightarrow{\mu}_{N_\mathrm{S}}(j))] \approx \sum_{n_1\in\phi_i}\sum_{n_2\in\phi_j}\left[\frac{\partial C_i}{\partial \overrightarrow{Y}(n_1)}\frac{\partial C_j}{\partial \overrightarrow{Y}(n_2)}\Theta_{\overrightarrow{Y}}(n_1,n_2)\right]. \tag{5.22}$$

Note that in (5.22), only the covariance between the R-D OFDM subcarriers are taken into account, and in (5.17), all the channels are considered. This is because the correlation between the link capacities is caused only by the common channel between R and D.

Now, defining the N_S element threshold vector $\overrightarrow{\gamma}_{N_\mathrm{S}}$ as $\overrightarrow{\gamma}_{N_\mathrm{S}} = [\gamma_1, \ldots, \gamma_{N_\mathrm{S}}]$, the global probability of outage is

$$\begin{aligned}\widehat{P_{\mathrm{out}}} = \sum_{i_1} P_{\mathrm{out}}(i_1) - \sum_{i_1,i_2,i_1\neq i_2} T_2(i_1,i_2) + \ldots \\ + (-1)^{m+1}\sum_{i_1,\ldots,i_m,i_1\neq i_2\neq\cdots\neq i_m} T_m(i_1,\ldots,i_m) + \ldots \\ + (-1)^{N_\mathrm{S}+1} G(\overrightarrow{\gamma}_{N_\mathrm{S}}, \overrightarrow{\mu}_{N_\mathrm{S}}, \mathbf{Q}_{N_\mathrm{S}\times N_\mathrm{S}}),\end{aligned} \tag{5.23}$$

where all the indices i_m can take values in $\{1,\ldots,N_\mathrm{S}\}$, and

$$T_m(i_1,\ldots,i_m) = G\big(\overrightarrow{\gamma}_m(i_1,\ldots,i_m), \overrightarrow{\mu}_m(i_1,\ldots,i_m), \mathbf{Q}_{m\times m}(i_1,\ldots,i_m)\big). \tag{5.24}$$

In the above equation, $\overrightarrow{\gamma}_m(i_1,\ldots,i_m)$ and $\overrightarrow{\mu}_m(i_1,\ldots,i_m)$ are m element vectors obtained by removing all the elements except the $i_1,\ldots,i_m$ elements from $\overrightarrow{\gamma}_{N_\mathrm{S}}$ and $\overrightarrow{\mu}_{N_\mathrm{S}}$, respectively, and $\mathbf{Q}_{m\times m}(i_1,\ldots,i_m)$ is an $m\times m$ element covariance matrix obtained by removing all the rows and columns except the $i_1,\ldots i_m$ rows and columns from $\mathbf{Q}_{N_\mathrm{S}\times N_\mathrm{S}}$. As an example, for the the case of $N_\mathrm{S} = 2$ we have

$$\widehat{P_{\mathrm{out}}} = P_{\mathrm{out}}(1) + P_{\mathrm{out}}(2) - G(\overrightarrow{\gamma}_2, \overrightarrow{\mu}_2, \mathbf{Q}_{2\times 2}). \tag{5.25}$$

5.3 Numerical simulation results

In this section, we examine the accuracy of our global outage analysis against Monte Carlo simulation. In our simulations, we have considered three cases of $N_S = 2, 3$ and 4, under equal power budgets at the sources and the relay, and a reduced power budget at the relay

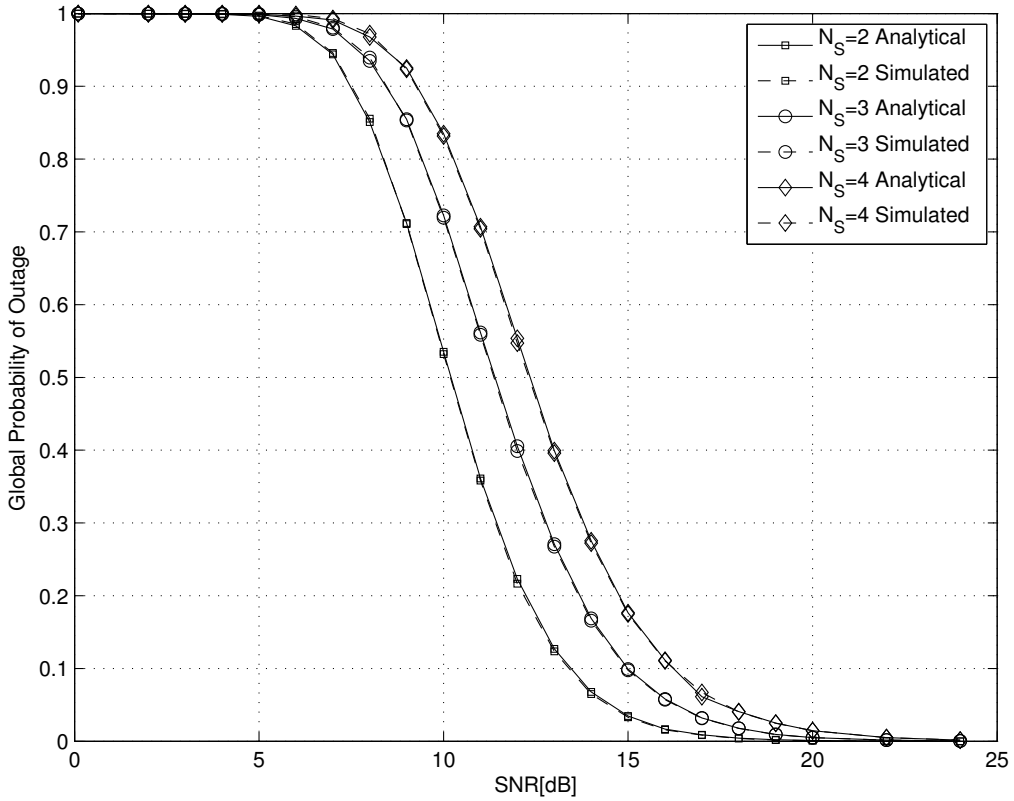

Figure 5.2: Global outage probability against transmitted SNR when $P_R = P_S$ for $N_S = 2, 3, 4$

by a factor of 10, in Fig. 5.2 and Fig. 5.3, respectively. The number of channel taps on all the links is set to 4. It is assumed that the S_i-R distances and the R-D distance are all equal, and the variance of channel taps is set to 1/4 so that the channel powers on S_i-R and R-D channels are normalized to 1. The sources are uniformly located on 1/3 arc of a circle with R at the center and radius of the R-D distance, farthest from the D. Assuming the path loss exponent of 4, the S_i-D channel powers are scaled by the ratio of S_i-D distance to S_i-R distance to the power of 4. It is also assumed that each source is given 16 adjacent OFDM subcarriers. The noise variances at R and D are set to 1.

As it can be seen in both figures, the analytical solution to the global outage probability closely matches the simulated results in all cases. It can also be seen that increasing the number of sources worsens the probability of outage. This is because the outage occurs when at least one link goes into outage, and increasing the number of links increases the likelihood of this event. By comparing Fig. 5.2 and Fig. 5.3, it is apparent that the outage

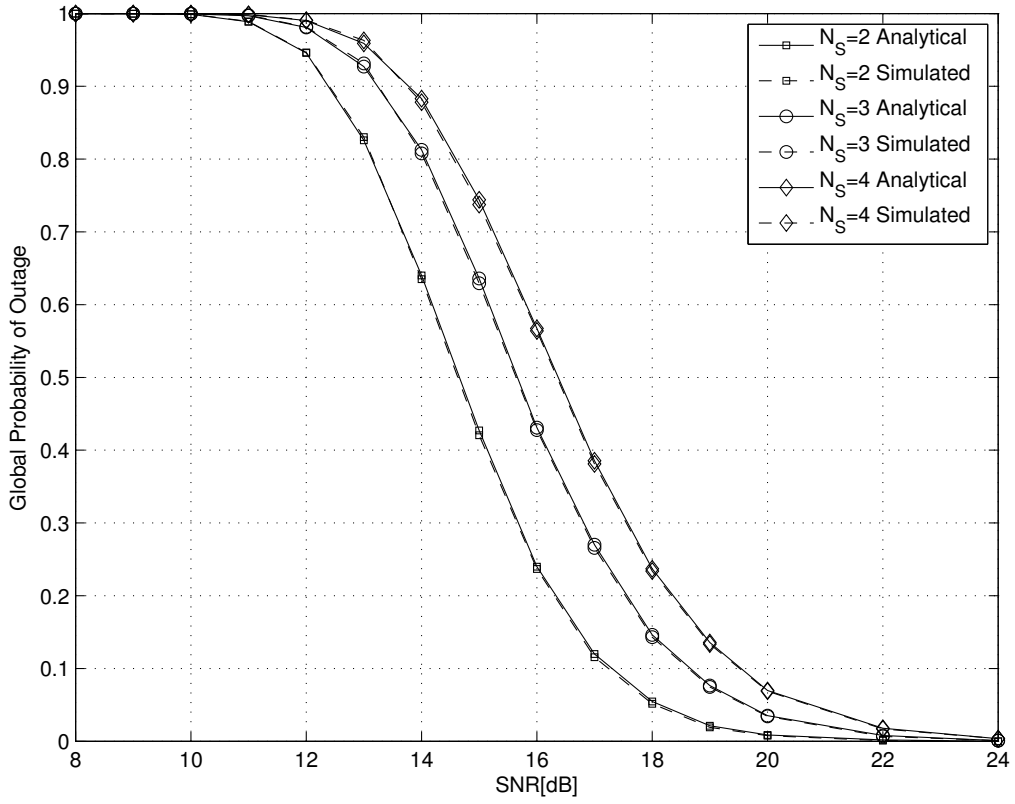

Figure 5.3: Global outage probability against transmitted SNR when $P_R = 0.1 \cdot P_S$ for $N_S = 2, 3, 4$

performance is better when the power budgets at the sources and the relay are equal. This trend is expected because reducing the power budget at the relay decreases the SNR levels in the network, which in turn decreases the link capacities and increases the likelihood of these capacities dropping below a threshold.

Chapter 6

Outage Analysis and Relay Allocation for Multi-Stream OFDMA Decode-and-Forward Rayleigh Fading Networks

In this chapter, we study a clustered OFDMA two-hop DF network consisting of a set of source-destination pairs, and a cluster of relays. We consider the case of no LOS between source cluster and the destination cluster, and it is assumed that individual source-relay and relay-destination channels suffer from Rayleigh frequency selective fading. The contributions of this chapter are summarized in the following:

- The global outage probability of described networks is approximated assuming correlated OFDM subcarrier gains on individual source-relay and relay-destination channels along with the freedom of allocating arbitrary number of bits to each OFDM subcarrier. The global outage event is defined as the event where at least one source-relay-destination link goes into outage.

- It is also shown that the outage probability on a single source-relay-destination link does not depend on the choice of OFDMA subcarrier subset as long as there is equal number of subcarriers in each subset and a given subset is formed from contiguous subcarriers in the frequency domain.

- The problem of relay allocation to minimizing the obtained global outage probability is formulated and it is shown it can be converted to a standard assignment problem. Then, a novel and low complexity centralized relay allocation scheme based on Hungarian method is proposed to minimize the global outage probability. The proposed relay allocation scheme is based on knowing only some statistical characteristics of the channel, as opposed to high complexity methods based on having access to full channel state information.

Before proceeding further, some notations used in this chapter are clarified. We use $|\cdot|$ to denote magnitude of a complex argument, and $\delta(\cdot)$ and $U(\cdot)$ to represent the unit impulse and step functions. The Cartesian product of two sets is represented by $(\cdot)\times(\cdot)$, and defined as the set of all ordered pairs whose first element is a member of the left argument, and the second element is a member of the right argument. Moreover, $\bar{\cdot}$ and $\mathrm{E}[\cdot]$ indicate the expected value, $\mathrm{var}(\cdot)$ symbolizes the variance, $\mathrm{cov}(\cdot,\cdot)$ indicates the covariance of the two arguments, while the PDF of X is denoted by $f_X(\cdot)$, and $\mathcal{N}(0,\sigma^2)$ and $\mathcal{CN}(0,\sigma^2)$ denote the normal, and complex normal PDFs with zero mean and variance σ^2. Vectors and matrices are represented by bold letters, the i^{th} element of vector $\mathbf{V}$ is denoted by $\mathbf{V}(i)$, $\mathrm{diag}(\cdot)$ is a matrix with elements on the main diagonal taken from the elements of the input vector and zeros elsewhere, and $\mathrm{trace}(\cdot)$ is a scalar obtained by adding up the elements on the main diagonal of the input matrix.

The rest of this chapter is organized as follows. In the following section, the system model is defined. In Section 6.2, The outage probability of a single source-destination stream through a relay is obtained. Then, in Section 6.3, we characterize the global probability of outage and propose our relay allocation scheme. The performance of our proposed method is examined through numerical simulations in Section 6.4.

6.1 System model

In a Rayleigh frequency selective wireless environment, N_{s} sources (s_i, $i\in\{1,\ldots,N_{\mathrm{s}}\}$) wish to communicate to their intended destinations (d_i, $i\in\{1,\ldots,N_{\mathrm{s}}\}$), establishing N_{s} source-destination pairs, using the help of N_{r} relays (r_j, $j\in\{1,\ldots,N_{\mathrm{r}}\}$) in between, as shown in Fig. 6.1. Each relay can support only one s_i-d_i pair, i.e., at least N_{s} relays are needed to support all s_i-d_i pairs. It is assumed that there is no LOS between sources and destinations, and all the nodes are half-duplex, capable of only transmitting or receiving data at a specific time and frequency band. Therefore, a two time slot OFDMA scheme is employed. The frequency band consisting of N_{sc} flat faded OFDM subcarriers is divided into M non-overlapping subsets of subcarriers $\{\phi_1,\ldots,\phi_M\}$, each formed from N_ϕ contiguous OFDM subcarriers (i.e., $M\cdot N_\phi = N_{\mathrm{sc}}$)[5]. These OFDMA subcarrier subsets are allocated to s_i-d_i pairs, one to each pair, in order to realize more than one s_i-d_i pair at a time. In the first time slot, the sources transmit on their allocated OFDMA subset, and relays listen.

[5]In this chapter, all indices i refer to sources, and to be more precise, source-destination pairs, all indices j refer to relays, and indices n, n_1, and n_2 refer to the OFDM subcarriers. Where not indicated, indices i and j can take any value in $\{1,\ldots,N_{\mathrm{s}}\}$ and $\{1,\ldots,N_{\mathrm{r}}\}$, respectively, while n, n_1, and n_2 can take values in $\{1,\ldots,N_{\mathrm{sc}}\}$.

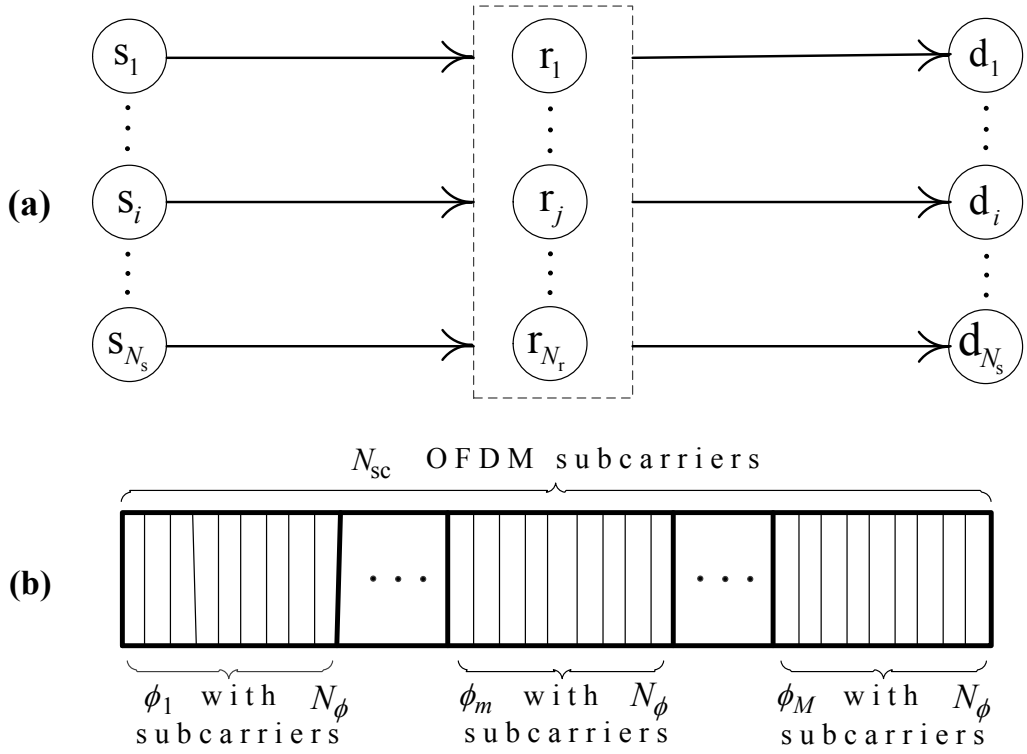

Figure 6.1: System model (a) System configuration (b) OFDMA setup

Assuming that one relay is allocated to each source, in the second time slot, the relays retransmit the information on the allocated OFDMA subset to the destinations under DF protocol. We also assume perfect time and frequency synchronization along with a cyclic prefix that is long enough to overcome the channel delay spread.

There are $2 \cdot N_{\mathrm{s}} \cdot N_{\mathrm{r}}$ physical channels in this system, $N_{\mathrm{s}} \cdot N_{\mathrm{r}}$ channels between sources and relays, and $N_{\mathrm{s}} \cdot N_{\mathrm{r}}$ channels between relays and destinations, where all these channels are statistically independent, due to the random nature of multi-paths fading in wireless channels. Indicating by $L_{\mathrm{s}_i\mathrm{r}_j}$ and $L_{\mathrm{r}_j\mathrm{d}_i}$ the number of channel taps on s_i-r_j and r_j-d_i channels, respectively, the channel impulse responses are

$$\begin{aligned} h_{\mathrm{s}_i\mathrm{r}_j}(\tau) &= \sum_{l=0}^{L_{\mathrm{s}_i\mathrm{r}_j}-1} \mathbf{h}_{\mathrm{s}_i\mathrm{r}_j}(l)\delta(\tau - l \cdot T_c), \\ h_{\mathrm{r}_j\mathrm{d}_i}(\tau) &= \sum_{l=0}^{L_{\mathrm{r}_j\mathrm{d}_i}-1} \mathbf{h}_{\mathrm{r}_j\mathrm{d}_i}(l)\delta(\tau - l \cdot T_c), \end{aligned} \tag{6.1}$$

where T_c indicates the coherence time, and the channel tap coefficients are taken from the

following $L_{\mathrm{s}_i\mathrm{r}_j}$ and $L_{\mathrm{r}_j\mathrm{d}_i}$ element random vectors

$$\begin{aligned}\mathbf{h}_{\mathrm{s}_i\mathrm{r}_j} &= [\mathbf{h}_{\mathrm{s}_i\mathrm{r}_j}(1)\ \mathbf{h}_{\mathrm{s}_i\mathrm{r}_j}(2)\ \ \ldots\ \ \mathbf{h}_{\mathrm{s}_i\mathrm{r}_j}(L_{\mathrm{s}_i\mathrm{r}_j})]^T,\\ \mathbf{h}_{\mathrm{r}_j\mathrm{d}_i} &= [\mathbf{h}_{\mathrm{r}_j\mathrm{d}_i}(1)\ \mathbf{h}_{\mathrm{r}_j\mathrm{d}_i}(2)\ \ \ldots\ \ \mathbf{h}_{\mathrm{r}_j\mathrm{d}_i}(L_{\mathrm{r}_j\mathrm{d}_i})]^T.\end{aligned} \tag{6.2}$$

It is assumed that the channel tap coefficients on a given physical channel are statistically independent, zero mean, and complex normally distributed RVs. Therefore, channel tap coefficient vectors, $\mathbf{h}_{\mathrm{s}_i\mathrm{r}_j}$ and $\mathbf{h}_{\mathrm{r}_j\mathrm{d}_i}$, are modelled as complex normal vectors with covariance matrices $\mathbf{\Gamma}_{\mathrm{s}_i\mathrm{r}_j}$ and $\mathbf{\Gamma}_{\mathrm{r}_j\mathrm{d}_i}$, as follows

$$\mathbf{h}_{\mathrm{s}_i\mathrm{r}_j} \sim \mathcal{CN}(0, \mathbf{\Gamma}_{\mathrm{s}_i\mathrm{r}_j}) \quad , \quad \mathbf{h}_{\mathrm{r}_j\mathrm{d}_i} \sim \mathcal{CN}(0, \mathbf{\Gamma}_{\mathrm{r}_j\mathrm{d}_i}), \tag{6.3}$$

where

$$\begin{aligned}\mathbf{\Gamma}_{\mathrm{s}_i\mathrm{r}_j} &= \mathrm{diag}\left[\mathrm{var}\left(\mathbf{h}_{\mathrm{s}_i\mathrm{r}_j}(1)\right)\ \ \ldots\ \ \mathrm{var}\left(\mathbf{h}_{\mathrm{s}_i\mathrm{r}_j}(L_{\mathrm{s}_i\mathrm{r}_j})\right)\right],\\ \mathbf{\Gamma}_{\mathrm{r}_j\mathrm{d}_i} &= \mathrm{diag}\left[\mathrm{var}\left(\mathbf{h}_{\mathrm{r}_j\mathrm{d}_i}(1)\right)\ \ \ldots\ \ \mathrm{var}\left(\mathbf{h}_{\mathrm{r}_j\mathrm{d}_i}(L_{\mathrm{r}_j\mathrm{d}_i})\right)\right].\end{aligned} \tag{6.4}$$

Having defined the channels in time domain, the Rayleigh OFDM subcarrier gains can be modelled as N_{sc} element vectors, which are obtained by performing N_{sc}-point Discrete Fourier Transform ($\mathrm{N_{sc}}$- DFT) on channel tap coefficient vectors,

$$\begin{aligned}\mathbf{H}_{\mathrm{s}_i\mathrm{r}_j} &= [\mathbf{H}_{\mathrm{s}_i\mathrm{r}_j}(1), \ldots, \mathbf{H}_{\mathrm{s}_i\mathrm{r}_j}(N_{\mathrm{sc}})] = N_{\mathrm{sc}}\text{- DFT}\{\mathbf{h}_{\mathrm{s}_i\mathrm{r}_j}\},\\ \mathbf{H}_{\mathrm{r}_j\mathrm{d}_i} &= [\mathbf{H}_{\mathrm{r}_j\mathrm{d}_i}(1), \ldots, \mathbf{H}_{\mathrm{r}_j\mathrm{d}_i}(N_{\mathrm{sc}})] = N_{\mathrm{sc}}\text{- DFT}\{\mathbf{h}_{\mathrm{r}_j\mathrm{d}_i}\}.\end{aligned} \tag{6.5}$$

The channel power gain vectors on s_i-r_j and r_j-d_i channels are represented by $\mathbf{X}_{ij}$ and $\mathbf{Y}_{ji}$, respectively. These two N_{sc} element vectors are formally defined as

$$\begin{aligned}\mathbf{X}_{ij} &= [|\mathbf{H}_{\mathrm{s}_i\mathrm{r}_j}(1)|^2, \ldots, |\mathbf{H}_{\mathrm{s}_i\mathrm{r}_j}(N_{\mathrm{sc}})|^2],\\ \mathbf{Y}_{ji} &= [|\mathbf{H}_{\mathrm{r}_j\mathrm{d}_i}(1)|^2, \ldots, |\mathbf{H}_{\mathrm{r}_j\mathrm{d}_i}(N_{\mathrm{sc}})|^2].\end{aligned} \tag{6.6}$$

Here, we can deduce that the elements of $\mathbf{X}_{ij}$ are exponentially distributed, since the channel gains in frequency are Rayleigh distributed. Moreover, elements of $\mathbf{X}_{ij}$ for a specific i and j are identical RVs, thus all associated with exponential parameter $\lambda_{\mathrm{s}_i\mathrm{r}_j}$. The same arguments hold for $\mathbf{Y}_{ji}$, its elements, and $\lambda_{\mathrm{r}_j\mathrm{d}_i}$. Hence, the elements of $\mathbf{X}_{ij}$ and $\mathbf{Y}_{ji}$ are taken from the following distributions

$$f_{\mathbf{X}_{ij}(n)}(x) = \lambda_{\mathrm{s}_i\mathrm{r}_j} e^{-(\lambda_{\mathrm{s}_i\mathrm{r}_j})x} \cdot U(x),\ \forall n \in \{1, \ldots, N_{\mathrm{sc}}\},$$

$$f_{\mathbf{Y}_{ij}(n)}(y) = \lambda_{\mathrm{r}_j\mathrm{d}_i} e^{-(\lambda_{\mathrm{r}_j\mathrm{d}_i})y} \cdot U(y),\ \forall n \in \{1,\ldots,N_{\mathrm{sc}}\}, \tag{6.7}$$

where the exponential distribution parameters are obtained to be

$$\lambda_{\mathrm{s}_i\mathrm{r}_j} = \frac{1}{\mathrm{trace}[\mathbf{\Gamma}_{\mathrm{s}_i\mathrm{r}_j}]} \quad , \quad \lambda_{\mathrm{r}_j\mathrm{d}_i} = \frac{1}{\mathrm{trace}[\mathbf{\Gamma}_{\mathrm{r}_j\mathrm{d}_i}]}. \tag{6.8}$$

Furthermore, denoting by $\Theta_{X_{\mathrm{s}_i\mathrm{r}_j}}(n_1,n_2)$ and $\Theta_{Y_{\mathrm{r}_j\mathrm{d}_i}}(n_1,n_2)$ the cov $\big(\mathbf{X}_{ij}(n_1),\mathbf{X}_{ij}(n_2)\big)$ and cov $\big(\mathbf{Y}_{ji}(n_1),\mathbf{Y}_{ji}(n_2)\big)$, respectively, they easily can be obtained to be [78]

$$\begin{aligned}
\Theta_{X_{\mathrm{s}_i\mathrm{r}_j}}(n_1,n_2) &= \Big| \sum_{l=0}^{L_{\mathrm{s}_i\mathrm{r}_j}-1} \mathrm{var}\left(\mathbf{h}_{\mathrm{s}_i\mathrm{r}_j}(l)\right) e^{-\hat{j}2\pi l\frac{n_1-n_2}{N_{\mathrm{sc}}}} \Big|^2, \\
\Theta_{Y_{\mathrm{r}_j\mathrm{d}_i}}(n_1,n_2) &= \Big| \sum_{l=0}^{L_{\mathrm{r}_j\mathrm{d}_i}-1} \mathrm{var}\left(\mathbf{h}_{\mathrm{r}_j\mathrm{d}_i}(l)\right) e^{-\hat{j}2\pi l\frac{n_1-n_2}{N_{\mathrm{sc}}}} \Big|^2,
\end{aligned} \tag{6.9}$$

where $\hat{j}$ is the imaginary unit $\sqrt{-1}$. It should be noted that cov $\big(\mathbf{X}_{ij}(n_1),\mathbf{X}_{\acute{i}\acute{j}}(n_2)\big) = 0$ if $i \neq \acute{i}$ or $j \neq \acute{j}$, because in this case, the arguments of cov(.,.) are obtained from two independent events. Following the same reasoning, it is trivial that cov $\big(\mathbf{X}_{ij}(n_1),\mathbf{Y}_{\acute{i}\acute{j}}(n_2)\big) = 0$ for all $(i,j) \in \{1,\ldots,N_{\mathrm{s}}\} \times \{1,\ldots,N_{\mathrm{r}}\}$ and $(\acute{i},\acute{j}) \in \{1,\ldots,N_{\mathrm{s}}\} \times \{1,\ldots,N_{\mathrm{r}}\}$.

Now, let us assume that s_i with power budget of P_{s_i} wants to transmit its information to d_i using the help of r_j with power budget of P_{r_j}. Further, let us assume that this communication is taking place through m^{th} OFDMA subcarrier set, i.e., s_i and r_j are allowed to use OFDM subcarriers $n \in \phi_m$. Also, s_i and r_j equally distribute their power budget among their N_ϕ available OFDM subcarriers, allocating $\frac{P_{\mathrm{s}_i}}{N_\phi}$ and $\frac{P_{\mathrm{r}_j}}{N_\phi}$ to each subcarrier in ϕ_m, respectively. Having defined these parameters, the capacity of s_i-r_j-d_i link on the n^{th} OFDM subcarrier, where $n \in \phi_m$, is [27]

$$C_{ij}(n) = \frac{1}{2}\log\left(1 + \min\left\{\mathbf{X}_{ij}(n)\frac{P_{\mathrm{s}_i}}{N_\phi\sigma_{\mathrm{r}}^2}, \mathbf{Y}_{ji}(n)\frac{P_{\mathrm{r}_j}}{N_\phi\sigma_{\mathrm{d}}^2}\right\}\right), \quad n \in \phi_m, \tag{6.10}$$

where σ_r^2 and σ_d^2 are noise variances at relays and destinations, respectively. Finally, the overall capacity of s_i-r_j-d_i link through ϕ_m is

$$C_{ij}^m = \frac{1}{N_\phi} \sum_{n=(m-1)N_\phi+1}^{mN_\phi} C_{ij}(n). \tag{6.11}$$

In this chapter, the eventual goal is to allocate relays to s_i-d_i pairs such that the global outage probability of the system is minimized. Hence, obtaining the global outage probability

as the main objective function is one of the crucial steps. On the way to achieving this purpose, evaluating the outage probability of a single s_i-r_j-d_i link through ϕ_m is of higher priority. We denote this probability by $P^m_{\text{out}}(i,j)$, and analyze it in the next section. Then, in Section 6.3, we formulate the overall outage probability minimization problem through relay allocation and propose our solution.

6.2 Outage probability of a single source-relay-destination link

In Chapter 4, we have presented an analysis to obtain the outage probability of an OFDM DF relay system, consisting of one source, one relay, and one destination, in which LOS between source and destination is also present. By modifying the system model in Chapter 4 by removing the LOS and allowing the active nodes to use only a subset of available OFDM subcarriers, $P^m_{\text{out}}(i,j)$ can be characterized. The outline of deriving $P^m_{\text{out}}(i,j)$ is described here.

The event of outage on s_i-r_j-d_i link occurs if the link's capacity from (6.11) drops below a certain threshold γ_i

$$P^m_{\text{out}}(i,j) = \Pr[C^m_{ij} < \gamma_i]. \tag{6.12}$$

In order to find $\Pr[C^m_{ij} < \gamma_i]$, the PDF of C^m_{ij} is required. According to (6.11) and (6.10), the link capacity C^m_{ij} is a summation over identical RVs $C^m_{ij}(n)$, where $n \in \phi_m$. If these RVs were statistically independent, the link capacity would be expected to follow a Gaussian PDF according to the central limit theorem. But, although the RVs $C^m_{ij}(n)$ are correlated through (6.9), still the link's capacity approximately follows the normal distribution. On the other hand, to fully characterize a normal RV, calculating the mean and variance is adequate.

As for the mean of C^m_{ij}, we introduce the following set of RVs

$$\mathbf{V}_{ij}(n) = \min\left\{\mathbf{X}_{ij}(n)\frac{P_{\mathrm{s}_i}}{N_\phi \sigma_r^2}, \mathbf{Y}_{ji}(n)\frac{P_{\mathrm{r}_j}}{N_\phi \sigma_d^2}\right\}, \forall n \in \phi_m. \tag{6.13}$$

Given the PDFs of $\mathbf{X}_{ij}(n)$ and $\mathbf{Y}_{ji}(n)$ in (6.7), the PDF of the above RVs is calculated to be

$$f_{\mathbf{V}_{ij}(n)}(v) = (\alpha_{\mathrm{s}_i\mathrm{r}_j} + \alpha_{\mathrm{s}_i\mathrm{r}_j}) e^{-(\alpha_{\mathrm{s}_i\mathrm{r}_j} + \alpha_{\mathrm{r}_j\mathrm{s}_i})v} \cdot U(v), \tag{6.14}$$

where

$$\alpha_{\mathrm{s}_i\mathrm{r}_j} = \frac{\lambda_{\mathrm{s}_i\mathrm{r}_j} \cdot N_\phi \sigma_{\mathrm{r}}^2}{P_{\mathrm{s}_i}} \quad , \quad \alpha_{\mathrm{r}_j\mathrm{d}_i} = \frac{\lambda_{\mathrm{r}_j\mathrm{d}_i} \cdot N_\phi \sigma_{\mathrm{d}}^2}{P_{\mathrm{r}_j}}. \tag{6.15}$$

By substituting (6.13) into (6.10) we have

$$\mathrm{E}[C_{ij}^m] = \frac{1}{N_\phi} \sum_{n=(m-1)N_\phi+1}^{mN_\phi} \mathrm{E}[C_{ij}(n)] = \mathrm{E}[C_{ij}(n)] = \int_0^\infty \frac{1}{2}\log(1+v) f_{\mathbf{V}_{ij}(n)}(v)\mathrm{d}v. \tag{6.16}$$

Finally, by calculating the above integral, the mean of C_{ij}^m is

$$\mathrm{E}[C_{ij}^m] = \frac{-\log_2(e)}{2} e^{(\alpha_{\mathrm{s}_i\mathrm{r}_j}+\alpha_{\mathrm{r}_j\mathrm{s}_i})} \mathrm{Ei}\big(-(\alpha_{\mathrm{s}_i\mathrm{r}_j}+\alpha_{\mathrm{r}_j\mathrm{s}_i})\big), \tag{6.17}$$

in which $\mathrm{Ei}(\cdot)$ is the exponential integral and defined as $\mathrm{Ei}(x) = \int_{-\infty}^{x} \frac{\exp(t)}{t}\mathrm{d}t$ [81]. Note that $\mathrm{E}[C_{ij}^m]$ is independent of m and n, i.e., choice of ϕ_m does not change the mean of a link's capacity.

Considering that the joint PDF of any two OFDM subcarrier gains $|\mathbf{H}_{\mathrm{s}_i\mathrm{r}_j}(n_1)|$ and $|\mathbf{H}_{\mathrm{s}_i\mathrm{r}_j}(n_2)|$, or $|\mathbf{H}_{\mathrm{r}_j\mathrm{d}_i}(n_1)|$ and $|\mathbf{H}_{\mathrm{r}_j\mathrm{d}_i}(n_2)|$, follows a bivariate Rayleigh distribution [82, 83], obtaining a solution in closed form to the variance of C_{ij}^m is not straight-forward. Therefore, we use the delta method [84] to estimate the variance as follows

$$\sigma_{C_{ij}^m}^2 \approx \sum_{n_1\in\phi_m}\sum_{n_2\in\phi_m} \left[\frac{\partial C_{ij}^m}{\partial \mathbf{X}_{ij}(n_1)} \frac{\partial C_{ij}^m}{\partial \mathbf{X}_{ij}(n_2)} \Theta_{X_{ij}}(n_1,n_2) + \frac{\partial C_{ij}^m}{\partial \mathbf{Y}_{ji}(n_1)} \frac{\partial C_{ij}^m}{\partial \mathbf{Y}_{ji}(n_2)} \Theta_{Y_{ji}}(n_1,n_2) \right], \tag{6.18}$$

where $\frac{\partial C_{ij}^m}{\partial \mathbf{X}_{ij}(n)}$ and $\frac{\partial C_{ij}^m}{\partial \mathbf{Y}_{ji}(n)}$ denote the partial derivatives of link's capacity C_{ij}^m from (6.11) and (6.10) with respect to $\mathbf{X}_{ij}(n)$ and $\mathbf{Y}_{ji}(n)$. The derivatives are evaluated at $\mathrm{E}[\mathbf{X}_{ij}(n)]$ and $\mathrm{E}[\mathbf{Y}_{ji}(n)]$ as the following

$$\frac{\partial C_{ij}^m}{\partial \mathbf{X}_{ij}(n)} = \beta \begin{cases} \frac{a_{x,i}}{1+a_{x,i}\mathrm{E}[\mathbf{X}_{ij}(n)]} & a_{x,i}\mathrm{E}[\mathbf{X}_{ij}(n)] \le a_{y,j}\mathrm{E}[\mathbf{Y}_{ji}(n)] \\ 0 & \text{otherwise} \end{cases}, \tag{6.19}$$

$$\frac{\partial C_{ij}^m}{\partial \mathbf{Y}_{ji}(n)} = \beta \begin{cases} 0 & a_{x,i}\mathrm{E}[\mathbf{X}_{ij}(n)] \le a_{y,j}\mathrm{E}[\mathbf{Y}_{ji}(n)] \\ \frac{a_{y,j}}{1+a_{y,j}\mathrm{E}[\mathbf{Y}_{ji}(n)]} & \text{otherwise} \end{cases},$$

and

$$\beta = \frac{\log_2(e)}{2N_\phi} \ , \ a_{x,i} = \frac{P_{\mathrm{s}_i}}{N_\phi \sigma_{\mathrm{r}}^2} \ , \ a_{y,j} = \frac{P_{\mathrm{r}_j}}{N_\phi \sigma_{\mathrm{d}}^2}. \tag{6.20}$$

Inspecting (6.18), it is observed that $\sigma^2_{C^m_{ij}}$ is also independent of ϕ_m. This is because according to (6.9), $\Theta_{X_{ij}}(n_1, n_2)$ and $\Theta_{Y_{ji}}(n_1, n_2)$ are functions of OFDM subcarrier spacing $n_1 - n_2$. In other words, as long as there is equal number of OFDM subcarriers in each subset ϕ_m, and these subcarriers are contiguous, choice of ϕ_m does not change the mean and variance of link's capacity. Moreover, since the link's capacity is modeled as a normal RV which is fully represented by its mean and variance, choice of ϕ_m does not affect link's capacity C^m_{ij}, either. Therefore, we omit the index m from C^m_{ij} and $P^m_{\mathrm{out}}(i,j)$, and replace them by C_{ij} and $P_{\mathrm{out}}(i,j)$, respectively.

Having obtained the mean and variance of C_{ij} in (6.17) and (6.18), the outage probability on the s_i-r_j-d_i link is

$$P_{\mathrm{out}}(i,j) = \Pr[C_{ij} < \gamma_i] = 1 - Q\left(\frac{\gamma_i - \bar{C_{ij}}}{\sigma_{C_{ij}}}\right), \tag{6.21}$$

in which $Q(\cdot)$ is the standard Q-function.

6.3 Problem formulation and proposed relay allocation scheme

In this section, the problem of relay allocation for minimizing the global outage probability is formally stated, and a solution based on Hungarian method is proposed. We say the multi-stream system introduced in Section 6.1 is in outage if at least one of the N_{s} s_i-d_i links is in outage. In order to obtain an expression for the global outage probability P_{out}, we introduce relay assignment indices $\rho_{ij} \in \{0, 1\}$. The relay j is assigned to s_i-d_i pair if and only if $\rho_{ij} = 1$. Moreover, $\rho_{ij} = 1$ implies that $\rho_{\acute{i}\acute{j}} = 0$ if $i \neq \acute{i}$ or $j \neq \acute{j}$, because a relay can help at most one s_i-d_i pair. Following this definition, and considering the fact that the events of outage on single s_i-r_j-d_i links are statistically independent, the probability that none of the s_i-d_i pairs is in outage can be written in the form of

$$1 - P_{\mathrm{out}} = \prod_{i=1}^{N_{\mathrm{s}}} \prod_{j=1}^{N_{\mathrm{r}}} \left(1 - P_{\mathrm{out}}(i,j)\right)^{\rho_{ij}}, \tag{6.22}$$

in which $P_{\text{out}}(i,j)$ is the outage probability on a single s_i-r_j-d_i link through any of the M OFDMA subcarrier subsets ϕ_m, and this probability has been analyzed in Section 6.2. Finally, we are seeking a solution for the following optimization problem

$$\min_{\rho_{ij}} \quad 1 - \prod_{i=1}^{N_\text{s}} \prod_{j=1}^{N_\text{r}} \big(1 - P_{\text{out}}(i,j)\big)^{\rho_{ij}} \tag{6.23}$$

$$\text{subject to (s.t.)} \quad \sum_{i=1}^{N_\text{s}} \rho_{ij} \leq 1, \ \forall j \in \{1, \ldots, N_\text{r}\}, \tag{6.24}$$

$$\sum_{j=1}^{N_\text{r}} \rho_{ij} \leq 1, \ \forall i \in \{1, \ldots, N_\text{s}\}, \tag{6.25}$$

$$\rho_{ij} \in \{0,1\}, \forall (i,j) \in \{1, \ldots, N_\text{s}\} \times \{1, \ldots, N_\text{r}\}. \tag{6.26}$$

In this optimization problem, the objective function (6.23) is the global probability of outage, and constraints (6.24), (6.25) and (6.26) guarantee that each relay is at most assigned to one s_i-d_i pair. Further, by removing the constant term in (21) and taking the logarithm of the right hand side, the optimization problem (6.23)-(6.26) is transformed into the following optimization problem

$$\max_{\rho_{ij}} \quad \sum_{i=1}^{N_\text{s}} \sum_{j=1}^{N_\text{r}} \rho_{ij} \log\big(1 - P_{\text{out}}(i,j)\big) \tag{6.27}$$

$$\text{s.t.} \quad (6.24), (6.25) \text{ and } (6.26), \tag{6.28}$$

The above optimization problem is a standard 2-dimensional assignment problem [85]. To illustrate the nature of this problem, a gain matrix $\mathbf{A}$ is introduced, where the elements of this matrix are

$$A_{ij} = \log\big(1 - P_{\text{out}}(i,j)\big), \quad \forall (i,j) \in \{1, \ldots, N_\text{s}\} \times \{1, \ldots, N_\text{r}\}. \tag{6.29}$$

These elements are interpreted as the gain achieved by assigning r_j to s_i-d_i pair. Now, the problem of finding ρ_{ij} such that (6.23) is minimized is reduced to selecting N_s elements from $\mathbf{A}$, such that only one element is selected from each row and column, and the summation of these elements is maximized. In other words, if A_{ij} is selected, then $\rho_{ij} = 1$, and $\rho_{ij} = 0$ otherwise. This problem can be solved optimally by adopting the Hungarian method [85] with the complexity of $\mathcal{O}(\max(N_\text{s}, N_\text{r})^3)$. Forming the gain matrix $\mathbf{A}$ requires $N_\text{s} \times N_\text{r}$ calculations, giving the complexity of $\mathcal{O}(N_\text{s} \times N_\text{r})$; thus, the complexity of our proposed solution is dominated by the Hungarian method.

The proposed algorithm of relay allocation for minimizing the global outage probability is briefly described here. Given the statistical properties of the channel impulse responses between sources and relays, and relays and destination, the outage probability of all s_i-r_j-d_i links can be evaluated through the procedure described in Section 6.2. It is also observed in Section 6.2 that the outage probability of a specific link does not depend on the choice of OFDMA subcarrier subset ϕ_m. Therefore, the need for allocating OFDMA subcarrier subsets to s_i-d_i pairs is eliminated, leaving us only with relays to be allocated. In order to allocate relays, the gain matrix in (6.29) is formed, and then performing the Hungarian method on this matrix readily gives us the relay allocation pattern. Finally, the OFDMA subcarrier subsets ϕ_m can be allocated randomly to the s_i-r_j-d_i links, so that simultaneous communication of s_i-d_i pairs is not corrupted. This algorithm is evaluated through numerical simulation in the next section.

6.4 Numerical simulation results

In this section, the behavior of our system model and the performance of our proposed relay allocation scheme is examined through numerical simulations. In simulations, it is assumed that the number of channel taps on all the channels is equal, i.e., $L_{\mathrm{s}_i\mathrm{r}_j} = L_{\mathrm{r}_j\mathrm{d}_i} = L$, and the channel tap coefficients on a given channel have equal variance, while the variance of channel taps on different channels are not necessarily equal, as the following

$$\begin{aligned} \mathrm{var}\left(\mathbf{h}_{\mathrm{s}_i\mathrm{r}_j}(1)\right) = \cdots = \mathrm{var}\left(\mathbf{h}_{\mathrm{s}_i\mathrm{r}_j}(L)\right) = \sigma^2_{\mathrm{s}_i\mathrm{r}_j}/L, \\ \mathrm{var}\left(\mathbf{h}_{\mathrm{r}_j\mathrm{s}_i}(1)\right) = \cdots = \mathrm{var}\left(\mathbf{h}_{\mathrm{r}_j\mathrm{s}_i}(L)\right) = \sigma^2_{\mathrm{r}_j\mathrm{s}_i}/L. \end{aligned} \tag{6.30}$$

Furthermore, the total power of channels, $\sigma^2_{\mathrm{s}_i\mathrm{r}_j}$ and $\sigma^2_{\mathrm{r}_j\mathrm{s}_i}$, are taken from a uniformly distributed RV between 0 and 1

$$\sigma^2_{\mathrm{s}_i\mathrm{r}_j} \sim U[0,1] \quad , \quad \sigma^2_{\mathrm{r}_j\mathrm{s}_i} \sim U[0,1]. \tag{6.31}$$

Equal power budgets at all the source and relay nodes is also assumed ($P_{\mathrm{s}_i} = P_{\mathrm{r}_j} = P_{\mathrm{s}} = P_{\mathrm{r}}$), and the threshold rate is set to 1 for all s_i-d_i pairs ($\gamma_i = \gamma = 1$ bit/s/Hz), and noise variances at relays and destinations are $\sigma^2_{\mathrm{s}} = \sigma^2_{\mathrm{r}} = 1$. In addition, the users are allowed to use OFDMA subcarrier groups of $N_\phi = 16$, and the SNR is the transmit SNR per OFDM subcarrier.

In this section, all the demonstrated probabilities, whether analytical or simulated, are probabilities averaged over 1000 samples of $\sigma^2_{\mathrm{s}_i\mathrm{r}_j}$ and $\sigma^2_{\mathrm{r}_j\mathrm{s}_i}$ in (6.31). In case of analytical results, the global outage probability is obtained using (6.23) for each sample of $\sigma^2_{\mathrm{s}_i\mathrm{r}_j}$ and

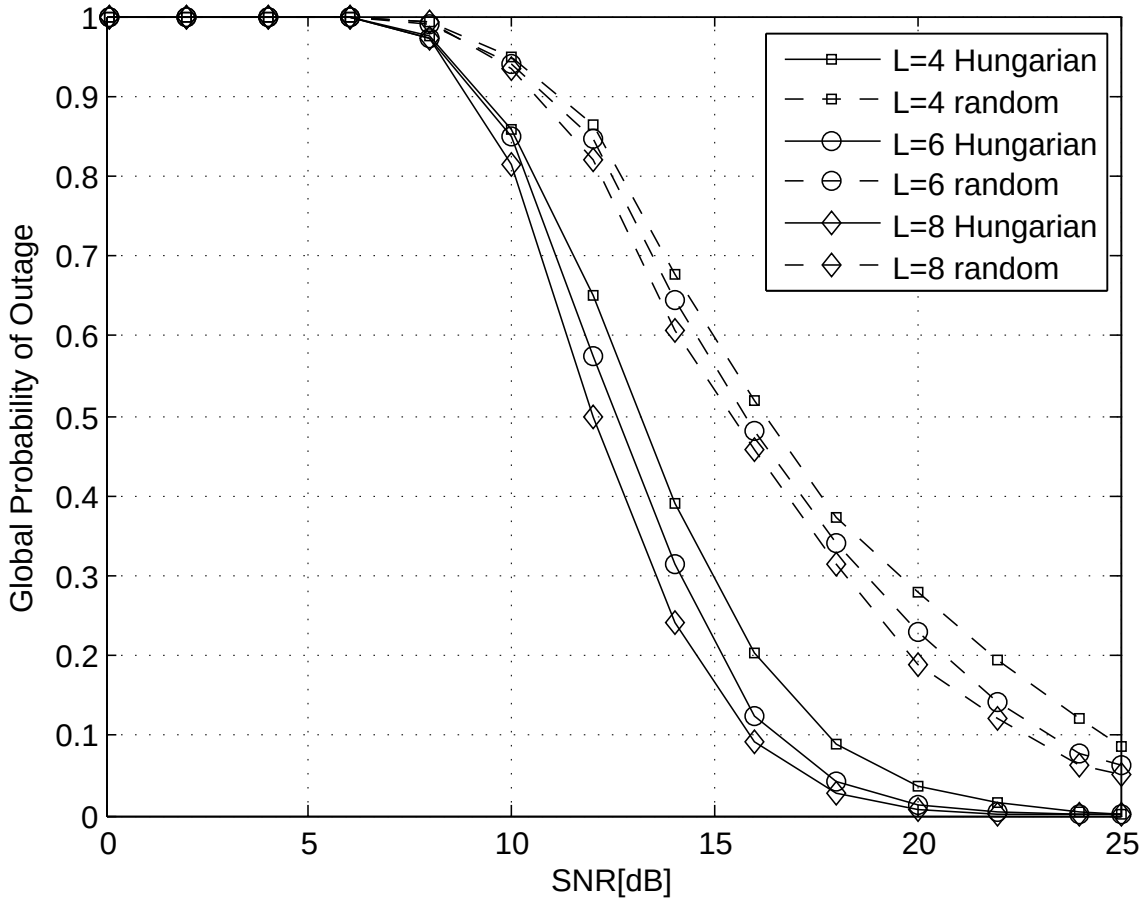

Figure 6.2: Simulated global outage probability against SNR when $N_{\mathrm{s}} = N_{\mathrm{r}} = 4$ and $N_{\phi} = 16$, for $L = 4, 6, 8$.

$\sigma^2_{\mathrm{r}_j\mathrm{s}_i}$, then the results are averaged. While regarding the simulated results, for each sample of $\sigma^2_{\mathrm{s}_i\mathrm{r}_j}$ and $\sigma^2_{\mathrm{r}_j\mathrm{s}_i}$, 1000000 samples of source-relay and relay-destination channels are generated according to (6.3) and (6.4), the number of outage events is counted, and the global outage probability is calculated. Then the outage probabilities associated with samples of $\sigma^2_{\mathrm{s}_i\mathrm{r}_j}$ and $\sigma^2_{\mathrm{r}_j\mathrm{s}_i}$ are averaged.

In Fig 6.2., the simulated global outage probabilities at different SNRs are shown for random relay allocation and our proposed relay allocation method. In this figure, keeping the number of source-destination pairs and relays at $N_{\mathrm{s}} = N_{\mathrm{r}} = 4$, the number of channel taps L is varied to study the effects of frequency diversity on the global outage probability. As it can be seen, the proposed relay allocation scheme outperforms random relay allocation significantly for all numbers of channel taps, which is due to the improved cooperative diversity in our method. Moreover, increasing the number of channel taps results in better

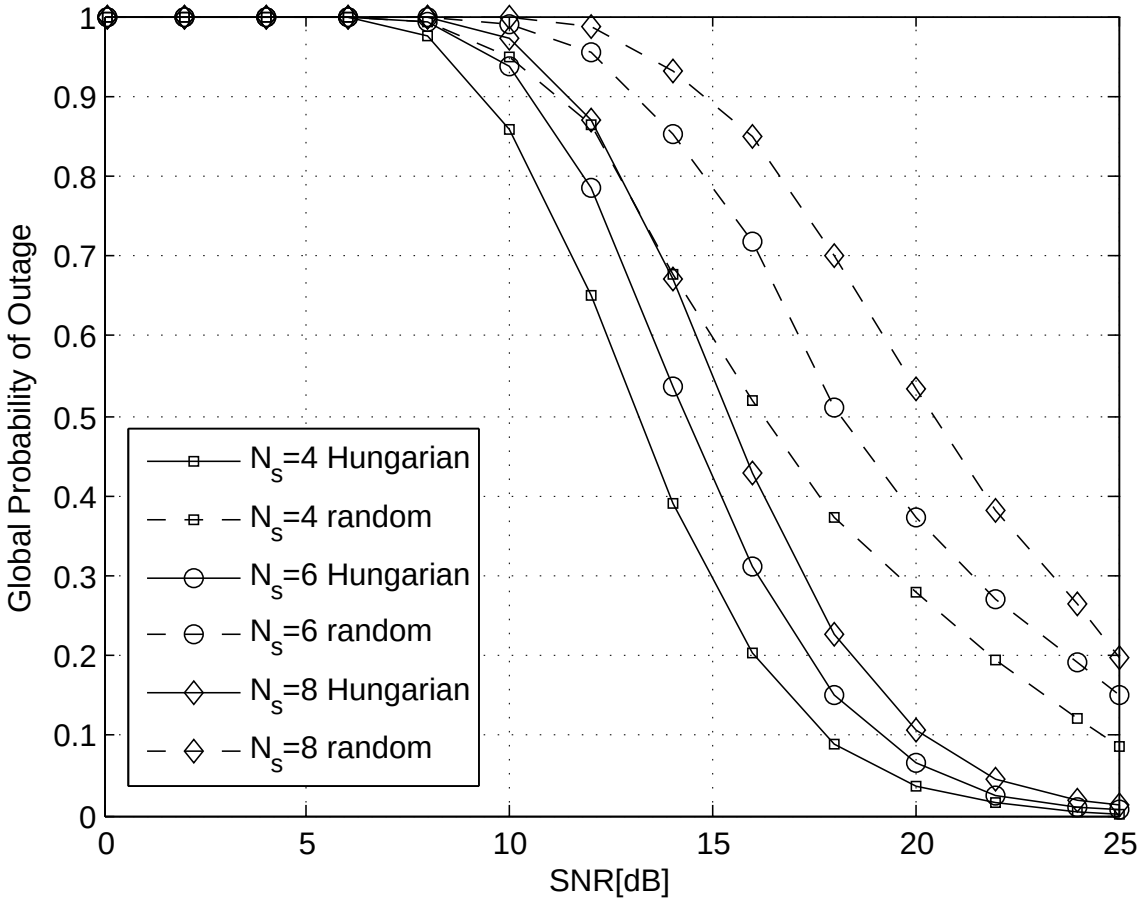

Figure 6.3: Simulated global outage probability against SNR when $L = 4$ and $N_\phi = 16$, for $N_\mathrm{s} = N_\mathrm{r} = 4, 6, 8$.

performance in both cases in terms of outage probability, which is due to the increased frequency diversity.

The simulated global outage probabilities at different SNRs for constant $L = 4$ and different numbers of source-destination pairs are demonstrated in Fig 6.3. Likewise, the results for random relay allocation and our proposed relay allocation method are shown in this figure, where our relay allocation algorithm beats the random allocation scheme with a considerable margin. In addition, increasing the number of users worsens the outage performance. This is because outage event happens even if only one source-destination pair is in outage, which is more likely when more pairs are to be realized. We have observed in our simulations that the analytical outage probabilities agree precisely with simulated results for all the cases of random relay allocation and relay allocation based on Hungarian method, which demonstrates the precision of our outage analysis. However, the analytical

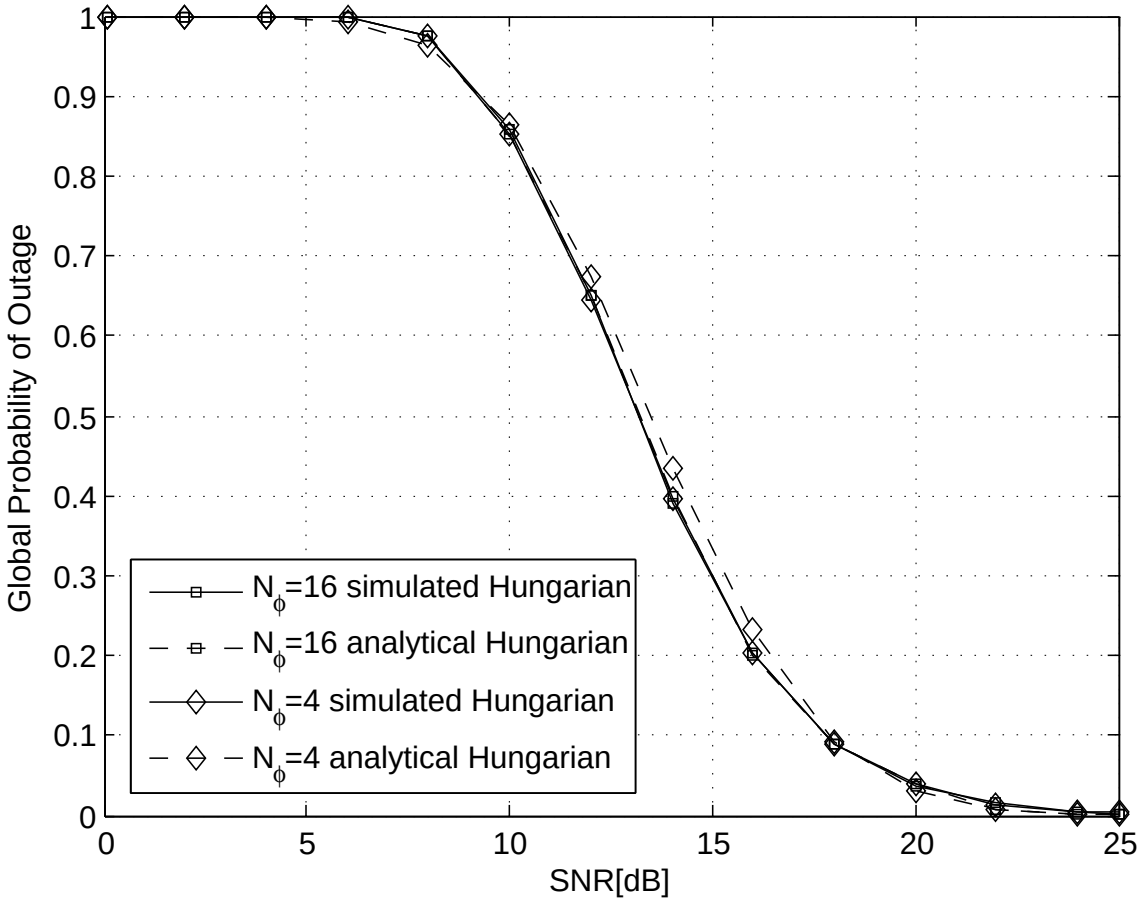

Figure 6.4: Simulated and analytical global outage probabilities against SNR when $L = 4$ and $N_{\mathrm{s}} = N_{\mathrm{r}} = 4$ for $N_\phi = 4, 16$.

results are not depicted in Fig. 6.2 and Fig. 6.3 to avoid impairing the readability of the figures. Analytical and simulated results can be compared in Fig. 6.4.

The effect of low number of subcarriers in OFDMA subsets is investigated in Fig. 6.4, where we keep both the number of sources and channel taps constant and vary N_ϕ. In this figure, the simulated and analytical outage probabilities with $N_\phi = 4$ and $N_\phi = 16$ are shown where the relays are allocated according to our proposed method. As it is mentioned in Chapter 4, approximating the capacity of a single s_i-r_j-d_i link by a Gaussian RV results in tight approximations of outage probability if the number of OFDM subcarriers is not too low. It can be seen in Fig. 6.4 that the simulated and analytical results match when $N_\phi = 16$, while the analytical results slightly deviate from simulated results when $N_\phi = 4$. However, although the analytical approximated outage probability is not exact for $N_\phi = 4$, we can see that the simulated performance of the system is identical to the case of $N_\phi = 16$.

We can deduce here that low number of subcarriers does not provide good approximations for the outage probability, but it does not degrade the effectiveness of our relay allocation method, either.

Chapter 7

Conclusions and Future Research Directions

7.1 Conclusions

In this thesis, we have addressed the cell association problem in HetNets, and performance evaluation as well as relay allocation in relay-based cooperative networks. We have proposed several cell association schemes in the context of HetNets, and characterized the outage behavior of cooperative relay-based systems in a broader system model compared to existing works in the literature. We also have proposed a relay allocation scheme based on our outage analysis. In the following, the concluding remarks on the contributions made in this thesis are brought.

First, in Chapter 2, we addressed the cell association problem in the downlink of a multi-tier HetNet in which BSs have finite number of RBs available to distribute among their associated users. We proposed a QoS-driven distributed cell association algorithm in which users receive only enough number of RBs to satisfy their QoS constraints. The algorithms are derived in two different frameworks. The first one is maximizing the sum utility of long term rate with long term rate QoS constraints. The second framework is minimizing the global outage probability with outage QoS constraints. The algorithm obtained in the first framework is suitable for environments with slow fading and low mobility users. On the other hand, the second framework is constructed in the context of outage to design cell association algorithms suitable for fast fading environments. It was shown that the cell association problem in both frameworks have the same structure. Therefore, a unified cell association algorithm was proposed by applying Lagrange dual decomposition method. The option of distributing the remaining RBs is also given to the BSs after the cell association phase. Distributing the rest of RBs improves the rates seen by the users significantly at the expense of consuming more energy and time and frequency resources. The derived algorithms are of low complexity, and low levels of message passing are required to render them distributed. Extensive simulation results that are brought in Chapter 2 show that our distributed cell association scheme outperforms the maximum SINR scheme. For instance, rate gains of up

to 2.4x have been observed in the simulations for the cell edge users in our distributed cell association algorithm over maximum SINR scheme. Most importantly, we provided a general framework for jointly associating users to BSs and RBs in LTE systems in which frequency reuse factor of 1 and no interference coordination are assumed.

Second, in Chapter 3, we extended the work in Chapter 2 by considering uplink as well as downlink. In Chapter 3 we addressed a joint downlink and uplink aware cell association problem in a multi-tier HetNet in which BSs have finite number of RBs to distribute among the users in the downlink and uplink. We proposed a distributed cell association scheme to maximize the downlink and uplink rates while maintaining outage QoS. The QoS is provided in both downlink and uplink by considering separate outage requirements for the user in downlink and uplink. Designing distributed and uplink aware cell association schemes is a major challenge in cellular networks since users cannot measure the uplink attributes including the uplink interference at their end. This is while users can measure some of the downlink attributes by listening to the reference signals that BSs are constantly transmitting. Therefore, we required the BSs to report the uplink interference using few number of bits. Few number of bits incurs negligible load on the already existing reference signals of the BSs. A low complexity distributed scheme is then proposed by introducing this limited amount of feedback and applying Lagrange dual decomposition method. In the proposed scheme, the users receive only enough number of RBs to satisfy their QoS constraints. Keeping the number of RBs minimum is in particular interesting from energy saving perspectives. Moreover, by assigning different weights to the downlink and uplink rates, the proposed scheme can be modified to be only downlink oriented, only uplink oriented, or both downlink and uplink aware. By comparing the proposed scheme with the downlink oriented maximum SINR scheme through simulations, significant uplink rate gains are observed. This is while the gains in the downlink rates are also considerable. Furthermore, simulation results verify the intrinsic asymmetries that exist between the attributes of downlink and uplink in HetNets. We also have considered a general system model in designing the distributed downlink and uplink aware cell association schemes, where frequency reuse factor of 1 and no interference coordination are assumed.

Next, in Chapter 4, we addressed the the outage behavior of the fundamental three-node cooperative model with one source, one relay, and one destination, in which OFDM technology is used to combat the frequency selectivity of the channel. We analyzed the outage probability and outage capacity of this OFDM DF network assuming Rayleigh frequency selective channel model. In our analysis, the correlation between OFDM subchannels along with arbitrary number of bits on each subchannel is considered. The analysis is carried out by fitting a normal distribution to the total capacity of the system. The normal distribution is

a suitable model for the total capacity of OFDM systems. This is because the total capacity is a summation of capacities on individual OFDM subcarriers which are usually identical random variables. The exact mean and approximated variance of the system capacity are obtained that result in tight approximations on the outage probability of the described systems. As a special case, the exact variance of the total capacity is derived for i.i.d. OFDM subchannels that results in even tighter approximations on the outage probability. Finally, the simulation results demonstrated the precession of our analysis even for low number of OFDM subchannels.

As an extension to Chapter 4, in Chapter 5, we let multiple users to communicate to a common destination through a single relay. The channel is assumed to be Rayleigh frequency selective. OFDMA is used as the multiple access scheme to realize multiple source-destination streams. We addressed the global outage behavior of this network in the sense that global outage occurs if at least one source-destination stream goes into outage. It is observed that the outage analysis for single source-relay-destination link is similar to the analysis provided in Chapter 4 if correlated OFDM subchannels and arbitrary number of bits on each subchannel are to be accounted for. However, it is observed that the capacity on different links are correlated RVs that complicates the global outage analysis. The correlation is created on the relay-destination channel that is common to all the steams. We proposed to fit a multi-variate normal distribution to the link capacities. Then, we approximated the covariance between the link capacities to characterize the global outage event. Monte Carlo simulations verified the validity of this analysis for multi-user single-relay OFDMA DF networks.

Finally, building upon Chapter 4, in Chapter 6, we investigated a clustered two-hop DF network consisting of a set of source-destination pairs, and a cluster of relays. It is assumed that there is no LOS between the source and destination clusters, and only one relay can help a particular source-destination pair in their communication. The channels are Rayleigh frequency selective on which OFDMA is employed to realize multiple simultaneous source-relay-destination links. Given some statistical parameters of the channels, the event of global outage is analyzed for the general case of correlated OFDM subcarrier gains, and arbitrary number of bits on each subcarrier. The global outage is again defined as the event where at least one source-destination pair experiences outage. The obtained global outage probability is then used to formulate a relay allocation optimization problem for which a low complexity solution based on Hungarian method is proposed. It is also shown that the outage probability on a single source-relay-destination link does not depend on the choice of OFDMA subcarrier subset if all the subsets consist of equal number of contiguous OFDM subcarriers. This observation simplified the relay allocation problem by removing the need

to allocate the OFDMA subcarrier subsets. In the end, the numerical results demonstrated the precision of the outage analysis, and effectiveness of the relay allocation method.

7.2 Future research directions

In this section, we propose some possible research directions that can be followed from this thesis:

- In our research on cell association problem in HetNets, we have not considered any ICIC. This is while considering resource partitioning, ICIC, and interference avoidance schemes can potentially enhance the overall user experience. Therefore, considering the mentioned techniques on top of the proposed cell association schemes can be a possible research venue.

- In the context of cell association in HetNets, we have assumed that the channel is frequency flat on the bandwidth of the BSs, i.e., the channel gain is identical on all the RBs of a BS at a certain time from user's point of view. This assumption is made to keep the system model simple and as general as possible. However, the BSs' reference signals are spread over time and frequency on the RBs so that a user can interpolate the channel gains on all the RBs. Meanwhile, different channel gains on different RBs highly complicates the analysis and designing distributed QoS-based cell association schemes. As a possible future research direction, the frequency selectivity of channels can be considered in the context of cell association in HetNets.

- In the context of cell association in HetNets, two admission control schemes are proposed in Chapters 2 and 3. The proposed admission control schemes are used to project a potential infeasible solution back to the feasible set. We have used heuristics to design these admission control schemes. Therefore, the dynamics of the optimization problems in Chapters 2 and 3 need to be investigated in more depth in search for optimal admission control schemes.

  From another perspective, in the proposed admission control schemes, we have not assumed any protocol for the communication of the BSs. However, in LTE-Advanced, BSs exchange information regarding load balancing and ICIC through X2 interface. Therefore, admission control schemes should be designed considering the protocol of X2 interface as well as the limitations that this interface imposes on the communication of BSs.

- In our research on cell association problem in HetNets, we have assumed the Rayleigh channel model. However, Rayleigh distribution captures only some characteristics of the wireless channel. More comprehensive wireless channel models such as Nakagami-m distribution should be considered. Also, the performance of the proposed cell association schemes need to be investigated with empirical channel models through simulations and experiments in order to modify these schemes to be suitable for practical implementation.

- In the context of relay-based cooperative communication, we have analyzed the outage behavior of OFDM DF relaying system in a Rayleigh fading environment in Chapters 4 and 5. However, Rayleigh distribution captures only some characteristics of the wireless channel. More comprehensive wireless channel models such as Nakagami-m distribution should be considered. The difficulty of considering statistical models such as Nakagami-m is that the analysis required to characterize the distribution of the total capacity becomes more complicated. In addition, OFDM cooperative systems operating under different protocols such as AF can be analyzed in the same manner.

- In our research on the problem of relay allocation in an OFDMA DF multi-source multi-destination scenario in Chapter 6, it is assumed that the number of OFDM subcarriers in all OFDMA subcarrier subsets is a constant, i.e., all users are allocated equal number of OFDM subcarriers. This assumption along with the obligation of choosing adjacent subcarriers in the spectrum for each subset result in independence of the link's capacity from the choice of OFDMA subset, which reduces one of the problem's dimensions. If the OFDMA subcarrier subsets are composed of varying number of subcarriers, or non-contiguous OFDM transmission takes place in the system, the choice of subcarrier subset will become one of the factors influencing the global outage probability. Adding the choice of OFDMA subcarrier subset to allocating relays to source-destination streams converts the two dimensional assignment problem we have encountered in Chapter 6 to a three dimensional assignment problem which is NP-hard in general [85]. Therefore, devising simplified low-complexity schemes to solve this complex problem for multi-stream OFDMA relayed systems can be another possible research direction.

- In general, in the context of OFDM cooperative communications, employing OFDM translates into sending information on parallel subcarriers, where the behavior of each subcarrier is an RV, and all the subcarriers show an identical behavior, meaning that the RVs associated with these subcarriers are identical. Since channel capacity or bit

rate is an additive parameter, the total capacity or bit rate is always obtained by adding up the capacities or rates on parallel OFDM subcarriers, resulting in Gaussian RVs according to central limit theorem. Devising a unified scheme to approximate the mean and variance of the resulting capacity or bit rate under any OFDM protocol considering general channel distributions is another research venue. As the next step, using the analysis for general distributions, designing distributed algorithms to allocate relays to source-destination pairs in multi-user scenarios can be considered.

Bibliography

[1] G. Wu, S. Talwar, K. Johnson, N. Himayat, and K. D. Johnson. M2M: From mobile to embedded internet. *IEEE Communications Magazine*, 49(4):36–43, Apr. 2011.

[2] LM Ericsson. More than 50 billion connected devices, Feb. 2011.

[3] Cisco. Cisco visual networking index: Global mobile data traffic forecast update, 2010 - 2015. *White Paper*, Feb. 2002.

[4] A. J. Viterbi. *CDMA: Principles of Spread Spectrum Communication*. Addison Wesley Longman Publishing Co., Inc., 1995.

[5] R. V. Nee and R. Prasad. *OFDM for Wireless Multimedia Communications*. Artech House, Inc., 1st edition, 2000.

[6] D. Gesbert, M. Shafi, D.-S. Shiu, P. J. Smith, and A. Naguib. From theory to practice: An overview of MIMO space-time coded wireless systems. *IEEE Journal on Selected Areas in Communications*, 21(3):281–302, Apr. 2003.

[7] R. Q. Hu and Y. Qian. *Heterogeneous Cellular Networks*. Wiley - IEEE Series. Wiley, 2013.

[8] S. Haykin. Cognitive radio: Brain-empowered wireless communications. *IEEE Journal on Selected Areas in Communications*, 23(2):201–220, Feb. 2005.

[9] Federal Communications Commission. Spectrum policy task force. Rep. ET Docket no. 02-135, Nov. 2002.

[10] S. Yeh, S. Talwar, G. Wu, N. Himayat, and K. Johnsson. Capacity and coverage enhancement in heterogeneous networks. *IEEE Wireless Communications*, 18(3):32–38, Jun. 2011.

[11] W. Song, H. Jiang, and W. Zhuang. Performance analysis of the WLAN-first scheme in cellular/WLAN interworking. *IEEE Transactions on Wireless Communications*, 6(5):1932–1952, May 2007.

[12] V. Chandrasekhar, J. G. Andrews, and A. Gatherer. Femtocell networks: A survey. *IEEE Communications Magazine*, 46(9):59–67, Sep. 2008.

[13] H. Claussen, L. T. W. Ho, and L. G. Samuel. Financial analysis of a pico-cellular home network deployment. In *Proc. of 2007 IEEE ICC*, pages 5604–5609.

[14] A. B. Saleh, S. Redana, B. Raaf, and J. Hamalainen. Comparison of relay and pico eNB deployments in LTE-advanced. In *Proc. of 2009 IEEE VTC*, pages 1–5.

[15] A. Damnjanovic, J. Montojo, Y. Wei, T. Ji, T. Luo, M. Vajapeyam, T. Yoo, O. Song, and D. Malladi. A survey on 3GPP heterogeneous networks. *IEEE Wireless Communications*, 18(3):10–21, Jun. 2011.

[16] T. Nihtila and V. Haikola. HSDPA performance with dual stream MIMO in a combined macro-femto cell network. In *Proc. of 2010 IEEE VTC*, pages 1–5.

[17] H. R. Karimi, L. T. W. Ho, H. Claussen, and L. G. Samuel. Evolution towards dynamic spectrum sharing in mobile communications. In *Proc. of 2006 IEEE PIMRC*, pages 1–5.

[18] M. Yavuz, F. Meshkati, S. Nanda, A. Pokhariyal, N. Johnson, B. Raghothaman, and A. Richardson. Interference management and performance analysis of UMTS/HSPA+ femtocells. *IEEE Communications Magazine*, 47(9):102–109, Sep. 2009.

[19] S.-M. Cheng, S.-Y. Lien, F.-S. Chu, and K.-C. Chen. On exploiting cognitive radio to mitigate interference in macro/femto heterogeneous networks. *IEEE Transactions on Wireless Communications*, 18(3):40–47, Jun. 2011.

[20] A. Khandekar, N. Bhushan, Ji Tingfang, and V. Vanghi. LTE-advanced: Heterogeneous networks. In *Proc. of 2010 European Wireless Conference*, pages 978–982.

[21] G. Boudreau, J. Panicker, N. Guo, R. Chang, N. Wang, and S. Vrzic. Interference coordination and cancellation for 4G networks. *IEEE Communications Magazine*, 47(4):74–81, Apr. 2009.

[22] K. Okino, T. Nakayama, C. Yamazaki, H. Sato, and Y. Kusano. Pico cell range expansion with interference mitigation toward LTE-advanced heterogeneous networks. In *Proc. of 2011 IEEE ICC*, pages 1–5.

[23] M. Shirakabe, A. Morimoto, and N. Miki. Performance evaluation of inter-cell interference coordination and cell range expansion in heterogeneous networks for LTE-advanced downlink. In *Proc. of 2011 ISWCS*, pages 844–848.

[24] E. C. Van der Meulen. Three-terminal communication channels. *Advances in applied Probability*, 3(1):120–154, Spring 1971.

[25] T. Cover and A. El Gamal. Capacity theorems for the relay channel. *IEEE Transactions on Information Theory*, 25(5):572–584, Sep. 1979.

[26] R. Pabst, B.H. Walke, D.C. Schultz, P. Herhold, H. Yanikomeroglu, S. Mukherjee, H. Viswanathan, M. Lott, W. Zirwas, M. Dohler, H. Aghvami, D.D. Falconer, and G.P. Fettweis. Relay-based deployment concepts for wireless and mobile broadband radio. *IEEE Communications Magazine*, 42(9):80–89, Sep. 2004.

[27] J. N. Laneman, D. N. C. Tse, and G. W. Wornell. Cooperative diversity in wireless networks: Efficient protocols and outage behavior. *IEEE Transactions on Information Theory*, 50(12):3062–3080, Dec. 2004.

[28] R. U. Nabar, H. Bolcskei, and F. W. Kneubuhler. Fading relay channels: Performance limits and space-time signal design. *IEEE Journal on Selected Areas in Communications*, 22(6):1099–1109, Aug. 2004.

[29] J. N. Laneman and G. W. Wornell. Energy-efficient antenna sharing and relaying for wireless networks. In *Proc. of 2000 IEEE WCNC*, pages 7–12.

[30] Z. Hasan, H. Boostanimehr, and V. K Bhargava. Green cellular networks: A survey, some research issues and challenges. *IEEE Communications Surveys and Tutorials*, 13(4):524–540, Nov. 2011.

[31] C. Hoymann, W. Chen, J. Montojo, A. Golitschek, C. Koutsimanis, and X. Shen. Relaying operation in 3GPP LTE: Challenges and solutions. *IEEE Communications Magazine*, 50(2):156–162, Feb. 2012.

[32] D. Astely, E. Dahlman, A. Furuskar, Y. Jading, M. Lindstrom, and S. Parkvall. LTE: The evolution of mobile broadband. *IEEE Communications Magazine*, 47(4):44–51, Apr. 2009.

[33] E. Dahlman, S. Parkvall, and J. Skold. *4G: LTE/LTE-Advanced for Mobile Broadband*. Academic Press, 2013.

[34] H. G. Myung, J. Lim, and D. Goodman. Single carrier FDMA for uplink wireless transmission. *IEEE Vehicular Technology Magazine*, 1(3):30–38, Sep. 2006.

[35] J. Li, X. Wu, and R. Laroia. *OFDMA Mobile Broadband Communications: A Systems Approach*. Cambridge University Press, 2013.

[36] G. Berardinelli, L. A. Ruiz de Temino, S. Frattasi, M. I. Rahman, and P. Mogensen. OFDMA vs. SC-FDMA: Performance comparison in local area IMT-A scenarios. *IEEE Wireless Communications*, 15(5):64–72, Oct. 2008.

[37] B. E. Priyanto, H. Codina, S. Rene, T. B. Sorensen, and P. Mogensen. Initial performance evaluation of DFT-spread OFDM based SC-FDMA for UTRA LTE uplink. In *Proc. of 2007 IEEE VTC*, pages 3175–3179.

[38] 3GPP. X2 general aspects and principles. TS 36.420, 3rd Generation Partnership Project (3GPP), Dec. 2009.

[39] 3GPP. X2 application protocol (x2ap). TS 36.423, 3rd Generation Partnership Project (3GPP), Sep. 2010.

[40] A. Ghosh, R. Ratasuk, B. Mondal, N. Mangalvedhe, and T. Thomas. LTE-advanced: Next-generation wireless broadband technology. *IEEE Wireless Communications*, 17(3):10–22, Jun. 2010.

[41] Y. Nam, Y. Akimoto, Y. Kim, M. Lee, K. Bhattad, and A. Ekpenyong. Evolution of reference signals for LTE-advanced systems. *IEEE Communications Magazine*, 50(2):132–138, Feb. 2012.

[42] Z. Shen, A. Papasakellariou, J. Montojo, D. Gerstenberger, and Fangli X. Overview of 3GPP LTE-advanced carrier aggregation for 4G wireless communications. *IEEE Communications Magazine*, 50(2):122–130, Feb. 2012.

[43] D. Lee, H. Seo, B. Clerckx, E. Hardouin, D. Mazzarese, S. Nagata, and K. Sayana. Coordinated multipoint transmission and reception in LTE-advanced: Deployment scenarios and operational challenges. *IEEE Communications Magazine*, 50(2):148–155, Feb. 2012.

[44] J. G. Andrews. Seven ways that HetNets are a cellular paradigm shift. *IEEE Communications Magazine*, 51(3):136–144, Mar. 2013.

[45] H. Kim, G. de Veciana, X. Yang, and M. Venkatachalam. Distributed α-optimal user association and cell load balancing in wireless networks. *IEEE/ACM Transactions on Networking*, 20(1):177–190, Feb. 2012.

[46] K. Son, S. Chong, and G. Veciana. Dynamic association for load balancing and interference avoidance in multi-cell networks. *IEEE Transactions on Wireless Communications*, 8(7):3566–3576, Jul. 2009.

[47] Q. Ye, B. Rong, Y. Chen, M. Al-Shalash, C. Caramanis, and J. G. Andrews. User association for load balancing in heterogeneous cellular networks. *IEEE Transactions on Wireless Communications*, 12(6):2706–2716, Apr. 2013.

[48] Q. Ye, M. Al-Shalash, C. Caramanis, and J. G. Andrews. On/off macrocells and load balancing in heterogeneous cellular networks. *arXiv preprint arXiv:1305.5585*, 2013.

[49] S. Corroy, L. Falconetti, and R. Mathar. Dynamic cell association for downlink sum rate maximization in multi-cell heterogeneous networks. In *Proc. of 2012 IEEE ICC*, pages 2457–2461.

[50] E. Stevens-Navarro, Y. Lin, and V. W. S. Wong. An MDP-based vertical handoff decision algorithm for heterogeneous wireless networks. *IEEE Transactions on Vehicular Technology*, 57(2):1243–1254, Mar. 2008.

[51] S. E. Elayoubi, E. Altman, M. Haddad, and Z. Altman. A hybrid decision approach for the association problem in heterogeneous networks. In *Proc. of 2010 IEEE INFOCOM*, pages 1–5.

[52] E. Aryafar, A. Keshavarz-Haddad, M. Wang, and M. Chiang. RAT selection games in HetNets. In *Proc. of 2013 IEEE INFOCOM*, pages 998–1006.

[53] D. Niyato and E. Hossain. Dynamics of network selection in heterogeneous wireless networks: An evolutionary game approach. *IEEE Transactions on Vehicular Technology*, 58(4):2008–2017, May 2009.

[54] H. S. Dhillon, R. K. Ganti, and J. G. Andrews. Load-aware modeling and analysis of heterogeneous cellular networks. *IEEE Transactions on Wireless Communications*, 12(4):1666–1677, Apr. 2013.

[55] H.-S. Jo, Y. J. Sang, P. Xia, and J. G. Andrews. Heterogeneous cellular networks with flexible cell association: A comprehensive downlink SINR analysis. *IEEE Transactions on Wireless Communications*, 11(10):3484–3495, Oct. 2012.

[56] H. S. Dhillon S. Singh and J. G. Andrews. Offloading in heterogeneous networks: Modeling, analysis, and design insights. *IEEE Transactions on Wireless Communications*, 12(5):2484–2497, Dec. 2013.

[57] S. Singh and J. G. Andrews. Joint resource partitioning and offloading in heterogeneous cellular networks. *IEEE Transactions on Wireless Communications*, 13(2):888–901, Feb. 2014.

[58] X. Chen and R. Q. Hu. Joint uplink and downlink optimal mobile association in a wireless heterogeneous network. In *Proc. of 2012 IEEE GLOBECOM*, pages 4131–4137.

[59] V. Emamian, P. Anghel, and M. Kaveh. Multi-user spatial diversity in a shadow-fading environment. In *Proc. of 2002 IEEE VTC*, pages 573–576.

[60] M. O. Hasna and M.-S. Alouini. Optimal power allocation for relayed transmissions over Rayleigh-fading channels. *IEEE Transactions on Wireless Communications*, 3(6):1999–2004, Nov. 2004.

[61] M.O. Hasna and M.-S. Alouini. Performance analysis of two-hop relayed transmissions over Rayleigh fading channels. In *Proc. of 2002 IEEE VTC*, pages 1992–1996.

[62] L. Dai, B. Gui, and L. J. Cimini. Selective relaying in OFDM multihop cooperative networks. In *Proc. of 2007 IEEE WCNC*, pages 963–968.

[63] M. Kaneko, K. Hayashi, P. Popovski, K. Ikeda, H. Sakai, and R. Prasad. Amplify-and-forward cooperative diversity schemes for multi-carrier systems. *IEEE Transactions on Wireless Communications*, 7(5):1845–1850, May 2008.

[64] W. Yang, W. Yang, and Y. Cai. Outage performance of OFDM-based selective decode-and-forward cooperative networks over Nakagami-m fading channels. *Wireless Personal Communications*, 56:503–515, Apr. 2011.

[65] B. Gui, L. Dai, and L. J. Cimini. Selective relaying in cooperative OFDM systems: Two-hop random network. In *Proc. of 2008 IEEE WCNC*, pages 996–1001.

[66] W. Siriwongpairat, A. Sadek, and K. J. R. Liu. Cooperative communications protocol for multiuser OFDM networks. *IEEE Transactions on Wireless Communications*, 7(7):2430–2435, Jul. 2008.

[67] T. S. Rappaport. *Wireless Communications: Principles and Practice*. Prentice Hall, Inc., second edition, 2002.

[68] S. Kandukuri and S. Boyd. Optimal power control in interference-limited fading wireless channels with outage-probability specifications. *IEEE Transactions on Wireless Communications*, 1(1):46–55, Jan. 2002.

[69] Y. D. Yao and A. U. H. Sheikh. Outage probability analysis for microcell mobile radio systems with cochannel interferers in Rician/Rayleigh fading environment. *Electronics Letters*, 26(13):864–866, Jun. 1990.

[70] H. W. Kuhn. The Hungarian method for the assignment problem. *Naval Research Logistics Quarterly*, 2:83–397, Mar. 1955.

[71] D. W. Pentico. Assignment problems: A golden anniversary survey. *European Journal of Operational Research*, 176(2):774–793, Nov. 2007.

[72] S. P. Boyd and L. Vandenberghe. *Convex Optimization*. Cambridge University Press, 2004.

[73] S. H. Low and D. E. Lapsley. Optimization flow control I: Basic algorithm and convergence. *IEEE/ACM Transactions on Networking*, 7(6):861–874, Dec. 1999.

[74] D. P. Bertsekas. *Convex Optimization Theory*. Athena Scientific, 2009.

[75] D. P. Bertsekas and J. N. Tsitsiklis. *Parallel and Distributed Computation: Numerical Methods*. Prentice-Hall, Inc., 1989.

[76] C. E. Leiserson, R. L. Rivest, C. Stein, and T. H. Cormen. *Introduction to Algorithms*. The MIT Press, 2001.

[77] G. B. Dantzig. *Linear Programming and Extensions*. Princeton University Press, 1998.

[78] A. Assalini and S. Pupolin. On second-order statistical description of mutual information for OFDM systems. In *Proc. of 2008 Wireless Personal Multimedia Communications*, pages 1–5.

[79] A. Assalini. Maximizing outage capacity of OFDM transmit diversity systems. *IEEE Transactions on Vehicular Technology*, 58(9):4786–4794, Nov. 2009.

[80] M. R. McKay, P. J. Smith, H. A. Suraweera, and I. B. Collings. On the mutual information distribution of OFDM-based spatial multiplexing: Exact variance and outage approximation. *IEEE Transactions on Information Theory*, 54(7):3260–3278, Jul. 2008.

[81] M. Abramowitz and I. A. Stegun. *Handbook of Mathematical Functions with Formulas, Graphs, and Mathematical Tables*. Dover, ninth dover printing, tenth gpo printing edition, 1964.

[82] N. Nakagami. The m-distribution, a general formula for intensity distribution of rapid fading. In *Statistical Methods in Radio Wave Propagation*. Oxford, England: Pergamon, 1960.

[83] S. O. Rice. Mathematical analysis of random noise. *Bell System Technical Journal*, 24(1):46–156, Jan. 1945.

[84] W. H. Greene. *Econometric Analysis*. Prentice Hall, fifth edition, 2000.

[85] R. E. Burkard, M. Dell'Amico, and S. Martello. *Assignment Problems*. Society for Industrial and Applied Mathematics, 2009.